A Novel Approach to DNA Analysis by Surface Enhanced Resonance Raman Scattering

Ljiljana Fruk

PhD Thesis

March 2004.

University of Strathclyde
Department of Pure and Applied Chemistry

A Novel Approach to DNA Analysis by Surface Enhanced Resonance Raman Scattering

Ljiljana Fruk

2004.

The copyright of this thesis belongs to the author under the terms of the United Kingdom Copyright Acts as qualified by University of Strathclyde regulation 3.49. Due acknowledgement must always be made of the use of any material contained in, or derived from, this thesis.

Abstract

A number of methods for detecting specific DNA sequences have been used to provide data for diagnosis of diseases and examination of gene expression. The most favoured is fluorescence detection although the addition of fluorescent labels can be disadvantageous due to the complex and expensive labelling chemistry.

A novel method of oligonucleotide labelling was devised and surface enhanced resonance Raman scattering (SERRS) used as a detection technique. Single and dual labelled oligonucleotides were produced by first tagging the oligonucleotide with a furan or butadiene moiety at the 5' terminus to act as a diene in the subsequent Diels Alder cycloaddition with specifically designed SERRS active dienophiles. Four benzotriazole azo maleimide dyes were synthesised. Benzotriazole group is known to complex strongly to the silver metal surface, which is one of the requirements for SERRS. The maleimide group in turn serves as a dienophile to undergo the cycloaddition with the furan or butadiene modified oligonucleotide to generate a SERRS active probe. These probes gave excellent SERRS signals from both silver-polyvinyl alcohol (PVA) discs and silver colloid enabling the detection of ultra low concentrations of DNA.

Benzotriazole maleimide dye and fluorescein were used in the design of a novel class of biosensor, SERRS Beacons. In this type of molecular probe both SERRS and fluorescence were used as the detection techniques. The significant changes in the SERRS spectra of the Beacon indicated the presence of complementary sequence, while there were just slight changes when single base mismatch sequence was added. Both silver-PVA discs and silver colloid were used as SERRS surfaces, which demonstrated the flexibility of the SERRS Beacon to be used in different formats.

Low detection limits, simplicity of both the labelling chemistry and SERRS surface preparation, makes SERRS an excellent technique for oligonucleotide detection with the possibility of use in the rapidly growing DNA microarray and proteomic area.

Acknowledgements

First of all my sincere gratitude goes to my supervisors; Professor Smith for his endless enthusiasm, care and genuine interest in everything that was going on during my research and Dr. Graham for ideas, talks, encouragement and all the entertainment he provided when the things in lab got difficult.

My sincere thanks goes to Dr. Grondin who introduced me to the secrets of organic synthesis and unsuccessfully tried to convince me to learn French. I have to mention Gerry who made SERRS looking so easy and thank Rachel for talks, coffees and after lab discussions and Callum for allowing me to share his glassware and for discussing the beauties of dyes.

I would like to thank Dave for allowing me to sit in his office and complain and for using all of his phosphoramidites. I also want to thank all the members of the Graham group (Mark, Andrew, Leann, Alexis, Matt, Aaron, Dart and Strongbad) for creating entertaining work atmosphere. Thank you goes to all past and present Raman and Prof. Mulvey group members who gave entirely new meaning to lab sharing and made me feel good by eating my cakes.

Thank you goes to Dr. A. R. Kennedy for help with crystal structures and discussions, Professor A. Mills for sharing his knowledge on TiO_2 disc, Martin for help with substrate experiments, Shona Ross for excellent work on quenching and Dr. R. Martin for help with EMPA measurements.

Big thank you goes to Imran for badminton and sitting in the sun, Ian for all the talks, late evening SERRS, delicious turkeys and movies and Alison for all her help in the lab and outside.

Life during the PhD would have been much more difficult without all my friends both in Croatia and elsewhere. My special thanks goes to all of them for filling my days with funny e-mails and phone calls.

At the end, thank you goes to my dad, mum and Davorka for making the home feeling strong even when away and to Kai for the patience, support, delicious food and continuous struggle to put my articles in the right place.

Abbreviations

ABT	- aminobenzotriazole
AFM	- atomic force microscopy
ASV	- anodic stripping voltammetry
BHQ	- Black Hole quenchers
BOC	- *tert*-butoxycarbonyl
br	- broad
BT	- benzotriazole
CDF	- cold deposited film
CDI	- carbonyldiimidazole
CI	- chemical ionisation
CPG	- controlled pore glass
d	- doublet
DABCYL	- 4(4-dimethylaminophenylazo) benzoic acid
DCC	- 1,3-dicyclohexylcarbodiimide
DCM	- dichloromethane
DFT	- density functional theory
DIPEA	- diisopropylethylamine
DMA	- dimethylacetamide
DMF	- dimethylformamide
DMTr	- dimethoxytrityl
DNA	- deoxyribonucleic acid
dsDNA	- double stranded deoxyribonucleic acid
dT	- deoxytymidine
dUTP	- deoxyuridine triphosphate

EDANS	-5-(2-aminoethyl) aminonaphtalene-1-sulfonic acid
EI	- electron impact
EMPA	- electron microprobe analysis
FAB	- fast atom bombardment
FAM	- carboxyfluorescein
Fmoc	- 9-fluorenylmethoxycarbonyl
FRET	- fluorescence resonance energy transfer
FT	- Fourier transform
GCE	- glassy carbon electrode
HBTU	- O-(1H-benzotriazole-1yl)-N,N,N',N'-tetramethyluranium hexaflurophosphate
HEX	- 6-carboxy-2',4,4',5',7,7'-hexachlorofluorescein
HOBt	-1-hydroxybenzotriazole
HPLC	- high performance liquid chromatography
IR	- infrared
MALDI	- matrix assisted laser desorption
MMT	- monomethoxytrityl
m/z	- mass/charge ratio
NHS	- N- hydroxysuccinimide ester
PCR	- polymerase chain reaction
ppm	- parts per million
PVA	- polyvinyl alcohol
QD	- quantum dot
QPCR	- quantitative polymerase chain reaction

QSY7	- xanthylium, 9-[2-[[(2,5-dioxo-1-pyrrolidinyl)oxy]carbonyl]-1-piperidinyl]sulfonyl]phenyl]-3,6-bis(methylphenylamino)-chloride
RNA	- ribonucleic acid
RSD	- relative standard deviation
s	- singlet
SE	- secondary electron
SEM	- scanning electron microscopy
SERRS	- surface enhanced resonance Raman scattering
SNP	- single nucleotide polymorphism
SSB	- single strand (DNA) binding protein
t	- triplet
TAMRA	- tetramethylrhodamine
TEM	- transmission electron microscopy
TLC	- thin layer chromatography
UV	- ultraviolet

Contents

Page

Abstract…… iii
Acknowledgements…… iv
Abbreviations…… vi
Contents…… ix

Chapter 1: Introduction

1.1. General…….. 1
1.2. DNA Synthesis and Labelling…… 1
1.2.1. Synthesis of DNA…… 1
1.2.2. Automated solid phase synthesis of DNA……... 3
1.2.3. Labelling of DNA…… 5
1.2.3.a) Labelling using amino link……... 7
1.2.3.b) Labelling using a thiol linker……... 9
1.2.3.c) Direct coupling using label phosphoramidites or label CPG's……. 11
1) The 5' labelling…… 11
2) Internal labelling…… 13
3) The 3' labelling – use of CPG supports……. 14
1.2.3.d) Other labelling methods……... 16
1.3. DNA Microarrays……... 19
1.4. Polymerase chain reaction (PCR)……. 22
1.5. Molecular Beacons…….. 25
1.5.1. Introduction…….. 25
1.5.2. Design of molecular beacons and fluorescence quenching…….. 26
1.5.3. Application of molecular beacons……... 29
1.6. Surface Enhanced Resonance Raman Scattering (SERRS)…….. 33
1.6.1. Raman and Resonance Raman…….. 33
1.6.2. Surface Enhanced Raman and Resonance Raman Scattering…….. 34

Chapter 2: Synthesis and properties of benzotriazole dyes and dye maleimides

2.1. Introduction…… 40
2.2. Experimental…….. 40
2.3. Synthesis of benzotriazole dyes……. 41
2.4. Synthesis of dye maleimides from dyes…… 42
2.5. Synthesis of maleimide 1-(4-amino-phenyl)-pyrrole 2, 5-dione…. 48
2.6. Diels Alder cycloaddition…….. 52

Chapter 3: SERRS substrates

3.1. Introduction…… 55
3.2. Experimental…….. 56
3.3. Results and Discussion…….. 57
3.3.1. SERRS substrates…….. 57

3.3.2. Electron microprobe analysis of PVA-Ag discs…… 64

Chapter 4: Surface enhanced resonance Raman scattering of the benzotriazole dyes and dye maleimides

4.1. Introduction…….... 67
4.2. Experimental……. 67
4.3. Results and discussion…….. 68
4.3.1. UV/Vis and SERRS spectra of synthesised dyes…….. 68
4.3.2. Assignment of the SERRS spectra of BT dyes……. 72
4.3.3. The concentration study of BT dyes……. 77
4.3.4. Multiplexing by SERRS……... 80
4.3.4.a) Dye maleimides in the mixture…….. 80
*4.3.4. b) Dye maleimide **10** and Diels Alder cycloadducts in the mixture*…….. 83

Chapter 5: Oligonucleotide labelling and detection using Diels Alder cycloaddition and SERRS

5.1. Introduction……. 86
5.2. Experimental……... 87
5.3. Results and Discussion……...
5.3.1. Synthesis of modified oligonucleotides for Diels Alder cycloaddition…….. 88
5.3.1. a) Furan modification…….. 88
5.3.1. b) Butadiene modification…… 89
5.3.2. Labelling of diene modified oligonucleotides with SERRS active dyes…….….. 90
5.3.3. SERRS detection of the oligonucleotide cycloadduct……... 92
5.3.4. Oligonucleotide labelling with fluorophores……. 97

Chapter 6: Principle and design of SERRS Bacons

6.1. Introduction…….. 100
6.2. Experimental…… 100
6.3. Quenching potential of benzotriazole dyes…… 101
6.4. Fluorescence quenching of fluorescein labelled oligonucleotide……….. 104
6.5. SERRS Beacon……. 105
6.5.1. Design of SERRS Beacon…… 105
6.5.2. Detection of target DNA using silver colloid as a SERRS substrate……... 108
6.5.3. Detection of target DAN using PVA-Ag disc as a SERRS substrate…….. 115

Chapter 7: Conclusions……. 119

Chapter 8: Experimental data and procedures

8.1. Synthesis and properties of benzotriazole dyes and dye maleimides…… 122
8.1.1. General……. 122
8.1.2. Synthesis of benzotriazole dyes……. 122
8.1.3. Synthesis of the maleamic acids…….. 126

8.1.4. Synthesis of the dye maleimides from maleamic acid……..… 128
8.1.5.Synthesis of N-phenyl maleimides…….. 133
8.1.6. Diels Alder cycloaddition……. 140
8.2. SERRS substrates……. 142
8.2.1. General…….. 142
8.2.2. Silver colloid……. 142
8.2.3. Cold deposited films……. 143
8.2.4. Polyvinyl alcohol (PVA) substrates…….. 143
8.2.5. TiO2-silver discs……... 143
8.3. SERRS of dyes and dye maleimides…… 144
8.3.1. General……. 144
8.3.2. Molecular modelling and frequency calculations…… 144
8.4. Synthesis and labelling of modified oligonucleotides…… 145
8.4.1. General……. 145
8.4.2. Synthesis of furan modified oligonucleotides……... 146
8.4.3. Synthesis of butadiene modified oligonucleotide……. 147
8.4.4. Oligonucleotide deprotection and cleavage from solid support.. 147
8.4.5. Synthesis of oligonucleotide cycloadducts……..…. 147
8.4.6. HPLC purification of modified oligonucleotides……. 148
8.4.7. Desalting procedure after purification……. 148
8.4.8. Measurement of the concentration of the oligonucleotide stock solution……... 149
8.4.9. SERRS of the cycloadditon…….. 149
8.4.10. Fluorescence measurements of labelled oligonucleotides…… 149
8.5. SERRS Beacon…….. 150
8.5.1. General……. 150
8.5.2. Design and purification of SERRS Beacon……... 150
8.5.3. Hybridisation conditions…….. 151
8.5.4. SERRS measurements using silver colloid…… 151
8.5.5. SERRS measurements using PVA-silver discs…….. 151

References……. 152

Appendix…… 159

Chapter 1

Introduction

1.1. General

Modern DNA detection makes use of a number of techniques that are based on addition of the special labels to the DNA and their subsequent analysis. However, there is a constant search for new labelling and detection methods that will ease the chemistry involved and lower the detection limits. Surface enhanced resonance Raman scattering (SERRS) became a powerful technique throughout the last 15 years and it is now used in a wide number of analytical applications including the detection of DNA. Data presented in this thesis are the result of the work done to show the advantages of DNA detection by SERRS. The experiments performed indicate that there is potential for SERRS to be used not only in single and dual labelled DNA detection, but also in the DNA microarray field. *Chapter 1* gives a general overview of the most significant work done by a number of researchers in the area of DNA labelling and detection, including a short look at the microarray field. Dual labelled oligonucleotides are also discussed because of their growing significance and potential for genotyping and the identification of genetic diseases. A short overview of polymerase chain reaction (PCR) technique is given as an example of the practical use of labelled oligonucleotides. Finally, the last section describes, in brief, the theory of SERRS as well as a range of applications.

1. 2. DNA Synthesis and Labelling

1.2.1. Synthesis of DNA

DNA is a key molecule for the transfer of information in living organisms. Since the DNA model was described in 1953 (Fig. 1.1.)[1], the chemistry and biology behind nucleic acids has been of interest to many research groups. With the completion of the human genome sequence in 2003, the first chapter of the DNA book was closed.[2a,b] However, a huge number of questions are still to be answered. Although, 50 years after the discovery of the double helix, we understand the role of DNA better, the post genomic era focuses further on the link between the DNA structure, our genes and the proteins they encode.

The genetic information is encoded in the precise sequence of bases along each strand of DNA and when replication takes place, the complementary strand acts as a template. The flow of information in the cells, controlled by DNA, consists of

two basic steps; transcription and translation. In the transcription step, DNA serves as a template for RNA synthesis that in turn acts as a template for the protein synthesis in the subsequent process of translation.

When the importance of DNA was realised, scientists tried to synthesise DNA to investigate the link between its structure and the function of genes and the proteins that it encodes. Nowadays, synthetic oligonucleotides are one of the most powerful tools in biotechnology. They are used as probes in measuring gene expression in DNA arrays[3], as primers in polymerase chain reaction[4], antisense agents in therapeutic applications[5] and as molecular probes[6] for detecting unknown DNA and genetic mutations.

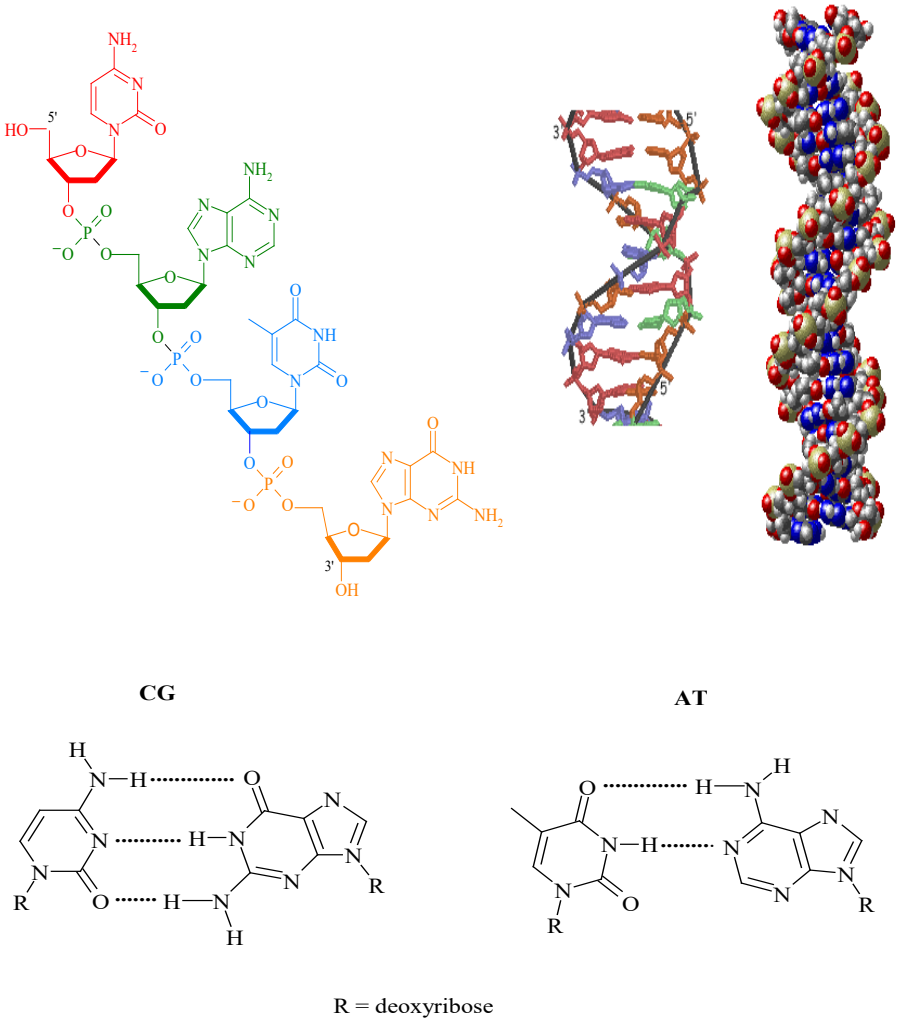

Figure 1.1. The basic structure of DNA and formation of the double helix by Watson Crick base pairing.

The successful solid phase synthesis of DNA used today is a product of the extensive research over the past 50 years and is a combination of the effective solid phase chemistry and phosphoramidite methodology first time used by Caruthers and Beaucage.[7] In their paper published in 1981 they describe the reaction of two modified nucleosides giving the product with a 3'-5' linkage in high yield.

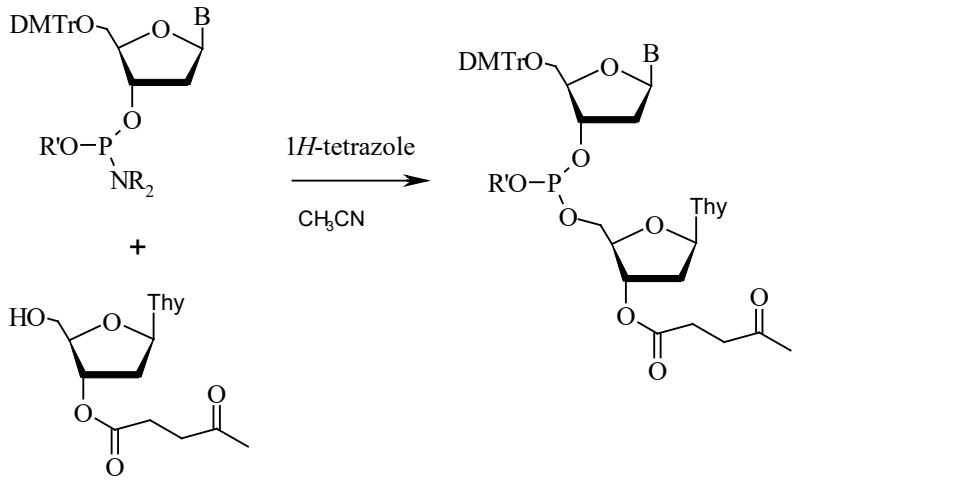

Figure 1.2. Formation of a 3'-5' internucleoside linkage by Caruthers and Beaucage.[7]

As a starting material they used protected thymidine phosphoramidite and reported that this type of nucleoside can be successfully used in the solid phase synthesis of dinucleoside phosphates. Significant credit for the development of phosphoramidite methodology also goes to Letsinger and Lunsfort who were the first to report that P (III) was considerably more reactive than the corresponding P (V) acylating agents[8] therefore providing the scientific base for the Caruthers and Beaucage (Fig. 1.2.) reaction and Koester *et al.*[9] for their work done with 2-cyanoethyl phosphoramidites which are used in solid phase oligonucleotide synthesis.

1.2.2. Automated solid phase synthesis of DNA

To ensure the formation of a specific 3'-5' linkage between two deoxynucloside units, all reaction centers not involved in the linkage must be protected.[10] Protected deoxynucleosides are then added to a CPG (controlled pore glass) support (Fig 1.3):

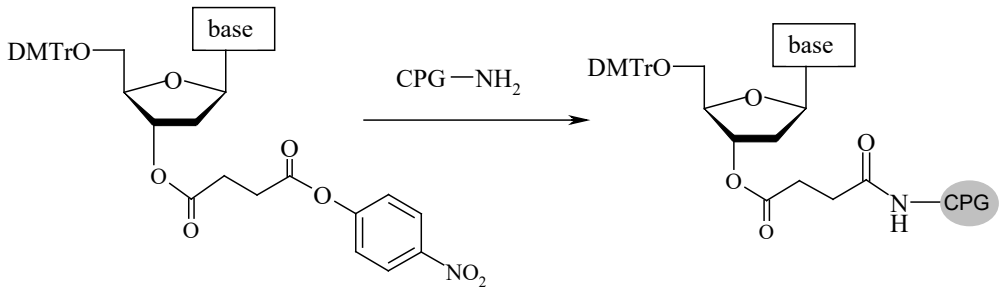

Figure 1.3. The addition of protected nucleosides to CPG.

When added to CPG, the 5'- hydroxyl is deprotected by treatment with $CHCl_2COOH$ to remove the DMTr group. The deprotected deoxynucleoside is then coupled with the protected deoxynucleoside containing a phosphoramidite group at the 3' alcohol. The phosphite product (P^{III}), which is very reactive, is oxidised to the phosphate triester by treatment with iodine and water (Fig 1.4).

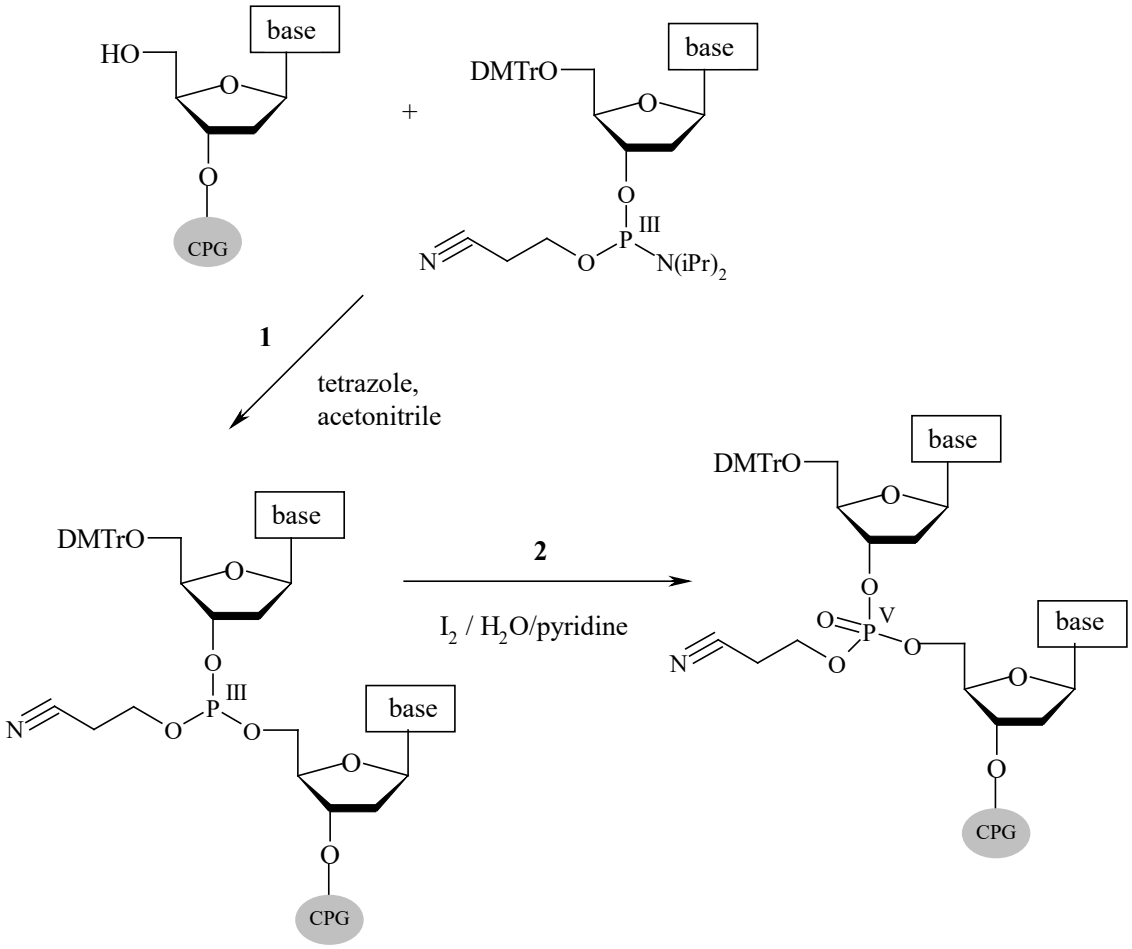

Figure 1.4. Principle of solid phase synthesis. **1**) Coupling of the CPG deoxynucleoside with deoxynucleoside phosphoramidite, **2**) oxidation of the phosphate product to the phosphate triester.

The desired sequence is built by adding the bases step by step using the same procedure in each cycle. The final step involves the cleavage of all protecting groups and the ester bond, holding the DNA onto the CPG, by treatment with ammonia.

DNA does not have intrinsic properties that allow direct, highly sensitive detection by a range of analytical methods. Therefore, it is necessary to make DNA detectable using non-covalent or covalent labelling methods. Non-covalent labelling includes stains (ethidium bromide) or intercalator dyes (SybrGreen) that enable detection and quantification of DNA in solution[11], immobilised in gels[12] or blotted on membranes[13]. However, they do not provide any specific information about the sequence nor discrimination between different sequences present in the same solution. To enable the detection of specific DNA it is necessary to label it covalently by introduction of functional groups that ease the subsequent detection.

1.2.3. Labelling of DNA

The desired characteristics of the label are its sensitivity, ease of detection, stability and the overall low cost of the label and its detection technique. There is a range of methods available for DNA detection, but fluorescence[14] and radioactive label detection[15] are most widely used. Although less sensitive, fluorescent dyes (Fig. 1.5) offer some advantages over radioactive labelling. One of the most important is the absence of radiation hazard and all related problems of waste handling and disposal. Moreover, several fluorescent dyes can be monitored in the same experiment and be detected in real time with high resolution.

Although fluorescence is a widely used method for DNA detection, especially in micorarrays, there are some disadvantages. Fluorescence is quantitative and highly sensitive and can be used to distinguish between labelled DNA strands. However, fluorescent dyes are difficult to synthesise and manufacture which makes them very expensive. Labelled strands also require the separation from the excess dye prior to analysis due to the overlapping fluorescence emission profiles. Moreover, some dyes are found to impair the biologically activity of DNA therefore effecting its analysis.[16]

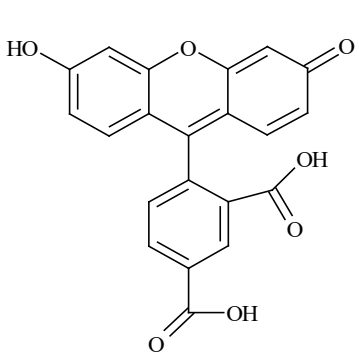

carboxyfluorescein (FAM)

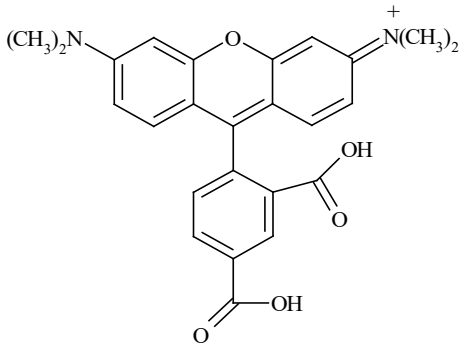

carboxytetramethylrhodamine (TAMRA

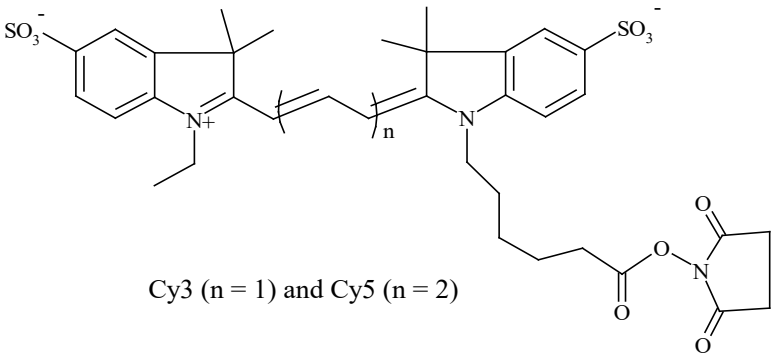

Cy3 (n = 1) and Cy5 (n = 2)

Figure 1.5. Some of the commonly used fluorophores.

Apart from fluorescent dyes, fluorescent inorganic microparticle labels called quantum dots have been developed.[17] Quantum dots (QD) have shell core construction, comprising of an outer shell of zinc sulphide surrounding the core containing a semiconductor material. Core composition and particle size determine the wavelength of emitted light. Highly luminescent CdSe QD's are extensively used as non radioactive labels.[18a,b] They are small, stable under a range of conditions, produce intense signals and have a potential for multicolour detection. However, the disadvantage still remains in the preparation of QD's as well as their insolubility in polar solvents due to the organic coating on the surface, but future research might offer the solutions to these problems.

Recently, Fang *et al*. described a new method of DNA detection.[19] They used anodic stripping voltammetry (ASV) to follow the hybridisation of a DNA probe labelled with the silver nanoparticle to a target DNA immobilized on a glassy carbon electrode (GCE). When a double strand is formed, silver nanoparticles linked to the double strands formed on the GCE surface are dissolved and the quantity of Ag(I)

ions measured. The target DNA was detected in pmol/dm^3 concentration and the electrochemical device designed is simple, compact and inexpensive. However, the lengthy preparation of immobilised GCE and labelled DNA still does not make it commercially viable. Other electrochemical DNA biosensors were also reported, all relying on the conversion of the hybridisation event into useful electrical signals.

All mentioned techniques require the attachment of a label to the oligo and the labels of interest are attached directly to the DNA probe during or immediately after automated solid phase synthesis.

The special labels that can be incorporated into DNA *in vivo* were also developed and they involve nucleotide modifications.[20] One of the most widely used *in vivo* labelling procedures involves the modification of deoxyuridine. In the study by Cook *at al.* dUTP labelled with fluorescent Cy5 dye was used as a thymidine triphosphate analogue for *in vivo* labelling of DNA to enable direct imaging of DNA in living cells.[21] Although the results of *in vivo* labelling are encouraging, the chemical synthesis of nucleoside triphosphates is complex and the determination of the right conditions for enzymatic reaction is a lengthy process. Therefore, preferred labelling methods used in laboratories around the world involve the incorporation of the labels by chemical means. The most commonly used methods are described below.

1.2.3 a) Labelling using amino link

Labelling of oligonucleotides through an amino link is a widely used post-synthetic approach. An alkyl amino phosphoramidite (Fig. 1.6) is routinely used in automated synthesis to introduce the primary amino group at the 5' end.[22] If label has to be attached at some other position of the DNA, internally or at the 3', nucleosides with an amino containing arm[23] or amino controlled pore glass[24] (CPG) can be also used respectively.

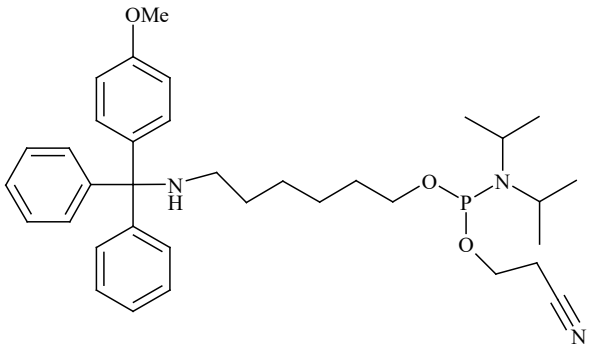

Figure 1.6. Commercially available MMT-5'-C6 amino linker.

The most common way of introducing a label to an amino linked oligonucleotide was by using the appropriate isothiocyanates (Fig. 1.7.).[25]

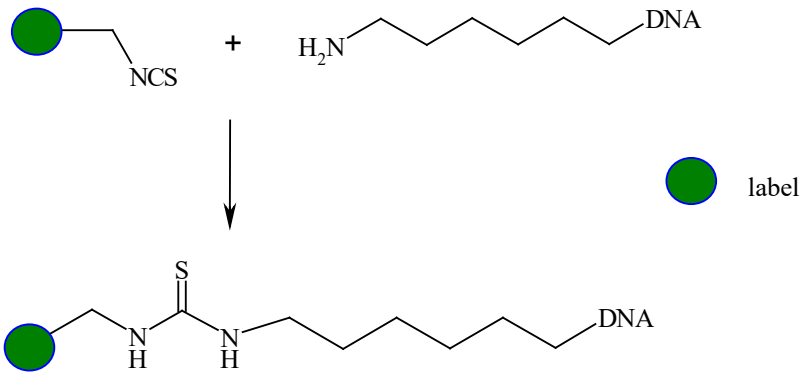

Figure 1.7. Labelling of amino linked oligonucleotide with an isothiocyanate label.

However, the problem with many isothiocyantes, especially fluorophore isothiocyanates is their instability. Banks *et al*. investigated the stability of the fluorescein isothiocyanate – lysine conjugate and showed that there is significant hydrolysis of the thiourea bond, especcially if the tempreature is increased above 37ºC. [26]

Another method, more favored, is use of an active ester, mainly a succinimidyl ester, which can be added to an amino linked oligonucleotide probe either in solution or on the solid phase (Fig. 1.8.). [27]

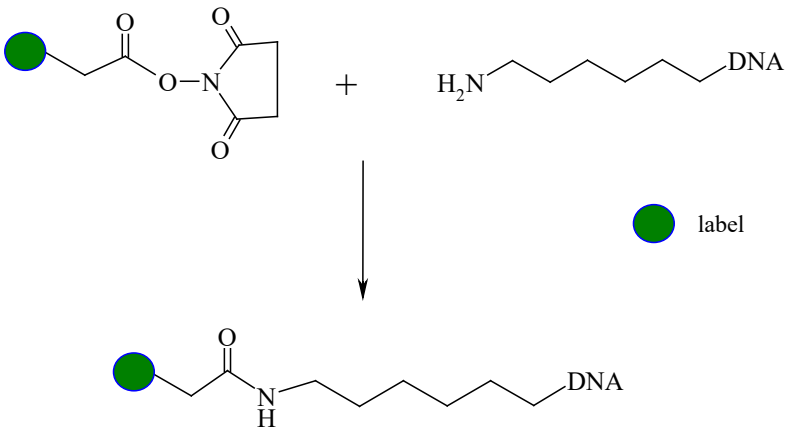

Figure 1.8. Labeling of amino linked oligonucleotide with a succinimidyl label.

Although this method is popular, the disadvantage is the hydrolysis of the succinimidyl ester moiety that can happen in the coupling reaction where aqueous conditions are required. Moreover, the succinimidyl ester of some dyes like rhodamine tends to decompose upon prolonged storage. To avoid this happening with rhodamine dye, which is particularly useful in DNA labelling, Vinyak developed a milder *in situ* procedure for the activation of the dye.[28] This involved activation of rhodamine carboxylic acid with HBTU and DIPEA and coupling to an amino linked oligonucleotide to achieve more than 85% coupling efficiency.

.

1.2.3.b) Labelling using a thiol linker

A thiol linker can be introduced to the different positions of an oligonucleotide allowing the maleimide derivative of different labels to undergo Michael addition (Figure 1.9).

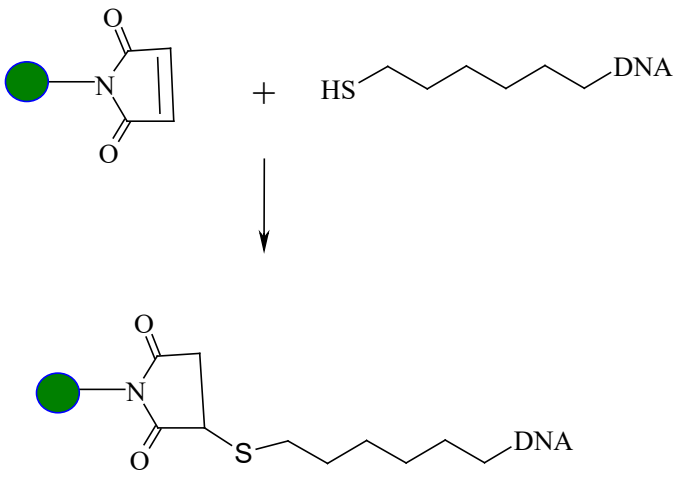

Figure 1.9. Michael addition of thiolated DNA to a label maleimide.

A range of fluorophore maleimides is commercially available and used in fluorescence detection. Thiol linked DNA is also widely used for surface attachment of DNA to the maleimide modified glass surfaces for production of DNA microarrays.[29a,b] Moreover, a new group of nanobiosensors was developed recently by labelling thiolated oligonucleotides with gold nanoparticles. Mirkin *et al*. developed heterogeneous colorimetric oligonucleotide detection system based on gold particles modified with alkylthiol oligonucleotides.[30a,b] In this system, dispersed oligonucleotide-modified gold nanoparticles were assembled into aggregated networks *via* hybridisation with the complementary target oligonucleotide. This process caused a change in colour thus enabling the detection of the hybridisation event. As mentioned earlier, one more group of labels, quantum dots (QD), has a growing significance. QD's are added to the oligonucleotide *via* a thiol linker. Mirkin *et al.* also succeeded in labelling thiol linked DNA probe with CdSe QD and determining the change in fluorescence upon the addition of the complementary strand.[18b] Thus, a thiol linker is used in DNA labelling with range of different labels (nanoparticles, fluorophores, QD's, fluorescent proteins[31]) and in their attachment to different surfaces (CPG, silica nanoparticles, paramagnetic beads). However, the main problem is still the rapid oxidation of the thiol to the disulphide.

1.2.3 c) Direct coupling using label phosphoramidites or label CPG's

1) The 5' end labelling

A phosphoramidite of the desired label (Fig. 1.10) can be sometimes synthesized and used in solid phase synthesis of oligonucleotides.

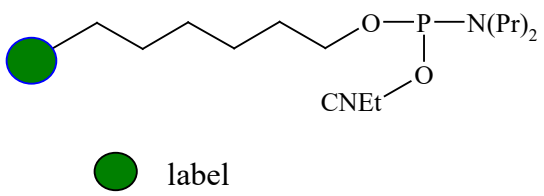

Figure 1.10. Phosphoramidite of the fluorescent labels.

Fluorescein phosphoamidite is a widely used fluorophore for 5' labelling. Therefore it is not surprising that there is a number of papers investigating different routes to fluorescein phosphoramidite synthesis. Nelson *et al*. reported the preparation of a fluorescein thioisocyanate based, 2-aminobutyl-1,3-propendiol linked prhosphoramidite.[32] Thiesen *et al*. were the first to synthesis FAM (5-carboxy fluorescein) phosphoramidite and used it in the solid phase synthesis of oligonucleotides.[33] They reacted NHS ester of 5-carboxyfluorescein with amine derivative prepared from solketal and resulting amide was then converted to the phosphoramidite by phosphitylation. The coupling of this phosphoramidite to the 5'-hydroxyl of the support bound oligonucleotides proceeded in 70% yield. 5- and 6-Carboxyfluorescein phosphoramidites are today commercially available from range of companies.

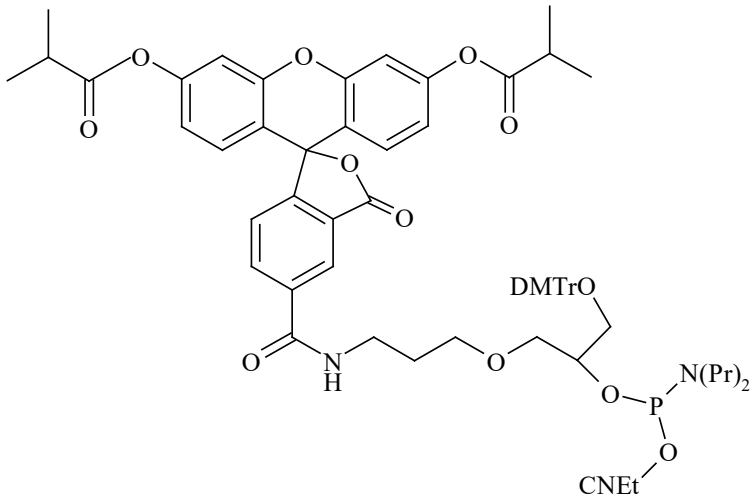

Figure 1.11. FAM phosphoramidite as prepared by Theisen *et al.*[33]

Recently Adamczyk and his research group additionally simplified fluorescein phosphoamidite synthesis. [34] They used the 5-hydroxymethyl fluorescein, which is an intermediate in the synthesis of 5–aminofluorescein, to make a monofunctional phosphoramidite (Fig. 1.12) for the 5' labelling in one step.

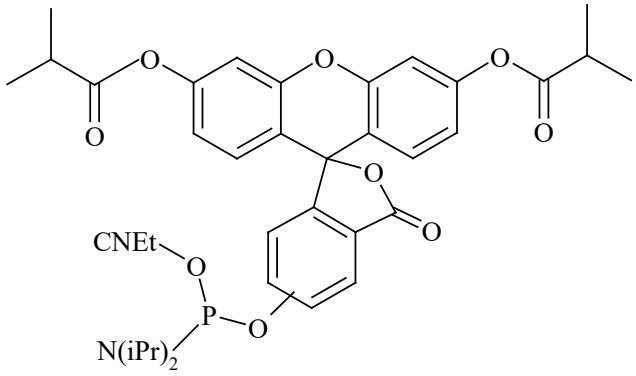

Figure 1.12. FAM phosphoramidite prepared by Adamczyk *et al.*[34]

A short linker between the fluorescein nucleus and the reactive phosphoramidite group did not have any effect on the oligonucleotide synthesis. Although they report high yields of phosphitylation and subsequent oligonucleotide synthesis, the preparation of the starting material takes 3 steps, of which the reduction of activated carboxyfluorescein to hydroxylfluorescein is the most important but least successful.

Rhodamine phosphoramidites were synthesised a few years after their fluorescein analogues due to the stability problems and complex chemistry exhibited by the rhodamine dyes. Lyttle *et al*. investigated the differences in rhodamine dye forms resulted from the disposition of the 3-carboxylate and succeeded in the synthesis of tetramethylrhodamine (TAMRA) phosphoramidite (Fig 1.13.). [35]

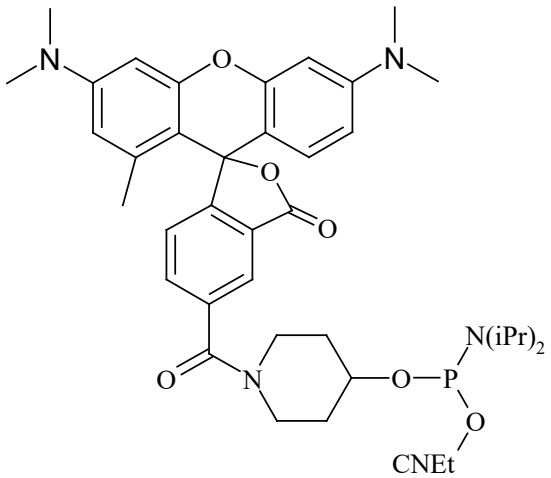

Figure 1.13. TAMRA phosphoramidite as synthesised by Lyttle *et al*.[35]

The coupling efficiencies in the DNA synthesiser were estimated at 90%, which is reasonably good taking into account the sensitivity of rhodamine dyes to coupling conditions.

The phosphoramidites of a number of other dyes are commercially available although very expensive. The synthesis of fluorescent phosphoamidites is difficult, usually requiring 4 or more steps, the yields are low and extensive purification is required. Moreover, phosphoramidites of some important fluorophores are difficult to prepare or not sufficiently stable.

2) Internal labelling

Internal labelling is even more complex than 5' labelling. It involves derivatisation of a nucleoside phosphoramidite with the label itself or the functional groups which can undergo subsequent reaction with the label. Hagmar *et al.*[23] synthesised an aminouridine phosphoramidite possessing a short alkylamino side arm which was used to react with fluorescein isothiocyanate. The yields for 1 μmol

synthesis of oligonucleotides containing the modified uridine base were about 50%. The other, improved approaches include the use of nucleotide phosphoramidite (dT is commonly used) derivatised with labels (Fig 1.14), which are commercially available (Glen Research)[36] but at considerable cost.

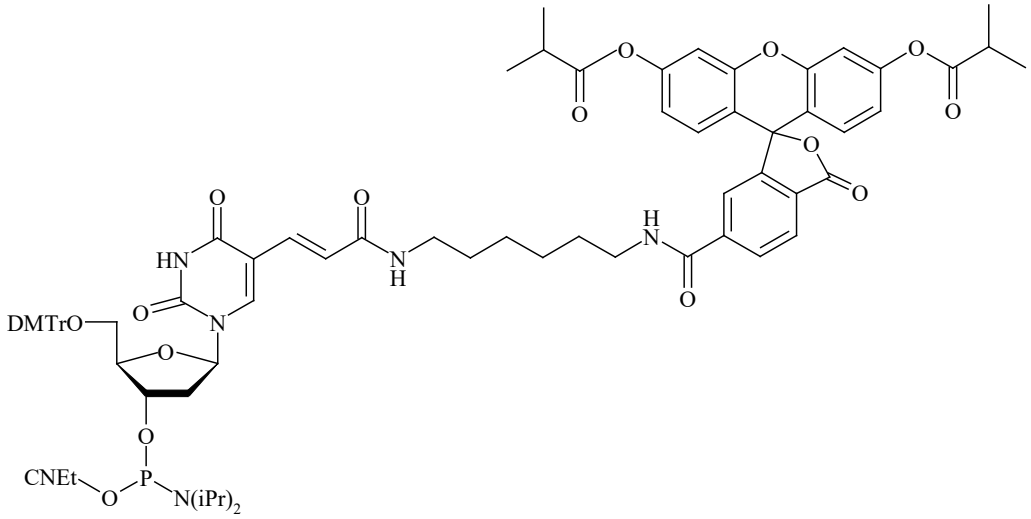

Figure 1.14. Fluorescein dT for internal labelling available from Glen Research. [36]

3) The 3' labelling – use of CPG supports

When 3' labelling of the oligonucleotide is required, different types of CPG supports are used. Lyttle *et al*. prepared CPG containing 3' terminal phosphodiesters modified with linkers bearing either an amine, thiol or hydroxy group (Fig.1.15). [24]

These CPG supports can be used in the solid phase synthesis and the desired label added to the synthesised oligonucleotides after cleavage from the support.

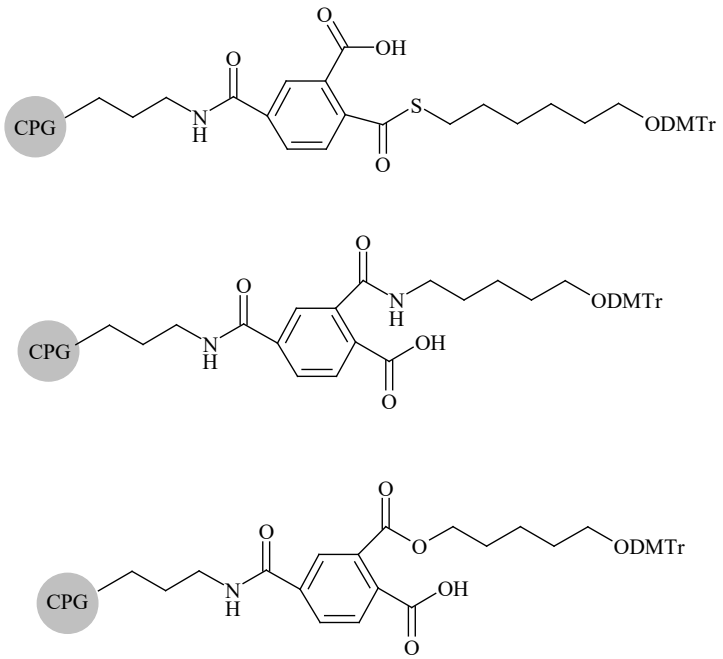

Figure 1.15. CPG supports for oligonucleotide synthesis prepared by Lyttle.[24]

Mullah and Andrus derivatised a CPG support with TAMRA (Fig. 1.16) and used it in DNA synthesis. [37]

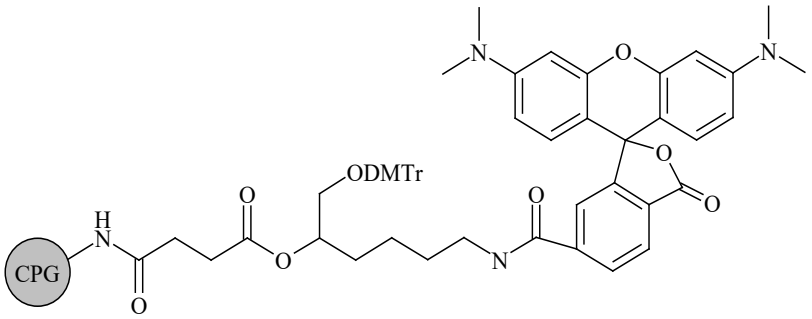

Figure 1.16. TAMRA CPG.

They also investigated the conditions for cleavage of the rhodamine oligonucleotide from the solid support because of the rhodamine sensitivity towards the standard cleavage procedure using ammonia.

A range of CPG supports with different fluorophores and other labels like biotin are commercially available. However, a problem encountered with CPG is the sensitivity of labels to the cleavage conditions limiting the number of available CPG supports to the most stable fluorophores (FAM, TAMRA).

Although the use of direct coupling of labels through label phosphoramidites or CPG supports has the advantage of being a fast way of making labelled oligos, the reagents are expensive and often very sensitive to both the standard conditions of coupling in DNA synthesis and cleaveage from the solid support leading to lower yields. Therefore their use is limited and there is a constant search for new labelling methods.

1.2.3. d) Other labelling methods

There are many other methods for fluorescent labelling of DNA that utilise different chemical methodologies to achieve the goal. Dey and Sheppard synthesised nucleoside phosphoramidite with a ketone arm on the C-5 of uridine and then used it in solid phase synthesis to make a 17mer oligonucleotide.[38] The ketone – DNA was then selectively modified with different aminooxy derivatives (glucose and biotin) (Fig. 1.17.) under physiological conditions.

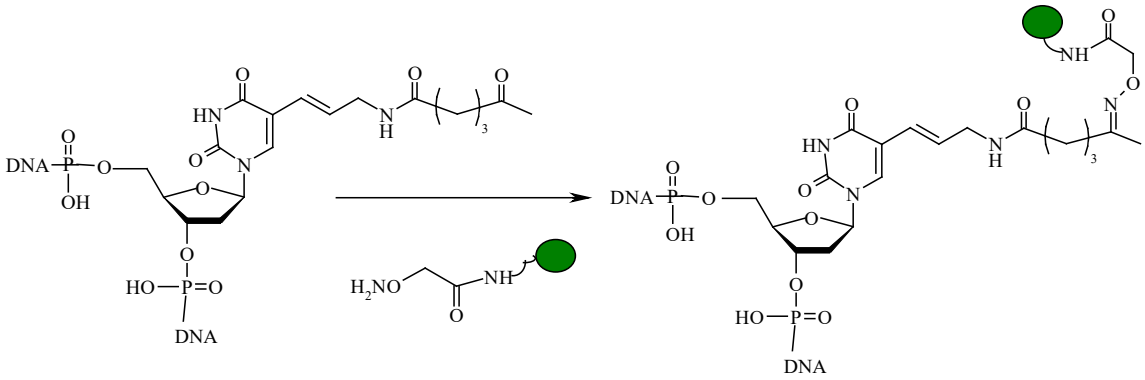

Figure 1.17. Labelling *via* ketone DNA.[38]

However, although the oligonucleotide was successfully labelled without any side products, the procedure is time consuming. It takes 24 h at 37°C for the reaction to be completed. Moreover, the synthesis of the ketone phosphoramidite required several steps, involving low yielding transformations.

The research group of J. Ju used “click chemistry” to construct a fluorescent oligonucleotide.[39] They used the coupling between azides and alkynes as the labelling method. However, they still used amino linked DNA to make an azide and commercially available fluorescein NHS ester to make alkynyl-6-carboxyfluorescein therefore not cutting the time nor effort significantly. Moreover, the “click reaction”

was carried out at 80°C, which is too harsh for some labels and it took 72 h to reach completion.

Brown *et al*. recently reported the use of Fmoc protected alkyl alcohol modified tymidine phosphoramidite.[40] Such phosphoramidite was incorporated into an oligonucleotide during routine automated solid phase synthesis, Fmoc group removed and the hydroxyl group coupled with commercially available dye phosphoramidite (Fig. 1.18.).

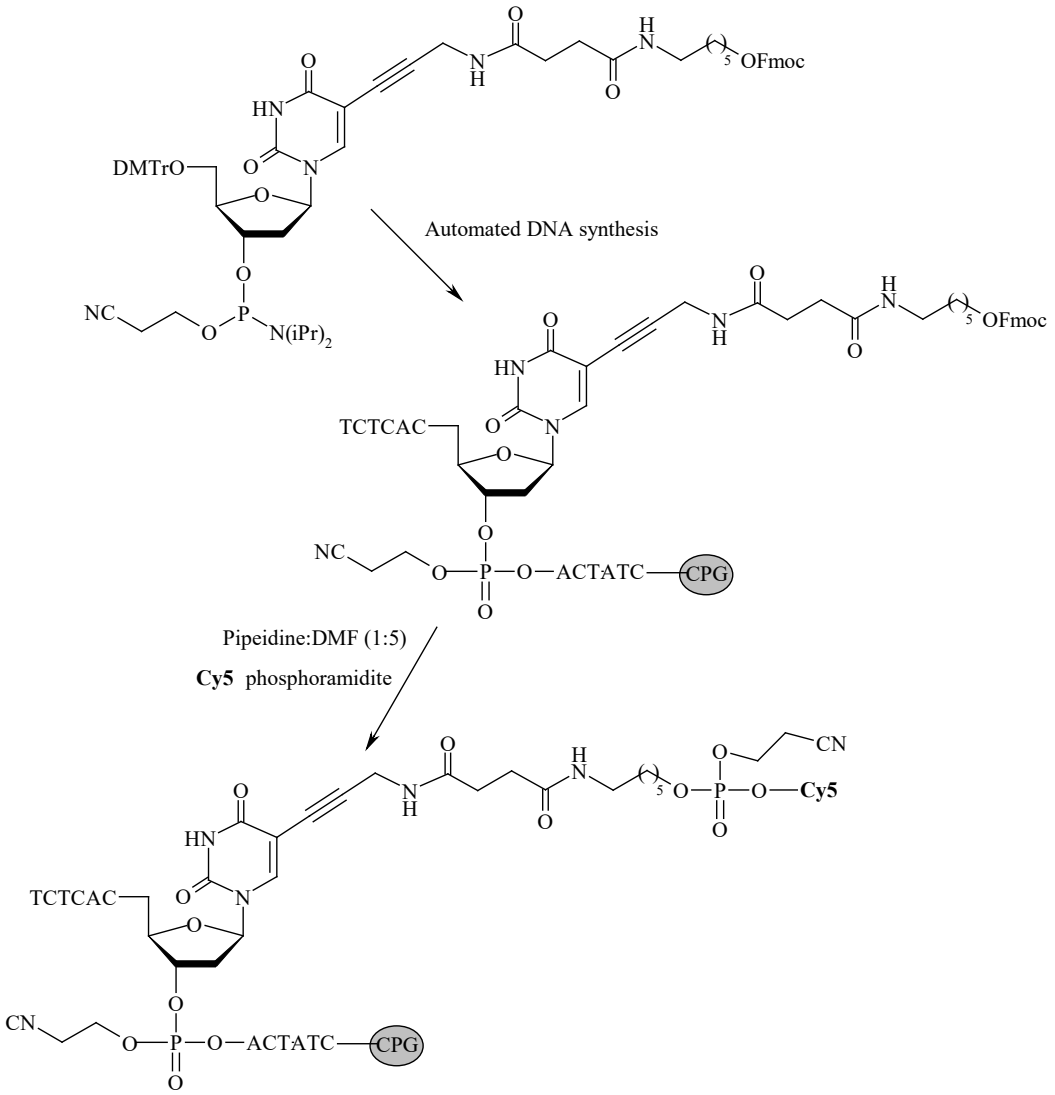

Figure 1.18. Modified tymidine phosphoramidite and its use in oligonucleotide synthesis as reported by Brown *et al*.[40]

This method was particularly useful for addition of Cy5 dye to oligonucleotides. Commercially available Cy5 monomer, when added internally to an oligonucleotide, causes destabilisation of the duplex. However, destabilisation was significantly

reduced by the use of modified tymidine and subsequent addition of Cy5 phosphoramidite.

Although there are many methods available for DNA labelling (as shown previously) there is still a need for faster, more effective and less expensive chemistry. The DNA microarray technology is developing rapidly and there is a need for fast screening of a large number of oligos, which requires sensitive detection techniques and simple labelling chemistry. The use of microarrays has revolutionised biotechnology and the DNA research and technology is now being applied to proteomics and drug testing. Microarrays are often referred to as “lab on the chip” since immobilised molecules retain the ability to undergo various reactions. DNA arrays were first introduced about 7 years ago, but the technology has developed and there are now three basic types: DNA, protein and chemical microarrays. A short overview of the DNA microarrays development and the chemistry and technology used in their production is given in the next section.

1.3. DNA Microarrays

The human genome project contributed to a significant progress in the creation of gene maps and the identification of genetic diseases. The vast amount of DNA information retrieved can be used further for complex genotyping and the screening of genetic illnesses. Microarray technology enables the quantification of thousands of DNA or RNA sequences in a single assay. A DNA array typically consists of thousands of immobilised DNA sequences, which are then hybridised to their complementary sequences and are usually radio or fluorescently labelled to enable the detection (Fig 1.19.).

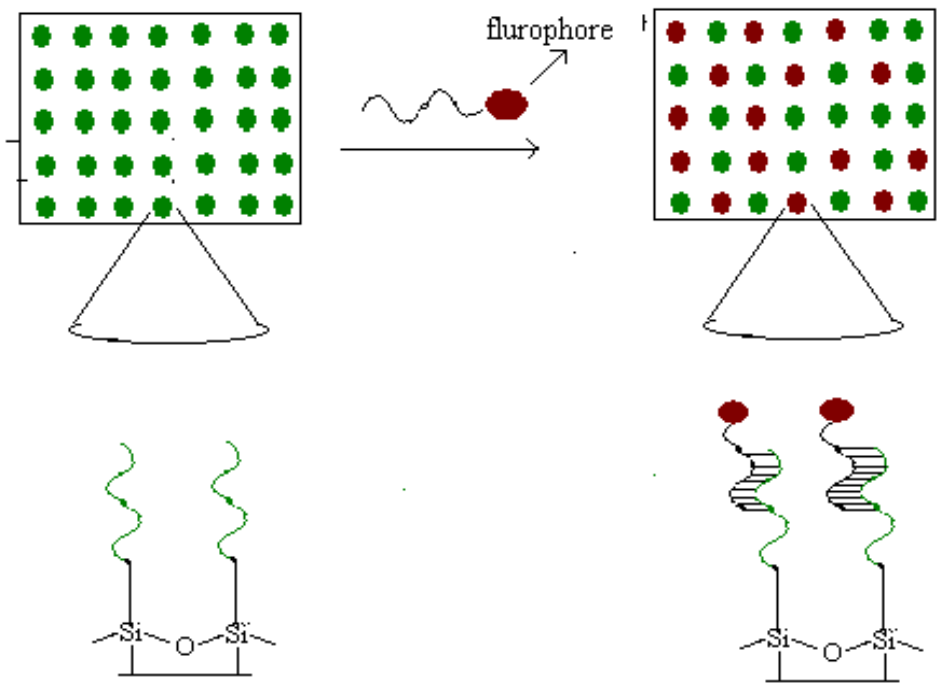

Figure 1.19. Principle of DNA microarray.

Shi defines arrays as a medium for matching known and unknown DNA samples based on base pairing rules and the automation of the process of identifying the unknowns.[41]

From the time microarrrays started to make their way into science and industry seven years ago, they have developed rapidly. There are two basic methods for their

manufacture. The first approach involves *in situ* synthesis of oligonucleotides using modified nucleotide phosphoramidites with a photo labile protecting group and photolithography.[42] In this approach, the oligonucleotide is synthesised directly on the surface of the chip. Lemieux reported that this method allows approximately 250 000 features per cm^2 for 20mer oligonucleotides.[43] The second method of array manufacture is spotting, which is widely used in industry as well as in research. Spotting actually means printing oligonucleotides onto the glass support using direct touch ink jet printing or fine pippetting. Glass surfaces are prepared to contain aminosilane layers on the glass slides or silicon wafers. Heterobifunctional linkers usually having the maleimide functional group are then linked to the surface amino groups allowing subsequent attachment of the thiolated DNA. Won Pak *et al.* recently investigated chemical homogeneity, surface roughness, density and spacing between surface functional moieties of these surfaces.[44] They also showed the importance of the density of the surface functional groups in the detection of DNA targets.

One limit of the microarrays is the length of the oligonucleotides which can be spotted onto the certain area. Most effective was synthesis of the 10-30 nucleotides sequence. However, Hughes *et al.* used microarrays based on *in situ* ink jet oligonucleotide synthesis to evaluate the effects of probe length.[45] They proved that oligonucleotides up to 60 nucleotides long could be used to monitor expression levels of a gene.

As mentioned previously, microarrays provide a rapid and cost-effective method of genotyping, facilitating the diagnosis of disease by identification of gene mutation. Dhanasekaran used the technique to obtain prognostic markers for prostate cancer.[46] Chee *et al.* simultaneously analysed the entire human mitochondrial genome producing a DNA array containing up to 135 000 probes complementary to mitochondrial DNAs.[47] In an extensive study, Shoemaker *et al.* succeeded in experimental annotation of the human genome using microarray technology.[48] They managed to validate exons and group them into genes. The method involved fabrication of ‘exon arrays’ consisting of long (50-60 bases) oligonucleotide probes derived from predicted exons followed by hybridisation with fluorescently labelled cDNAs derived for specific cell lines using normal or diseased tissues.

Microarrays can also be useful in pharmacology, particularly for drug selection and the prediction of drug or toxin activity. The abnormal expression of genes involved in drug metabolism of a patient can be compared in a high throughout manner with the expression of the genes from a control and ease the understanding of the complex biochemical pathways. Recently, Church *et al*. investigated the DNA sequence specific recognition by zinc finger proteins using DNA arrays.[49] It was one of the first studies of DNA protein interactions, which enabled quantitative mapping of the regulatory pathways within cells. They used a custom built arraying robot equipped with piezoelectric print heads to print the set of 64 oligonucleotides onto modified glass surfaces. Then they monitored their interaction with fluoroscently labelled zinc fingers by fluorescence screening.

DNA microarrays are now a powerful technique used widely in molecular biology, genetics, pharmacology. The principle of arrays is simple; technology to produce them is developing rapidly. However, there are still problems to be addressed and solved. One of them is finding the right technique of detection or visualisation of processes occurring on the chip. Fluorescence is the most widely used technique. However, labels are bulky and sometimes impair the biological activity of the probe. The array technology will have to improve in the direction of reducing the manufacturing cost and increase the throughput by reduction of the quantity of the DNA spotted. Moreover, the novel screening techniques could offer greater reproducibility, quantification of the result and cut the time necessary to prepare labelled oligonucleotides. Therefore the search for detection techniques continues. One candidate is surface enhanced resonance Raman scattering (SERRS), which can overcome the problems of visualization and determination of the interaction between molecules and is discussed in more detail later. First, one more example of the use of labelled DNA will be discussed in the following section that gives a short overview of the polymerase chain reaction.

1.4. Polymerase chain reaction (PCR)

Quantitative polymerase chain reaction (Q PCR) involves both amplification and analysis of a specific fraction of DNA with no need for additional sample manipulation.[50a,b] The method uses a pair of synthetic oligonucleotides as forward and reverse primers, each hybridising to one strand of a double stranded DNA (ds DNA) target. The hybridised primer acts as a substrate for a Taq DNA polymerase enzyme (source of which is the thermophilic bacterium *Thermus aquaticus* and therefore the name Taq), which creates a complementary strand *via* sequential addition of deoxynucleotides (Fig. 1.20).

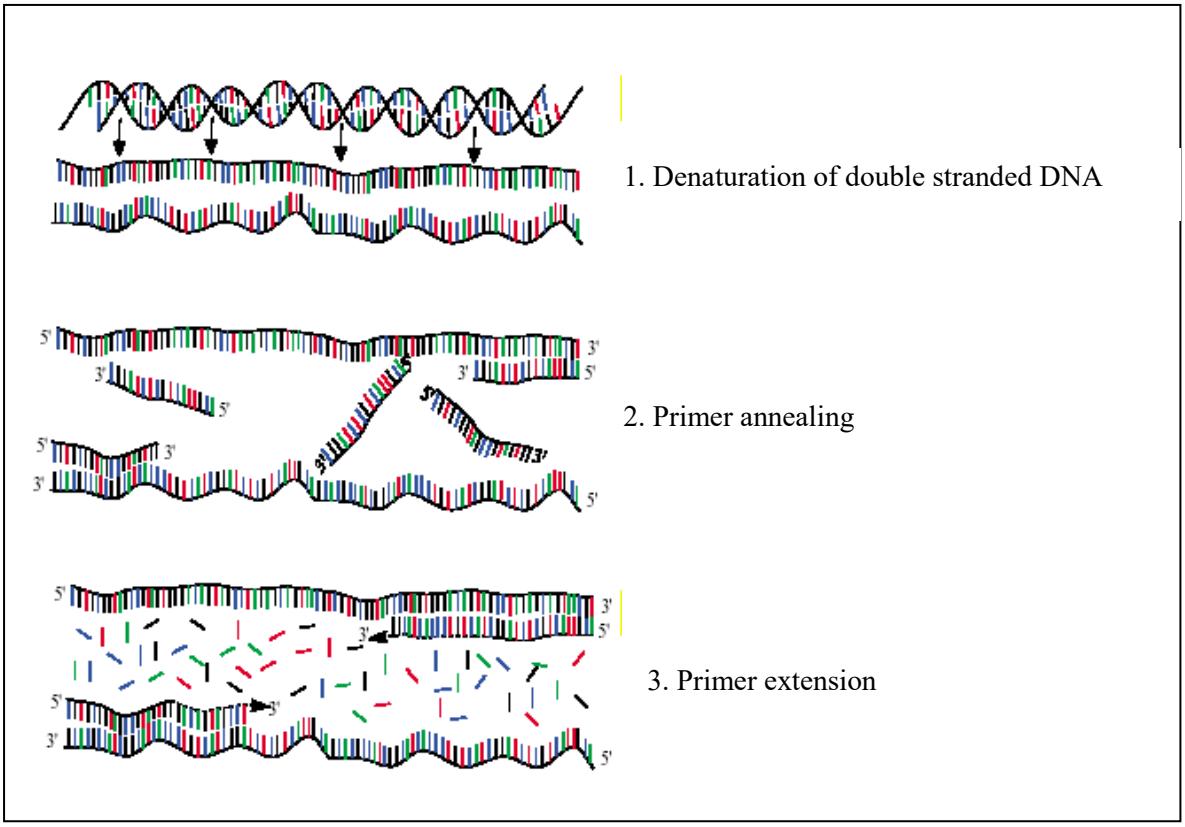

Figure 1.20. The principle of PCR.

As shown in the Fig. 1.20., the PCR process can be summarised in three steps:

1) denaturation of ds DNA at temperatures higher than 90°C

2) primer annealing at 50 - 75°C

and 3) primer extension at 72-78 °C

Detection of the PCR amplified DNA was originally based on the use of non-specific detection methods. These included post –amplification staining with ethidium bromide or use of intercalator dyes which bind to the double stranded DNA. However, the main drawback of these methods is that both specific and non specific products generate signal leading often to the false reads and misinterpretation of the results.[51]

The PCR system was improved by introducing specially designed oligonucleotide probes enabling the detection in real time and in a closed tube format, completely eliminating post amplification manipulation of the sample.

In 1991., Holland *et. al.* described the use of fluorogenic oligonuclotide probes in homogenous PCR.[52] In their experiment the amplified sequences (amplicon) were detected by monitoring the effect of Taq DNA polymerase's 5'→3' endonuclease activity on specific oligoprobe/target DNA duplexes. Lee *at al*. used this concept and introduced TaqMan probes in 1993 (Fig. 1.21.).[53] A TaqMan probe containing a reporter and quencher dye is designed to anneal between the forward and reverse PCR priming sites. During PCR, the probe anneals to the specific sequence location with high specificity and is subsequently cleaved by the endonuclease activity of the Taq DNA polymerase. When the probe is cleaved, the reporter dye is displaced and separated from the quencher dye which results in the increase of the fluorescence signal.

The fluorescence data collected indicated the extent of amplification. Since this type of assay involved measuring fluorescence without opening PCR tubes, the risk of carry over contamination was reduced. Furthermore, this type of assay is not labour intensive and is easily automated. However, when single nucleotide polymorphisms (SNP) have to be detected, TaqMan probes can assay only one to three SNP at the time.[54]

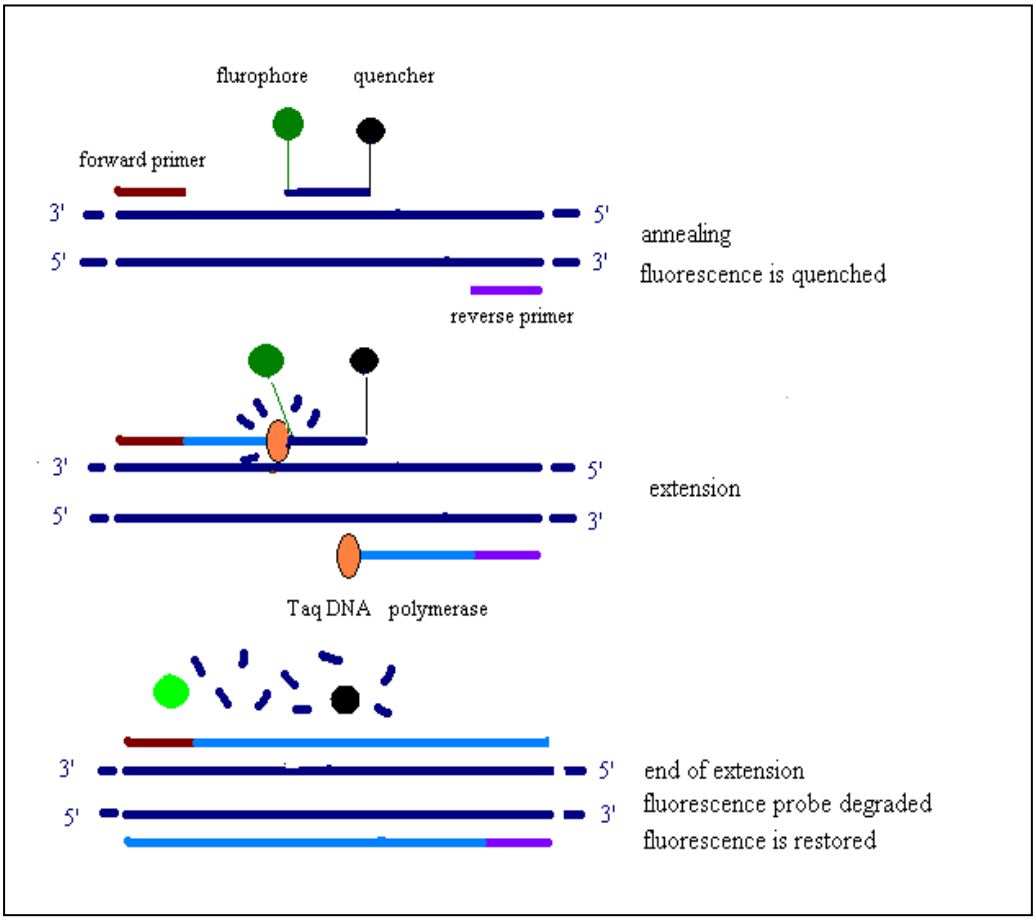

Figure 1.21. The principle of TaqMan. First step is annealing of forward and reverse primer sequences and TaqMan probe containing reporter and quencher dye. Second step is extension of DNA sequences using TaqDNA polymerase. During extension the TaqMan probe is cleaved by the endonuclease activity of the Taq DNA polymerase. This leads to the displacement of the reporter dye and its separation from a quenching dye, which results in the increase of the fluorescence signal.

The additional improvement of Q PCR amplicon detection came with the development of haripin oligonucleotides, molecular beacons (described in more detail in the following section). Amplifluor hairpin pimers[55] and Scorpion probes [56a,b] were also designed based on the molecular beacon concept. All of these probes provided higher specificity in SNP detection and, more importantly, enabled mulitplexing. The most widely used and simplest in design of these probes are molecular beacons where the simple concept proved highly effective in the detection of genetic polymorphisms and identification of genetic diseases.

1.5. Molecular Beacons

1.5.1. Introduction

First described by Tyagi and Kramer in 1996, molecular beacons are oligonucleotide probes with a fluorophore at one end and a fluorescence quencher at the other (Fig. 1.22.).[57] In solution, they form a hairpin structure which brings the fluorophore and quencher close together and causes a large or complete decrease of fluorescence signal through fluorescence resonance energy transfer (FRET) or static quenching. The probes are designed in such a way that the loop part of probe is complementary to the target nucleic acid and annealing of complementary sequences on the opposite ends forms the stem. In practice, stems of 5-6 bases and probe sequences of 16-22 bases are most commonly used and can be changed depending on the G/C and A/T content of the target.

When the target sequence is present, hybridisation occurs and the molecular beacon undergoes a spontaneous conformational reorganisation that forces the stem apart and causes the fluorophore and quencher to move away from each other, leading to the restoration of fluorescence. Thus, the conformational state of the beacon is directly reported by fluorescence.

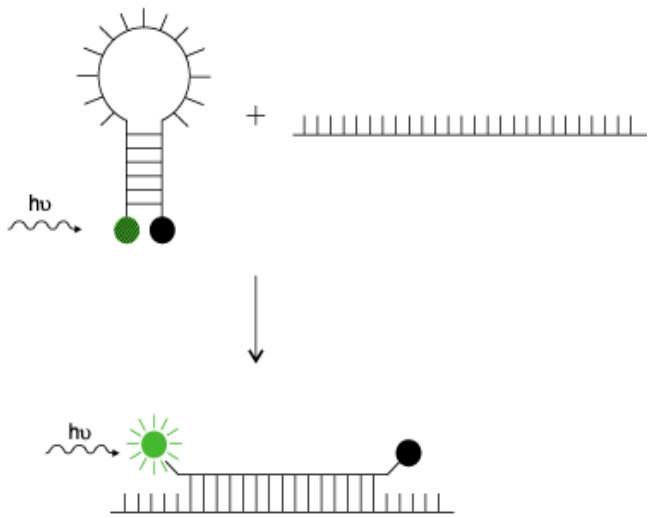

Figure 1.22. The principle of molecular beacons

The advantage of molecular beacon probes over single labelled oligonucleotides is that they allow the detection of a probe target sequence without

separation from unhybridised probes. They are also target specific, particularly in detecting single base mismatches and are therefore suitable for identification of alleles or particular strains of viruses or bacteria. Moreover, the specificity of molecular beacons enables the detection of many specific targets. Several molecular beacons with different fluorophore/quencher pairs can be used simultaneously in the same system enabling the multiplex detection without performing additional manipulations.

1.5.2. Design of molecular beacons and fluorescence quenching

The fluorophore is introduced to one end of the beacon (usually 5' end) using standard oligonucleotide labelling techniques. A range of fluorophores can be used, although fluorescein, rhodamine and Cy dyes are favoured. On the other end the quencher dye is added. Most commonly used is (4-(4' dimethylaminophenylazo) benzoic acid (DABCYL) (Fig. 1.23.).

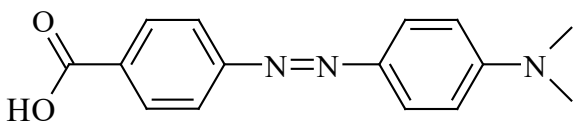

Figure 1.23. The structure of DABCYL, widely used quencher in molecular beacon design.

When the fluorophore and quencher are in proximity at the end of the hairpin structure they form a nonfluorescent complex that absorbs the energy of light and looses energy as heat. This phenomenon is called static quenching. When two fluorophores with different excitation and emission profiles are used in the same system we talk about fluorescence resonance energy transfer (FRET). FRET occurs when a matched donor and acceptor fluorophore are used and brought within 20-100 Å range. In that case the intensity of acceptor fluorophore increases, while donor decreases. FRET has been successfully applied in biotechnology[58] and used in molecular beacons as well as in Scorpion probes[56] and TaqMan[53]. The efficiency of FRET is dependent on the transition dipole orientation of donor and acceptor, distance between molecules and the overlap between the emission spectrum of the fluorophore

and absorption spectrum of the quencher (more details on the theory of FRET can be found in the Appendix).[59]

Different pairs of flurophores and quenchers have been used in design of molecular beacons. Tyagi and Kramer used EDANS and DABCYL in the first molecular beacon published.[57] Most widely used, however, are fluorescein and DABCYL.[60a,b] Other more efficient quenchers like Black Hole Quenchers (BHQ)[61], QSY 7[62] or 1,4-diaminoanthoquinone based quenchers[63] have also been utilised for molecular beacon design. However, the great challenge is still to find one with even better quenching ability. For example, DABCYL quenches at most 95% of the FAM fluorescence depending on the conditions and its quenching ability decreases for dyes emitting at longer wavelengths. BHQ are a bit more efficient, quenching 98% of Alexa Fluor 568, but FAM only 93%.[64]

Incomplete quenching gives rise to substantial residual fluorescence which can impair with measurements and decrease the sensitivity making quantification more difficult. Therefore there is a constant search for more efficient quenchers.

Table 1. Percentage of quenching given in the study by Marras *et al.*[64]

Fluorophore*	DABCYL (λ_{max}= 475 nm)		BHQ (λ_{max}= 534 nm)		QSY 7 (λ_{max} = 571 nm)	
	FRET	Static	FRET	Static	FRET	Static
FAM	80	91	88	93	85	93
TAMRA	78	83	89	87	84	87
Alexa 488	86	94	91	95	86	95
Alexa 568	60	91	96	98	83	99
Texas Red	88	96	97	98	89	98
Cy3	69	94	92	97	78	95
Cy5	43	84	89	96	63	79

* structures of fluorophore are given in Appendix

Recently, a number of papers described the use of gold nanoclusters as quenchers. The metal nanoclusters have been known for their quenching ability for some time[65] but Dubertret *et al.*[66] did an extensive study of the quenching by gold

nanoparticles. They designed molecular beacons with different fluorophores (FAM, rhodamine, Texas Red, Cy5) on 3' end and a gold nanoparticle on the 5' end. The quenching efficiency of nanoparticles resulting from non radiative energy transfer from dye to the metal was increased compared to conventional quenchers giving 99.97% of quenching for rhodamine 6G and 99.42% for FAM. Improved quenching allowed detection of minute amounts (5nM) of oligonucleotides. It was shown in the paper that nanoparticle molecular beacons can be used to detect a point mutation in the presence of random sequences even if only 1 out of 50 sequences has one mutation. However, additional improvements in the design of the molecular beacon are required because of the instability of the DNA- nanoparticle link, especially under temperature cycling conditions of PCR.

Different types of molecular beacons were recently designed, all attempting to circumvent the problem of insufficient quenching. Zhang *et al.* designed a molecular beacon with two fluorophores, coumarin and FAM, and proved that by measuring the intensity and change of shape of fluorescence spectra they can quantify and detect the target DNA down to 10^{-7} M.[67]

Tyagi and Kramer went further and constructed wavelength shifting molecular beacons, which made use of both static quenching and FRET.[68] They wanted to overcome the problem of the use of monochromatic light sources in instruments available for QPCR. When monochromatic sources are used they excite some fluorophores optimally, but others less well or not at all. This limits the number of fluorophores that can successfully be used in multiplexing. The wavelength shifting molecular beacon is designed so that it has two fluorophores on the 5' end and a quencher on the 3'. One fluorophore, called the harvester is in close proximity with quencher while another called emitter is seven nucleotides away from the harvester (Figure 1.24.). The harvester absorbs strongly in the wavelength range of the monochromatic light source and depending on the type of emitter used, the detection can be done at different wavelength ranges.

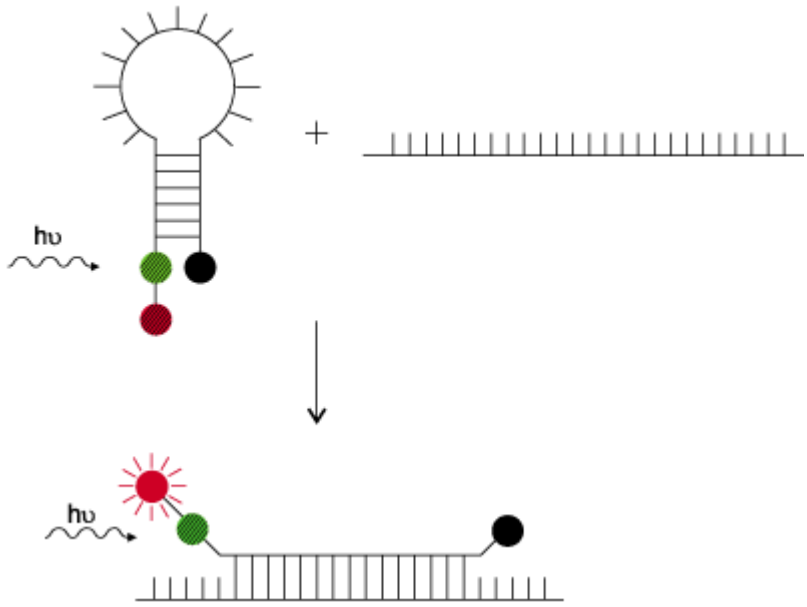

Figure 1.24. The wavelength shifting beacons by Tyagi and Kramer. FAM is the harvester (green), DABCYL, quencher (black) and TAMRA, Rhodamine 6G and Texas Red can be used as emitters (red).

When the molecular beacon is closed, in the absence of complementary sequence, the quencher and harvester are in close proximity, static quenching occurs and the probes are dark. When the target is present the beacon opens up. However, in contrast with normal molecular beacons, the energy stored in the harvester is transferred by FRET to the emitter and released at emitter's characteristic wavelength. Although the main disadvantage of this system is the complexity of the beacon synthesis, it enables the use of a single wavelength excitation light source in multiplex genetic analysis. Moreover, wavelength shifting molecular beacons are substantially brighter than conventional beacons, therefore the sensitivity of the system is increased.

1.5.3. Applications of molecular beacons

The first molecular beacons were used in the detection of single base mismatch and they showed remarkable efficiency.[69] Although this is still one of their main applications it is not the only one. Molecular beacons can be used in chemical diagnostics of infectious diseases. Wang *et al.* developed a fluorescent PCR assay

based on molecular beacon to detect *Mycrobacterium tuberculosis* at the 10 bacteria/mL level.[70]

In an other study by Chen and co workers[62] a FAM-DABCYL molecular beacon complementary to the *himA* gene of Salmonella was used in a real time PCR assay to detect the presence of the bacteria in the sample in as few as 2 colony forming units per PCR.[71]

Tan *et al.* reported the successful use of molecular beacons in the detection of DNA and protein interactions.[72] They designed TAMRA-DABCYL molecular beacons and studied the interaction with a well known single strand DNA binding protein (SSB) of *E. Coli*. When the molecular beacon was added to the solution of SSB, the fluorescence was restored in 10 sec, which indicated that the binding reaction is fast and the equilibrium is reached quickly. Moreover, the reaction occurred much faster than the one between the molecular beacon and cDNA. The experiments also showed that the binding constant for molecular beacon-SSB system was not significantly different from the DNA-SSB proving that the fluorophore and quencher do not influence the binding affinity. This study showed the potential for the use of molecular beacons in detection of different proteins. However, further improvements will have to be done to design specific molecular beacons that can be used in detection and discrimination of different proteins. The same research group used molecular beacons as a substrate for DNAase I and S1 nuclease to investigate the enzymatic cleavage of a single stranded DNA (Figure 1.25.).[73]

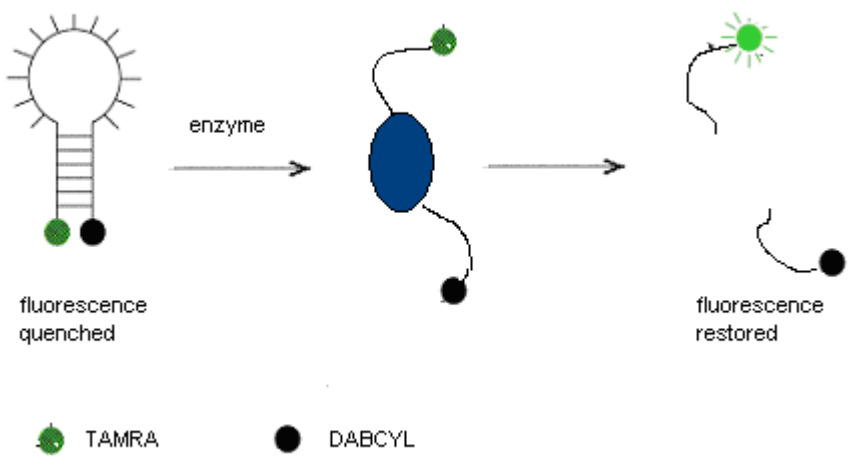

Figure 1.25. Enzymatic cleavage investigated by use of molecular beacon.[73]

Use of molecular beacons enabled the measurement of enzyme activity by calculating the average digestion rate based on the fluorescence spectra taken at different times of digestion. Moreover, the results provided the insight into the mechanism of DNA enzyme binding and cleavage.

One of the most exciting applications of molecular beacon is the real time detection of DNA-RNA hybridisation in living cells. In the study by Sokol *at al*. antisense and control molecular beacons were injected into living K562 human leukaemia cells and the fluorescence signal was measured.[74] When the molecular beacon with an antisense loop was injected, the fluorescence increased indicating the binding to complementary mRNA present. Moreover, it was possible to localise the signal within the cells, showing that hybridisation to mRNA is favoured in the cell cytoplasm. The study of antisense oligo – RNA binding is extremely important in the development of new DNA based drugs. Antisense oligos are known to perturb gene expression by hybridising to their complementary mRNA therefore promoting translation arrest. The problem encountered in the use of molecular beacons in cells is that fluorescence signal intensity varies when different targets are probed with the same molecular beacon pair. These fluctuations were attributed to the nature of the intermolecular coiling or hybridisation by the beacon sequences used. The degradation of the beacon in the cells also occurred after 45 min due to the attack of intracellular nucleases. It was indicated by the authors that better results could be achieved by changing the design of the beacon to make it more nucleases resistant and by improving the intensity of fluorescence signal.

Since the discovery, molecular beacons have been one of the most successful tools in biotechnology. They have provided valuable information in detection of infectious diseases, enabled the single base mismatch detection and multiplex genotyping, helped us to get an insight into enzyme action and to follow different process *in vivo*. Different types of molecular beacons are now available and further modifications are constantly introduced. However, it is still difficult to use them in quantification. The sensitivity of molecular beacon is determined by two parameters: residual fluorescence intensity when they are closed (incomplete quenching) and fluorescence intensity when they are in the open form. Although in theory fluorescence should be quenched completely, that does not really happen. Residual fluorescence varies greatly depending on the fluorphore/quencher selection, synthesis of molecular beacons and the way flurophore and quenchers are attached to

oligonucleotide. Therefore, the constant challenge in beacon chemistry is to find novel, more efficient quenchers or additional method of conformational change detection. There is also a limited number of fluorphore/quencher pairs limiting the multiplexing ability of molecular beacons. Additionally, although fluorescence is the technique routinely used in the laboratories around the world, there is a constant need to increase the sensitivity and multiplexing ability of the molecular probes used in biotechnology.

All of these created a need for novel methods of oligonucleotide labelling and the detection techniques that could compete with fluorescence. Surface enhanced resonance Raman scattering (SERRS) can provide solutions to some of the mentioned problems the practical aspects of this claim will be discussed in the following chapters.

1.6. Surface Enhance Resonance Raman Scattering (SERRS)

1.6.1. Raman and Resonance Raman

The investigation of processes that occur when electromagnetic radiation interacts with molecules gives information about their structure. The phenomena widely studied are absorption, emission and scattering of the light. Each one is the basis of different spectroscopic techniques but the most important for this work is the scattering of light. When radiation passes through a medium, the species present scatter a fraction of the beam in all directions. The Indian physicist Raman was the first to notice that a small fraction of the radiation scattered by certain molecules differs in wavelength from that of the incident beam and that the shift in wavelength can be linked to the structure of the molecule.[75] His discovery was the beginning of the development of Raman spectroscopy.

Raman spectra are acquired by irradiating a sample with a powerful laser source. It should be noted that classical and quantum theory show that there is one important requirement for the molecule to undergo Raman scattering and this is a change of polarizability of the molecule when irradiated.[76]

Three different types of scattered radiation are observed. When the incident radiation of energy $h\nu_0$ hits the sample, the collision with the photon excites the molecule from the ground electronic state to the virtual state of energy E_v. Immediately afterwards the photons are emitted and the molecule relaxes to the ground state. If the collision is elastic there is no exchange of energy between photon and molecule and no appreciable change in frequency. This scattering is called Rayleigh scattering and in that case the energy of scattering (E_s) is equal to incident energy $h\nu_0$. If the collisions are inelastic there is an exchange of energy in two possible ways. The molecule can receive some energy from the photon (ΔE) and get excited to a higher vibrational state. The scattered photon will then have a lower energy $E_s = h\nu_0 - \Delta E$. This process is called Stokes scattering and the resulting shift in wavelength the Stokes shift. If, on the other hand, molecules give some energy to the photon, the resulting E_s is equal to $h\nu_0 + \Delta E$ and the wavelength is shifted to lower values as a result of anti-Stokes scattering.

Resonance Raman scattering is a phenomenon in which an intensity enhancement of the Raman scattering (normally about 10^3 to 10^4 for effective chromophore) occurs when the excitation source is used with a wavelength that closely approaches that of an electron absorption peak of the analysed molecule. One more advantage, apart of the intensity enhancement, of resonance Raman is that the excitation is mainly frequency specific for absorption bands and can yield electronic as well as vibrational information

Although Raman spectroscopy is suitable for the study of aqueous solutions and resonance Raman gives marked increases in intensity, the scattering is still sufficiently weak which makes it difficult to work with low concentration of samples. The discovery of the surface enhanced Raman effect in 1974 by Fleischmann *et al.* led to the development of a new area of analytical chemistry as well as raising the questions concerning the basic theory of surface enhanced Raman scattering and the chemistry on the surface.[77] Three years later, in 1977, surface enhanced resonance Raman scattering (SERRS), which is a combination of resonance Raman and surface enhanced Raman scattering with enhancement of the Raman scattering claimed to be 10^{14}-10^{15}, was first observed by Van Duyne.[78]

The next section gives the overview of the basic theory behind SERRS as well as the applications. It should be noted that in many papers authors do not distinguish between SERS (which does not have a molecular resonance contributions) and SERRS. The theory behind both phenomena is based on the same principle, but the main differences lie in the size of enhancement and type of analytes used. Therefore, the development of SERRS theory and the application will be explained by referring to the published work on both types of Raman scattering.

1.6.2. Surface Enhanced Raman and Resonance Raman Scattering

SERS is a phenomenon observed for a range of different molecules when they are adsorbed onto roughened noble metal surfaces. Although a generally accepted account of SERS is still not available, SERS has developed as an important analytical tool. The magnitude of the SERS enhancement is usually determined as an enhancement factor, which is the ratio between measured Raman cross section in the

presence and in the absence of the metal surface. Typical values for enhancement range between 10^5 –10^6 for silver surface, although much larger enhancements of 10^{14} –10^{15} were recently reported in single molecule SERRS experiments using Ag and Au nanoparticles.[79] The overall observed enhancement is generally explained in terms of electromagnetic and chemical or "first layer" enhancement.[80]

The electromagnetic enhancement theory of SERS describes enhancement as being caused by an amplification of the electric field due to the response of the material surface to the incoming light wave.[81] The magnitude of the local field enhancement can vary depending on the material (Au, Ag, Cu) and the coupling between different surfaces. Therefore, the mathematical model has to account for a number of important factors, especially the shape and the size of metal particles. Xu *et al.* used a theoretical model and experimental results of single molecule measurements to estimate the electromagnetic contribution to SERS.[82] From their calculations it could be seen that in the case of nearly approaching Ag spheres, the enhancement factor is 10^{12} at 400 nm. On average, enhancement factors of 10^{10} can be attributed to the electromagnetic enhancement.

Chemical enhancement results from the charge transfer excitation of chemisorbed molecules. In this mechanism is it assumed that an adsorbed molecule has donor or acceptor levels (highest occupied and lowest unoccupied molecular orbital) at the right energy so that the charge transfer complex with the surface metal at so called "active sites" might be formed. Otto *et al*. reported that the strong electronic coupling between an adsorbed molecule and an active site generates new metal to ligand or ligand to metal charge transfer states that can be broadly excited at visible wavelengths.[83] The percentage of the contribution of each factor to the overall enhancement is still the matter of continuous debate, although experiments showed that chemical enhancement contributes to the overall effect much less then electrochemical and accounts for the difference between the electromagnetic and the overall enhancement reported in literature (10^{13}-10^{15}).

Krug *et al*. investigated the influence of size and shape of nanoparticles on the surface enhancement.[84] They screened Au particles of different sizes with adsorbed crystal violet molecules adsorbed on the surface and showed that SERS active particles have a narrow size range, about 63 ± 3 nm. Outside this range, particles have little or no SERS activity. They argue that in addition to the particle size, other factors like particle shape and specific adsorption sites are important for efficient optical

enhancement. The faceted particle shape could be important because the sharp points and edges can act as "lightning rods" to concentrate the incident electromagnetic field. Sharp points could also function as active sites and are believed to be responsible for chemical enhancement *via* a resonant charge transfer process. Hilderbrand and Stockburger suggested that SERS active sites are high affinity binding sites associated with adsorbed anions such as Cl^- and Br^-.[85] The number of active sites according to them is on average 3.3 per colloidal Ag particle.

The surfaces mainly used for SERS are silver and gold roughened surfaces. Using colloidal silver clusters, Kneipp *et al.* detected single adenine molecule using near infrared SERS showing that SERS could be used in detection of nucleotides in DNA sequencing.[86] Recently, Xia and Sun published the results of their research of the synthesis of gold and silver nanoparticles which will prove to be very useful for the application in SER(R)S in the near future.[87] They managed to make silver nanocubes with controllable dimensions (mean edge length of 175 nm) by a modified polyol process that involved the reduction of silver nitrate with ethylene glycol in the presence of a capping reagent such as poly(vinylpyrrolidone), PVP, at 160°C. The morphology and dimensions of the product were found to be strongly dependant on the reaction conditions. Subsequently, the authors also used silver nanocubes as templates to generate gold nanoboxes with a well defined shape. Since the optical and electrical properties as well as SERS enhancement, depend on the size and shape of the metal particles, it is clear that the chemical synthesis of nanoparticles of controlled shape, size and structure will have a huge impact on the future applications of SER scattering.

The same roughened metal surfaces are used in SERRS detection. As mentioned before, SERRS requires molecular as well as plasmon resonance and the main disadvantage in using it as a detection technique arises from the need for a specific chromophore that matches the excitation frequency. A significant amount of work has been done in the synthesis of new dyes that have both the desired chromophore and the ability to bind to the metal surface.[88]

SERRS is especially useful in the detection of biologically important molecules and compounds present in low concentration. Constantino *et al*. used the enhanced sensitivity of SERR scattering to achieve single molecule detection.[89] Bis(benzimidazo) perylene (AzoPTCD) was dispersed in the host fatty acid matrix using Langmuir Blodgett technique and transferred to the silver deposited films. The

SERRS spectra were then taken and the area mapped proving that spectra came from the single molecule detected in the matrix.

Although both surface enhanced Raman and resonance Raman scattering are proving to be extremely useful in fundamental studies on the single molecule level, they are also important analytical tools. SER(R)S has been used to detect a variety of different types of analytes present in low concentrations, including pollutants[90], explosives[91] and chemical warfare agents[92]. Recently, a glucose biosensor was developed using SERS detection on a silver film and the glucose level was quantitatively determined using partial least square method.[93]

Since Raman spectroscopy is suitable for studies of aqueous solutions, both SER and SERR scattering are used in the detection of important biological molecules, especially DNA. The interactions between anthracycline antibiotics, which have chromophore in the visible region, and DNA were investigated using SERRS.[94] Vibrational information for the antibiotic molecules themselves and a drug-DNA complex enabled the understanding of the DNA-drug binding. It was also shown that different modifications of the drug molecule effect its interaction with DNA. In a similar study, Ermishov *et al*. investigated the effect of antibiotic netropsin on double stranded DNA by SERS, making a significant contribution to the understanding of conformational changes when small molecules bind to different sites.[95]

Other important processes involving DNA, such as hybridisation and bending were also investigated using advanced Raman technigues.[96] The ability of DNA to wrap and bend around the substrates is important in packaging and transcription. Therefore, Gaerhart *et al.* prepared 14 nm protein sized gold particles and examined the adsorbtion and bending of 16 base pair DNA strands by SERS.[97] They found that the intensity of the enhanced vibrational modes of the bases within the sequences is dependant on the intrinsic DNA curvature and the way DNA binds around nanoparticles. This enabled the fast identification of strait, kinked or bent DNA in the solution.

However, the use of SERRS in DNA detection is less straightforward. Biomolecules, like DNA, do not posses a chromophore in the visible region and a label must be incorporated into the molecule to allow detection. Moreover, they do not have the ability to attach to the metal surface. Therefore, the direct analysis of DNA by SERRS is not possible without labelling the molecule with SERRS active species.

Recent work in our group focused on the SERRS detection of modified DNA.[98] Two fluorescent labels, HEX and rhodamine 6G were added to the 5' terminus of DNA. A colloid was used as a SERRS active surface. HEX is negatively charged and does not adsorb on to the colloid surface, but it was placed next to the modified base that attached to the surface and therefore was forced to come to close proximity facilitating the surface enhancement. On the other hand, rhodamine 6G has amino groups that attached to the colloid easily. Modified oligonucleotides were detected at about $2x10^{-13}$ mol dm^{-3}. Moreover, it was possible to discriminate between labels in a mixture without the separation. However, the problems with the surface attachment decreased the reproducibility of the measurements. Therefore a new approach made use of benzotriazole monoazo dyes specifically designed to attach strongly to the surface and provide reliable SERRS spectra.

Benzotriazole dye phosphoramidite was synthesised and coupled to a DNA sequence during automated synthesis.[99] In this way DNA was labelled at the 5' terminus with the dye that was acting both as chromophore and surface attaching group. Although good SERRS spectra were obtained, synthesis of dye phosphoramidites is tedious. Therefore, there was a need for a new, simpler and more effective approach.

Taking into account all these requirements and the work done previously on benzotriazole (BT) maleimides as a bifunctional reactant for SERS[100], Diels Alder cycloaddition was chosen as most suitable reaction to be investigated. Diels Alder cycloaddition describes the reaction between two groups of molecules referred to as the dienophile (e.g. vinyl groups, maleimide) and the dienes (e.g. furan).

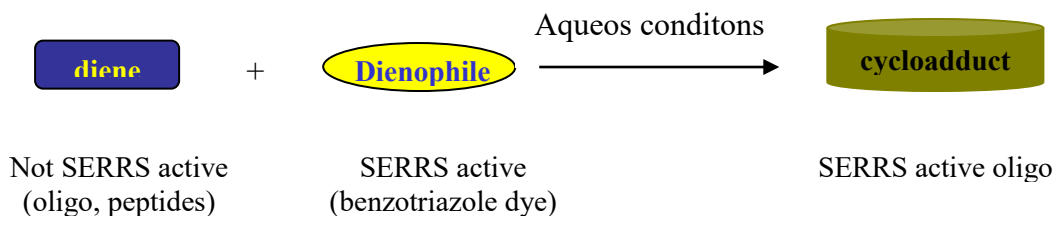

Scheme 1.1. Attachment of the non SERRS active molecules to the surface using Diels Alder cycloaddition.

If a BT dye with a maleimide functional group is synthesised, it would produce a cycloadduct with diene modified DNA therefore enabling fast, reliable, simple labelling of oligonucleotides in an aqueous environment.

This concept was investigated together with the use of SERRS as a novel technique in detection of single and dual labelled olligonucleotides and the results are presented in this thesis. In *Chapter 2* the synthesis of SERRS active benzotriazole dyes is discussed. *Chapter 3* presents the study of SERRS surfaces used throughout the project. The SERRS properties of dyes are discussed in *Chapter 4*. Labelling and SERRS detection of oligonucleotides is described in *Chapter 5* with the special section on labelling of DNA with fluorescent molecules using novel labelling chemistry. Finally, *Chapter 6* is based on the study of the fluorescence quenching properties of benzotriazole dyes and the design and function of a novel type of bioprobe, SERRS Beacons. Main conclusions are given in the *Chapter 7* and all experimental procedures are described in detail in *Chapter 8*.

Chapter 2

Synthesis and properties of benzotriazole dyes and dye maleimides.

2.1. Introduction

As demonstrated by previous research, different azo dyes with 1*H*-benzotriazole (BT) as a surface attachment group give strong and reproducible SERRS signals.[88] Benzotriazole is commonly used as an antitarnish agent on silver and is believed to act by forming a complex with more than one silver ion.[101] The main advantage of the attachment of BT to silver surfaces is that the process is essentially irreversible. Therefore, once attached, the orientation of the dye remains the same over a wide range of experimental conditions.

When designing benzotriazole dyes for Diels Alder cycloaddition the first aspect to consider is if the dye is going to be diene or dienophile. The synthesis of the suitable dye is the first step towards the use of Diels Alder cycloadditon in labelling of DNA. Taking into account the conditions required for the synthesis of DNA, which might be harsh for some dienophiles, and the previous experience in synthesis of BT dienophiles, the dyes suited as the dienophile. A number of different dienophiles such as vinyl derivatives or dihydroquinone could be used. Previously, Grondin *et al.* examined cycloaddition of a range of dienes with benzotriazole maleimide and recorded the differences between the starting material and cycloadduct by SERS.[100] Taking into account the excellent results obtained from this study, maleimide was chosen as the dienophile for oligonucleotide labelling. A number of synthetic routes were examined to produce a dienophile dye that could give excellent SERRS, conjugate to DNA and display a difference in signal as a result of cycloadduct formation. In order to produce the maximum differences in the cycloadduct from the dienophile dye, the maleimide needs to be part of the conjugated chromophore system of the dye. The benzotriazole dyes previously reported contain primary amine groups as part of the chromophore but due to extensive delocalisation they are unreactive towards conversion into maleimides.[102] Thus, a new class of benzotriazole azo dyes with reactive amine groups had to be produced. The results of the various synthetic strategies are reported in detail in this chapter.

2.2. Experimental

Experimental procedures and the data for all synthesised compounds are given in *Chapter 8*.

2.3. Synthesis of benzotriazole azo dyes

All dyes were prepared by diazotisation of aromatic amines followed by coupling of the diazonium salt to 5- or 4- aminobenzotriazole (Scheme 2.1). Diazotisation involved the treatment of a primary aromatic amine with nitrous acid to form a diazonium salt ($ArN_2^+Cl^-$). Since nitrous acid is unstable, it was generated in the reaction mixture by treatment of sodium nitrite with hydrochloric acid. The acidic conditions also enable the conversion of the insoluble aromatic amine into its water-soluble protonated form ($ArNH_3^+$). The diazotisation reactions were all carried out at 0°C as higher temperature promotes the decomposition of the nitrous acid and diazonium salt, which occurs readily with evolution of nitrogen gas. The second stage of the dye synthesis is an azo coupling of the diazonium salt with the coupling component 5- or 4-aminobenzotriazole. The temperature control in this step is less important and the reactions were carried out at room temperature. To obtain the dyes in high yield, the pH of the reaction was maintained at pH 6. Higher pH can cause the conversion of the diazonium cation (ArN_2^+) into the diazotate anion ($Ar\text{-}N{=}N\text{-}O^-$). Alternatively, more acidic conditions shift the equilibrium in the solution of the coupling component towards the protonated form, which is unreactive towards azo coupling.

The following dyes: 4- (4'-methoxy-phenylazo)-3*H*-benzotriazole-5-yl amine [**1**], 4-(3'-methoxy-phenylazo)-3*H*-benzotriazole-5-yl amine [**2**], 4-(3',5'-dimethoxy-phenylazo)-3*H*-benzotriazole-5-yl amine [**3**] and 4-(naphtalen-1-ylazo)-3*H*-benzotriazole-5-yl amine [**4**] were synthesised from 5-aminobenzotriazole (Scheme 2.1a.). These dyes were good SERRS dyes in their own right but unlike previous dyes had a nucleophilic aromatic amine available for further functionalisation.[88]

In a similar approach 4-ABT was used to synthesise 7-(4'-methoxy-phenylazo) –1*H*-benzotriazole-4-yl amine [**5**] (Scheme 2.1b). The primary amine in 4-aminobenzotriazole has a strong para directing effect towards the formation of the azo group. However, although a very good SERRS dye, the primary amine was not derivatised further. It is thought that the SERRS activity of this dye is due to its ability to complex silver through both the nitrogen of the triazole ring and the primary amine. Therefore, derivatisation of the primary amine could cause a decrease in SERRS activity.

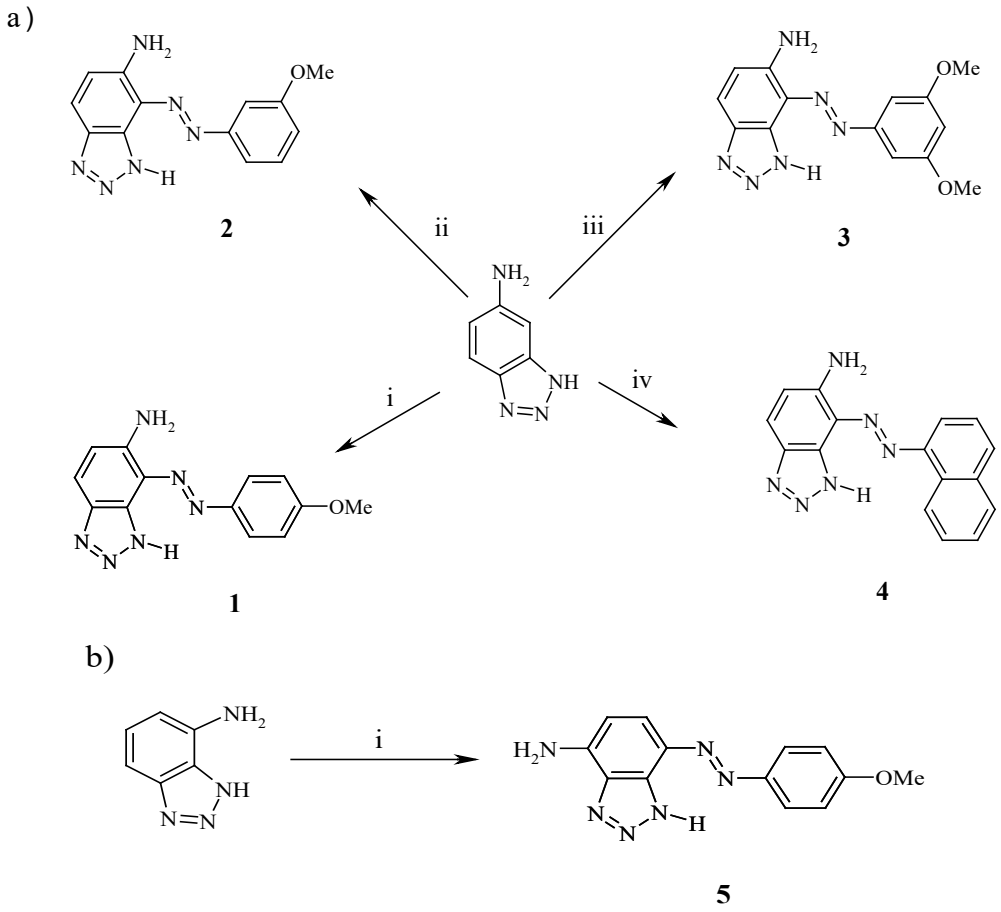

Scheme 2.1. Synthesis of the benzotriazole dyes from **a)** 5-ABT and corresponding primary amines (i) *p*-$CH_3OC_6H_4NH_2$, NaOAc buffer, pH 6, (ii) *m*-$CH_3OC_6H_4NH_2$, NaOAc buffer, pH 6, (iii) $NH_2C_6H_4(OCH_3)_2$, NaOAc buffer, pH 6 (iv) $C_{10}H_7NH_2$, NaOAc buffer, pH 6 and **b)** 4-ABT and (i) *p*-$CH_3OC_6H_4NH_2$, NaOAc buffer, pH 6 .

2.4. Synthesis of dye maleimides from dyes

Several different routes were investigated for the synthesis of dye maleimides (Scheme 2.2). The three-step synthesis employed in the synthesis of benzotriazole maleimide using acetic acid did not give the desired product after several attempts under different conditions.[100] The compound produced was the acetylated form of the dye **11** (Fig. 2.1) where the ability of the triazole ring to complex to the metal is decreased due to the presence of the acetyl group. The same compound is obtained as a side product in the maleimide **10** formation.

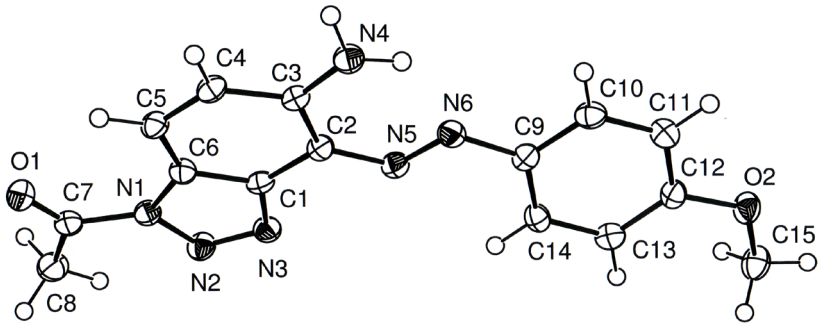

Figure 2.1. X-ray structure of the acetylated dye **11**.

Corrie *et al.* used a one pot procedure to prepare a fluorophore *N*-maleimide. The same procedure was employed in the synthesis of maleimide **11**.[103] Dye **1** was treated with maleic acid anhydride in dimethylacetamide (DMA) and the resulting solution of N-substituted maleamic acid was treated first with a small amount of cobalt(II) naphthenate followed by acetic anhydride and heated at 70-80°C for 1h to effect cyclisation.

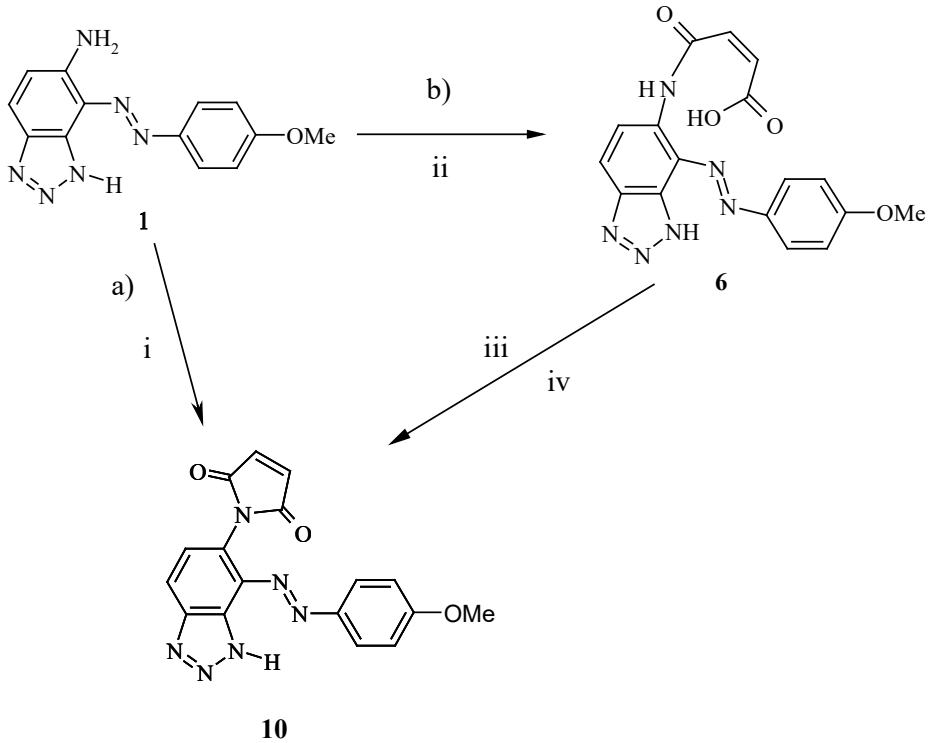

Scheme 2.2. Synthesis of dye maleimide **10 a)** directly from dye **1** using (i) maleic acid anhydride, Co(II) naphthenate, Ac_2O and **b)** from dye *N*-maleamic acid **6** (ii) maleic acid anydride, DCM and (iii) Co(II) naphthenate,Ac_2O or (iv) DCC, HOBt.

The role of cobalt is not fully understood but it is presumed that it acts as a coordinating template to assist cyclisation.[103] Maleimide **10** (Figure 2.2) obtained was contaminated with two side products of which one was successfully isolated and characterised to be acetylated form of the starting material **11**.

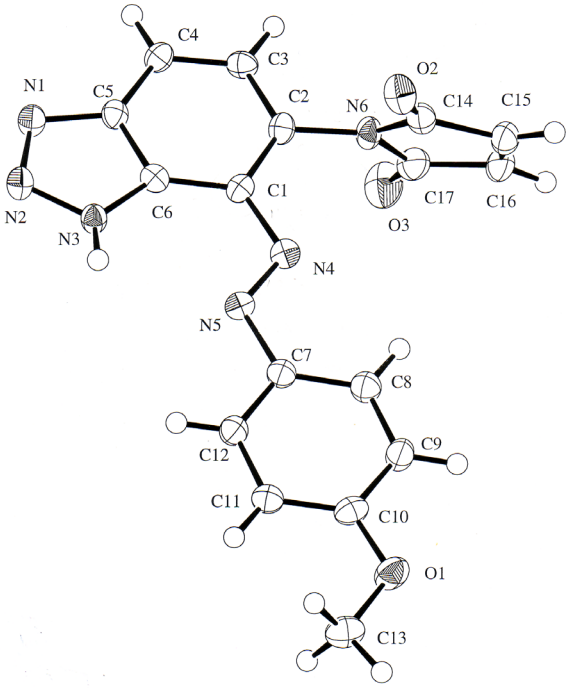

Figure 2.2. The X-ray structure of 1-[4-(4'-methoxy-phenylazo)-3*H*-benzotriazole-5-yl]-pyrrole–2,5-dione **10**.

The X-ray analysis of **10** showed that the values of N5-N4-C1-C6 and N4-N5-C7-C8 torsion angles are 0.9 and –2.1 respectively, which indicated that azo linkage adopted a planar conformation probably due to the presence of the bulky maleimide group that imposed some steric constrains.

The existence of the side product **11** was proved additionally when the maleimide **12** was synthesised from dye **2** (Scheme 2.3.). The acetylated side product **13** (Fig 2.3) was crystallised from hexane/ethyl acetate mixture after the purification of the maleimide.

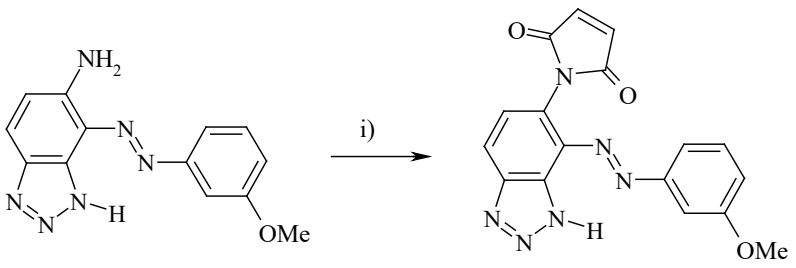

2 **12**

Scheme 2.3. Synthesis of dye maleimide **12** directly from dye **2** using (i) maleic acid anhydride, Co(II) naphthenate and Ac_2O.

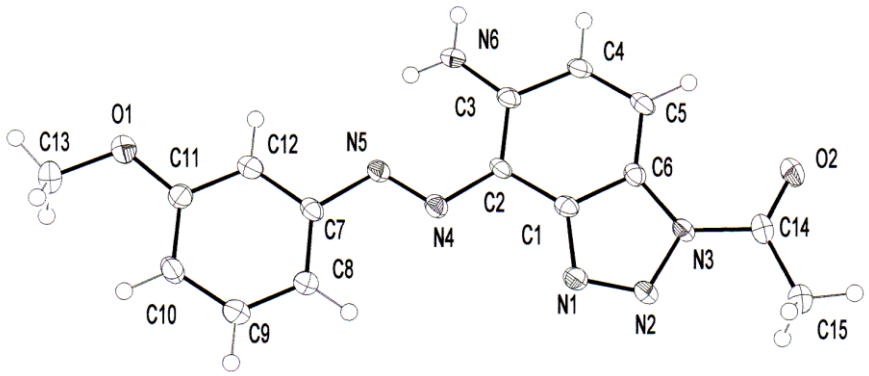

Figure 2.3. The X-ray structure of side product **13** from the maleimide **12** synthesis reaction using one pot Co(II) naphthenate procedure.

A strong intramolecular hydrogen bond is present between N6-H and N5 (2.00 Å). The comparison of selected bond lengths of dye maleimide **10** (without intramolecular hydrogen bonding) and dye **13** shows that there is a lengthening of C-C bonds and shortening of C-N bonds (Table 2.1). This is consistent with the existence of the strong hydrogen bonding that leads to the formation of a stabilised six membered ring.

Table 2.1. Selected bond lengths of the azo maleimide dye **10** and azo dye **13**.

Maleimide dye **10**		Dye **13**	
bond	bond length	bond	bond length
C2-N6	1.428 Å	C3-N6	1.341 Å
N4-C1	1.407 Å	N4-C2	1.389 Å
C1-C2	1.394 Å	C2-C3	1.415 Å

The angles N4-N5-C2 (115.0˚), N6-C3-C2 (122.9˚) and N4-C2-C3 (127.9˚) are close to idealised sp^2 geometry. The compression and expansion away from 120˚ is caused by steric contribution from the nitrogen lone pairs. The values of torsion angles N4-N5-C7-C8 (-8.7˚) and N5-N4-C2-C8 (3.1˚) demonstrate that as in the case of **10**, the azo linkage is adopting a planar conformation this time due to the stabilisation from the intramolecular hydrogen bond.

In order to increase the yield and avoid the formation of the side product, *N*-maleamic acids **6** and **7** were first synthesised and isolated and then treated with cobalt naphthenate and acetic anhydride. There was indeed no acetylated dye product formed and the maleimides were obtained in 51 % yield compared to 45% in the initial reaction.

Keanna *at al.*[104] suggested another method for the synthesis of N-maleimides from *N*-maleamic acids using dicylcohexylcarbodiimide (DCC) and 1-hydroxybenzotriazole hydrate which are commonly used in racemisation free peptide couplings[105]. When the cyclisation of acid **6** was attempted with the 1.2 equivalents of DCC as described by Keanna only traces of maleimides were found in the mixture of products. However, when the reaction procedure was modified to use 3 equivalents of DCC and the reaction mixture left to stir for 20 hours a 53% yield of dye maleimide **10** was achieved

Both methods were comparable in yields although the crude product obtained from the reaction with cobalt naphthenate was easier to purify. The cobalt (II) naphthenate residue and side products were removed by filtration and the filtrate was additionally purified by column chromatography.

Since the bifunctional benzotriazole dye maleimides were to be used for oligonucleotide labelling and further in multiplexing experiments, it is desirable to have several maleimides with distinguishable spectra in order to mark different oligonucloetides. Therefore, two more dye maleimides **14** and **15** were synthesised from dyes **3** and **4** respectively**.**

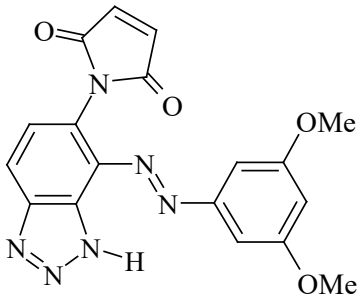

14

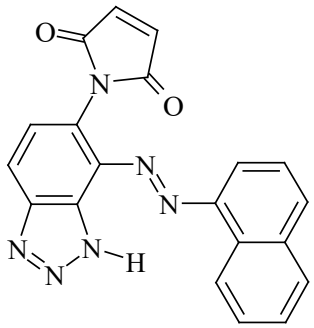

15

It was also assumed that the synthesis of different dye *N*-maleimides could be achieved, in high yield, by diazotisation of 1-(4-amino-phenyl)-pyrrole-2,5-dione and then coupling to 5-, 4-amino benzotriazole or other molecules with the ability to bind to a metal surface *e.g.* 8-hydroxyquinoline**.**[106] Therefore a number of experiments were performed to test this hypothesis leading to some interesting data concerning the conditions for the maleimide formation, which are presented in the following section.

2.5. Synthesis of maleimide 1-(4-amino-phenyl)-pyrrole-2,5-dione.

Although described in the literature[104] the synthesis of 1-(4-amino-phenyl)-pyrrole-2,5-dione (maleimide) (Fig. 2.4) was unsuccessful in our hands under a variety of conditions (Table 2.1).

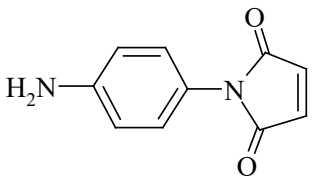

Figure 2.4. 1-(4-Amino-phenyl)-pyrrole-2,5-dione.

The synthesis of 1-(4-amino-phenyl)-pyrrole-2,5-dione was first attempted using acetic anhydride and sodium acetate as described by Cava and the maleamic acid produced from *p*-phenylendiamine.[107] However, *N*-[4-(2,5-dioxo-2,5-dihydro-pyrrol-1-yl] acetamide **17** was formed and the subsequent cleavage of the acetyl amide was unsuccessful leading instead to the undesired opening of the maleimide ring.

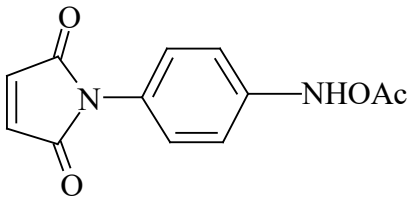

17

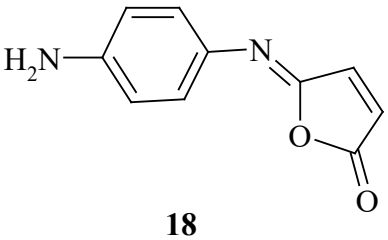

18

To avoid the use of the large access of acetic anhydride a range of other methods were used (Table 2.1) which all led to the formation of isomaleimide **18** in 63 to 75% yield depending on the procedure employed.

Table 2.1. Reagents and products of different cyclisation methods using 3-(4-amino-phenylcarbamoyl) acrylic acid **16.**

Reagents and conditions	Product
Acetic anhydride, sodium acetate, 40°C, reflux, 40 min	17
Co (II) naphthenate, acetic anhydride, 70°C, reflux, 1h	18
DCC (1.2 and 3 eqv), HOBt, DCM, rt, 12 h	18
DCC, HOBt, dry DMF, rt, 12 h	18
DCC, HOBt, DMA, 40°C, 1 h	18
Morpho CDI, HOBt, DCM, rt and 50°C, 12 h	18

Most of the reagents used were standard activating agents for carboxylic acids except for the cobalt naphtenate. Cobalt naphtenate was first used by Corrie in the preparation of fluorescent *N*-maleimides[103] and was successfully applied to the synthesis of BT dye maleimides. Previously it was reported that reactions conducted at low temperatures tended to favour isomaleimde formation but although the temperature was increased in some of the reactions only the isomaleimide **18** was isolated.[108]

In view of published results on the cyclisation of *N*-maleamic acids, the formation of isomaleimide under all of the above conditions was not expected.[104,109a,b,] Gill *et al*. prepared a series of simple maleimides in high yields by reaction of the appropriate maleic anhydride with either ammonium acetate or methylammonium acetate in boiling acetic acid.[109a] Chaurasia and coworkers synthesised 3-maleimidocoumarin in 40% yield using morpho CDI but did not mention any side products.[109b] *N*-(4-aminophenyl)- and *N*-(4-isothiocyanophenyl)maleimides were also prepared in other research labs using a DCC-HOBt procedure, which gave isomaleimide as the main product in our hands.[104] However, it should be noted that many authors investigating the synthesis of imides did not give a proper account of possible side products.

Further consideration of the reactions indicated that there was likely to be an electronic basis behind the observed results. Brady and Hegarty studied the imide–isoimide rearrangements (Figure 2.5.).[110] They studied the kinetics of the

rearrangement for a range of isoimides and determined the inductive effect of different substituents.

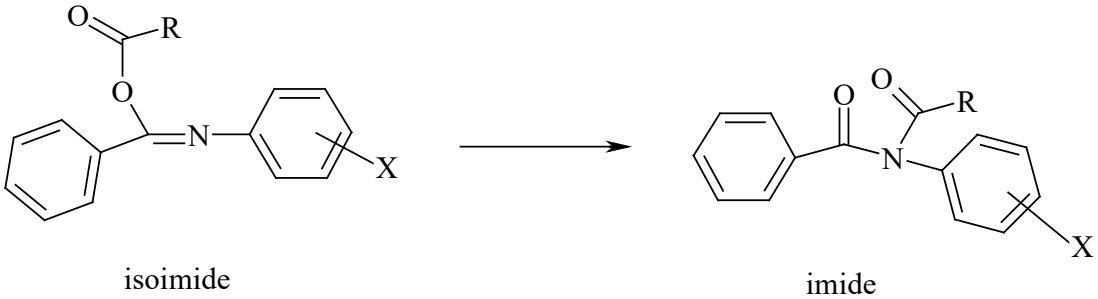

Figure 2.5. Isoimide –imide rearrangement studied by Brady and Hegarty.[110]

They observed that electron donating R or X groups shift the equilibrium towards isoimide. They also explained this result with the steric effects that occur in the highly restricted transition state. Therefore the formation of the isomaleimde **18** as the only product can be attributed to the electron-donating characteristic of the amino group on the aromatic ring. When the donating ability was decreased by acetylating, maleimde **17** was obtained.

On the basis of this observation, it was concluded that the presence of the electron withdrawing nitro group on the aromatic ring would favour the formation of maleimide. Thus, 1-(4-nitro-phenyl)-pyrrole-2,5-dione **20** was easily formed using acetic anhydride and sodium acetate (Figure 2.6.).

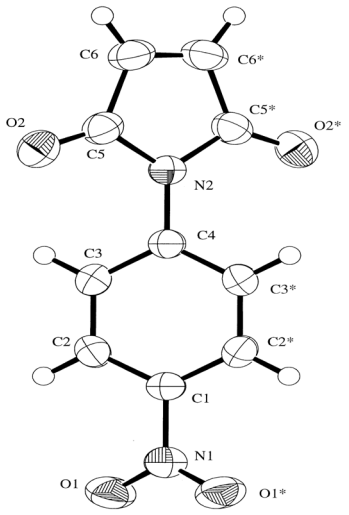

Figure 2.6. The X-ray structure of compound **20**.

However, reduction of the nitro group under a variety of conditions (hydrazine on graphite, Fe in acetic acid under inert atmosphere at different temperatures) failed to produce the desired amine. Although the products were not isolated, it can be assumed that the reduction of the maleimide double bond is favoured.[103]

m- and *p*-Anisidine were also used as reagents to make the corresponding maleamic acids which were then used in cyclisation reactions. The presence of the electron donating methoxy substituents was expected to give the isomaleimides **22** and **24** and was indeed the case.

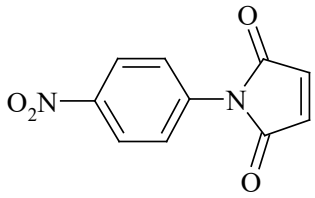

20

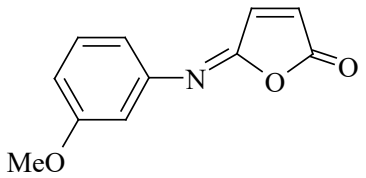

22

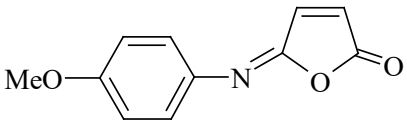

24

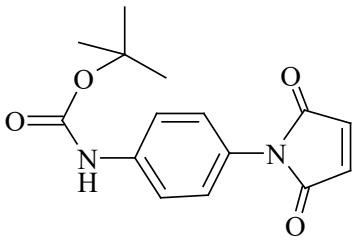

26

In order to obtain 1-(4-amino-phenyl)-pyrrole-2,5-dione another approach was adopted. The formation of the maleimide proceeded readily when the amino group was acetylated. Thus it was reasoned that if the amino group was protected with an alternative protecting group that did not utilise an amide linkage then the amine could be regenerated in the presence of the maleimide after the desired ring closure. The protecting group chosen for this was di-*t*-butyl carbonate, BOC, which can be removed either thermally or by acidic hydrolysis. Maleimides are stable to acidic conditions making BOC a compatible protecting group. The protection had two functions; firstly it prevented acetylation of the amine during ring closure by acetic anhydride and secondly, it decreased the electron donating character of the amino group therefore favouring the formation of the maleimide. Maleimide **26** was obtained in excellent yield using morpho CDI and HOBt as the reagents for cyclisation.

Removal of the BOC group was unsuccessful after several attempts with trifluoroacetic acid in different concentrations, hydrochloric acid and thermal deprotection. This means that a route to the synthesis of 1-(4-amino-phenyl)-pyrrole-2,5-dione has not been obtained but significant information on the formation of maleimides as opposed to isomaleimides has been gathered.

In conclusion, a range of aromatic isomaleimides and maleimides were formed to investigate the imide–isoimide formation under a range of conditions. The use of substituted aromatics allowed the effect of the substituent on maleimide formation to be determined. This indicated that the presence of an electron donating group favours the isomaleimide formation and is attributed to the favouring of the imino form of the amide that can then attack the carboxylic acid. Electron withdrawing groups favour the formation of maleimide and we propose that this allows the nitrogen of the amide to attack the carboxylic acid. This information is useful in designing the synthesis of new maleimides for use in a range of applications including biological labelling using Diels Alder chemistry.

2.6. Diels-Alder cycloaddition

The conditions for the Diels Alder cycloaddition were investigated with the phenyl maleimide and 2-furfurylaldehyde dimethylhydrazone as a diene. The reaction was attempted in water with acetonitrile as a co-solvent as this increases the rate of Diels Alder reactions due to the hydrophobic packing effect.[111a,b] The cycloadduct **27** (Fig. 2.7.) was obtained after 15 minutes of stirring in almost quantitative yield (93%) and crystallised from the solution in the form of bright yellow needles.

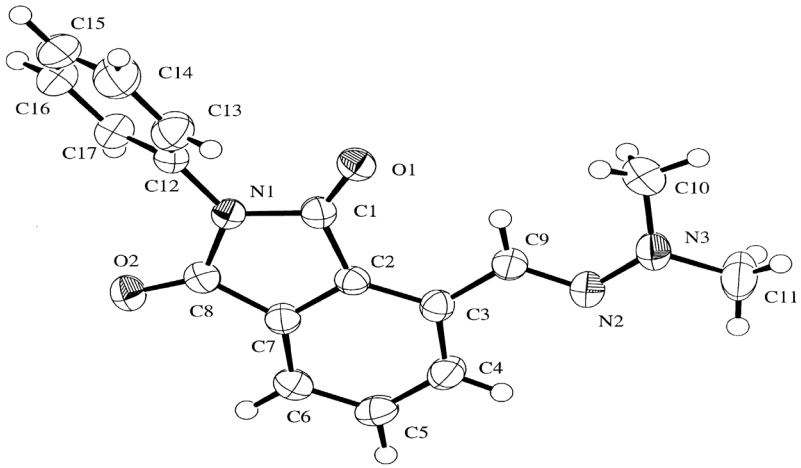

Figure 2.7. The X-ray structure of cycloadduct **27.**

The same diene was used in the reaction of dye maleimide **10** giving the yellow powder, which was characterised as the expected cycloadduct **28.** The reaction was fast and no side products were observed.

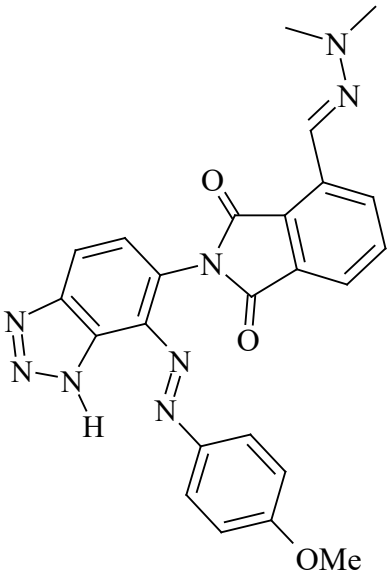

28

Therefore, the Diels Alder cycloaddition can be used to bind SERRS- inactive molecules to dye maleimides, which are attached to a silver surface, making them SERRS active.

A detailed account of SERRS activity of synthesised dyes as well as their use in the labelling of oligonucleotides using Diels Alder cycloaddition is given in following chapters.

Chapter 3

SERRS substrates

3.1. Introduction

One of the most common metal surfaces used in SERRS measurements is silver colloid. Recently, studies of colloids were done using high resolution electron micrography and SERRS.[112] It was observed that SERRS activity was increasing with the growing number of particles in the colloid aggregate. The aggregates of 4-9 silver particles gave higher intensity SERRS spectra of the investigated dye than aggregates of three or less particles. The saturation of the SERRS response was also noted above approximately 90 particles in an aggregate. This was the first extensive study of the correlation of the size of the aggregates in colloids with the intensity of SERRS spectra. Moreover, it was found that the SERRS enhancement could be correlated with interparticle gaps measuring 1 nm in width.

In general, colloids are particularly suitable in flow cell experiments and the production of colloid *in situ* in flow cell was recently developed.[113] However, in the experiments where a solid surface is required (array production, SERRS sensors), a colloid suspension is not useful. Therefore, there was a need for solid, rough metal surfaces for SERRS and a number of such surfaces was made. Cold deposited films (CDF) have been used as a substrates in numerous studies.[114,115]Although the roughness of those films can be adjusted by the rate of the silver deposition and a number of methods exist to control the quality of films, the roughness is lost with the time.[115] That causes the decrease in the intensity of the SERRS from an adsorbed molecule. Furthermore, the surface is susceptible to damage by mechanical stress or addition of a solution of analyte.

To make the films more robust, a polyvinyl alcohol (PVA) silver substrates were prepared by using PVA solution to coat the slides by a slightly modified Vo Dinh method.[116] The advantage of this surface is that a polymer, which accepts also hydrophilic molecules, protects the silver and this makes the surface more resistant to the damage.

Professor Mills at the University of Strathclyde provided the third type of SERRS substrates containing silver in TiO_2, which were evaluated to check their potential for SERRS measurements.

The PVA-Ag discs were analysed using electron microprobe analysis (EMPA). EMPA is based on X-ray fluorescence. It works by bombarding a micro

volume of the sample with a focused electron beam to excite X-rays from a small area of a sample. The resulting X-rays are diffracted by reference crystal and their intensities measured. The composition of the unknown sample is determined by comparison of the characteristic X-ray produced by the emitting species in the sample with X-rays intensities from materials with known composition. All elements from beryllium to uranium can be analysed. The sensitivity of EMPA is better and the risk of erroneous interpretation of qualitative spectra is less than with other techniques i.e. standard secondary electron microprobe (SEM).

When a sample is bombarded with fast electrons few other effects, apart from X-rays, can be noticed and they include production of backscattered and transmission electrons, secondary electrons (SE), Auger electrons and heat. Secondary electrons are particularly useful for the analysis of the sample surface. They are, by convention, those electrons with energies less than 50 eV and are produced when an incident electron excites an electron in the sample and loses some of its energy in the process. The excited electron then moves towards the surface of the sample undergoing elastic and inelastic collisions until it reaches the surface. Since the energy is lost in these collisions, for electrons to have some energy left when they reach the surface, their path length has to be small usually ≈10 Å. The volume of SE production is therefore very small allowing better spatial resolution. Moreover, since the depth of SE production is small, their measurement is very sensitive to the topography of the sample. This was very useful for the study of the discs.

3.2. Experimental

The concentration of dyes **1** and **10** used in all studies was $1 \cdot 10^{-7}$ mol dm^{-3} and that corresponds to less than monolayer coverage of the silver surface. 30 μL of the dye **1** or **10** was added to the colloid followed by aggregation with sodium chloride. The same quantity of dye was added also to a PVA-Ag disc and cold deposited film and allowed to adsorb for 10 min. All SERRS measurements were done using Renishaw 2000 Raman spectrometer with 514.5 nm laser excitation. The spectra were recorded using 3 accumulations of 3 s if not stated otherwise. Details of experimental setup and substrate preparation procedures are given in *Chapter 8*.

3.3. Result and Discussion

3.3.1. SERRS substrates

The main requirements for the metal surface for SERRS are roughness, resistance to the harsh conditions, stability over time and reproducibility of the SERRS signal.

The dye **1** and dye maleimide **10** were used as test analytes in the study of the substrates (for structures see *Chapter 2*, pages 42 and 43). Dye **1** was chosen because it is easily prepared in high yield and gives excellent SERRS spectra and dye **10** is the maleimide derivative of dye **1** that is interesting for further studies of oligonucleotide labelling.

Silver colloid was prepared according to a modified Lee and Meisel method[117] using citrate as a reducing agent. That resulted in a mean particle size of approximately 30 nm in diameter. Citrate reduced colloids are relatively stable with time compared to other colloids such as borohydrate reduced colloids. This is probably due to the formation of a citrate layer that reduces aggregation.[118] The TEM images (Fig. 3.1) of the silver colloid immobilised on the glass slides show the presence of particles and aggregates of different shapes and sizes.

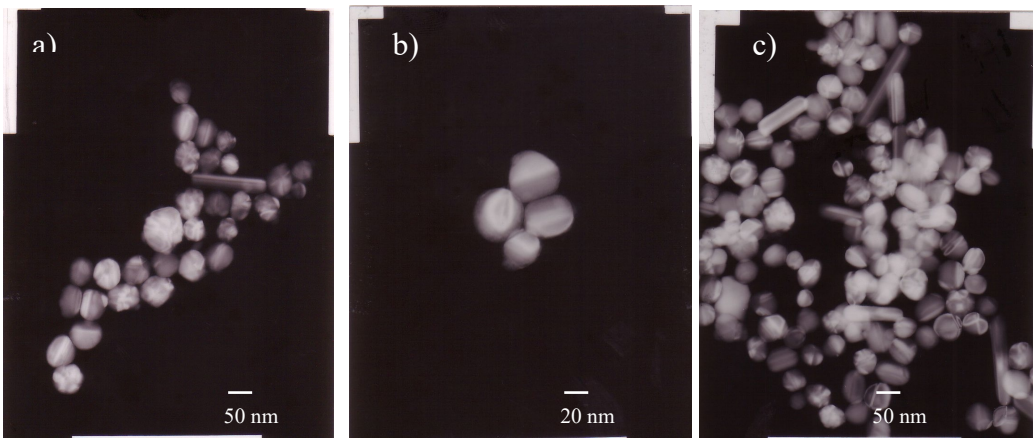

Figure 3.1. TEM pictures of Ag colloid immobilised on grid. Magnification of a) and c) was x120000 and b) x200000.

Figure 3.2 shows the spectra of dye **1** taken from the different substrates. The differences in the intensity of the bands are still not well understood but they may to the conformational changes of the dye on different surfaces.

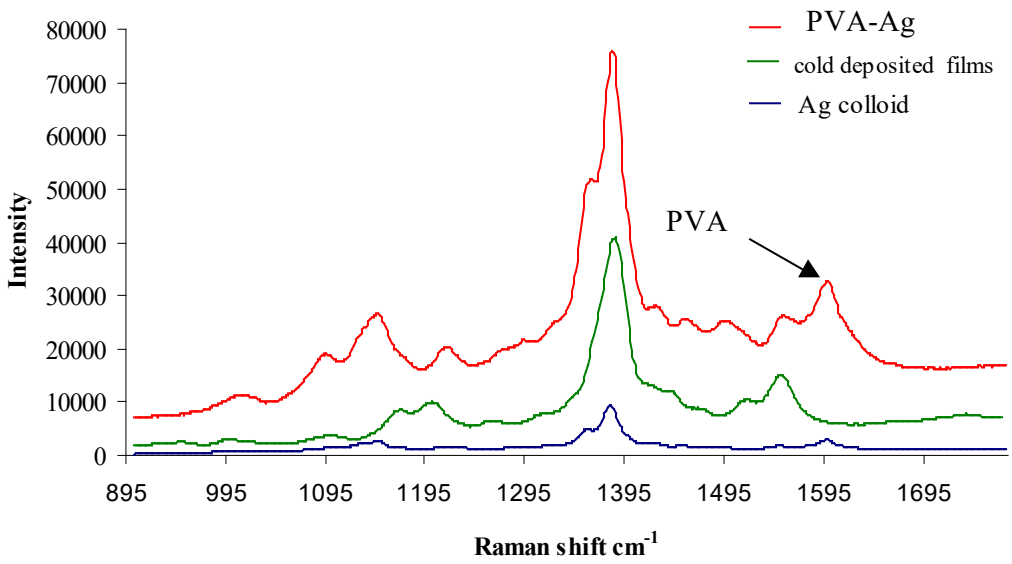

Figure 3.2. The comparison of the spectra of dye **1** taken using three different Ag substrates.

PVA-Ag discs were prepared by mixing PVA and silver nitrate, spin coating the mixture onto glass slides and then reducing Ag (I) with iron (II) sulphate. The stability of the novel PVA substrates with time was investigated. Dye **1** was adsorbed onto the surface and the spectra from the disc recorded over one year period. There were some differences in spectra after 1 year but they did not affect significantly the intensity and the signal to noise ratio of the dye spectra (Fig. 3.3).

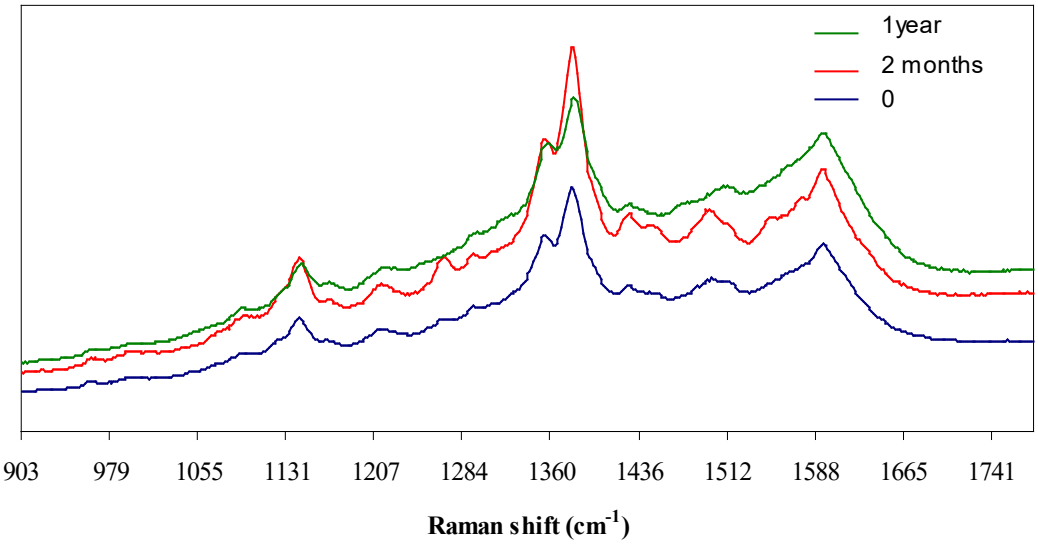

Figure 3.3. Spectra of dye **1** obtained in the time study of PVA-Ag substrate.

The surface maps of both dyes **1** and **10** showed that molecules absorbed on the surface of the PVA disc give intense spectra over the mapped area (Figure 3.4 and 3.5). A three dimensional representation of the surface clearly shows the variability in the SERRS signal over an area of the disc.

A)

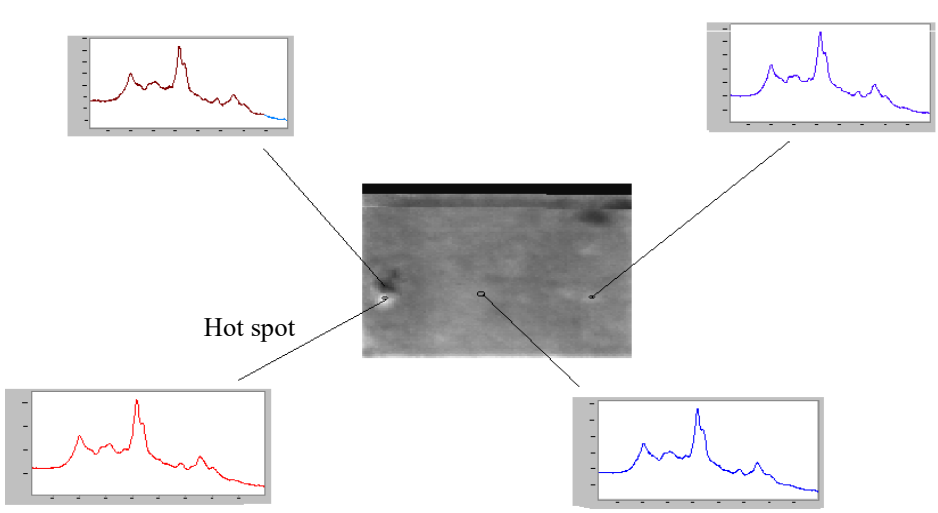

B)

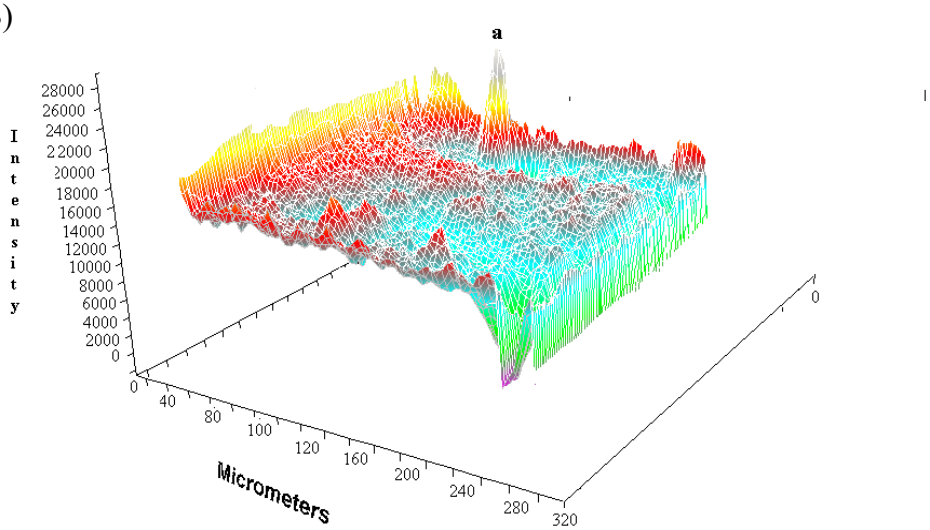

Figure 3.4. A grey scale surface map (A) and 3D representation (B) of the dye **1** on the PVA substrate. The white area on the surface map corresponds to area of the highest (hot spot) and the dark area to the lowest SERRS intensity. The peak a) in the 3D representation corresponds to the spectra taken at the hot spot.

A)

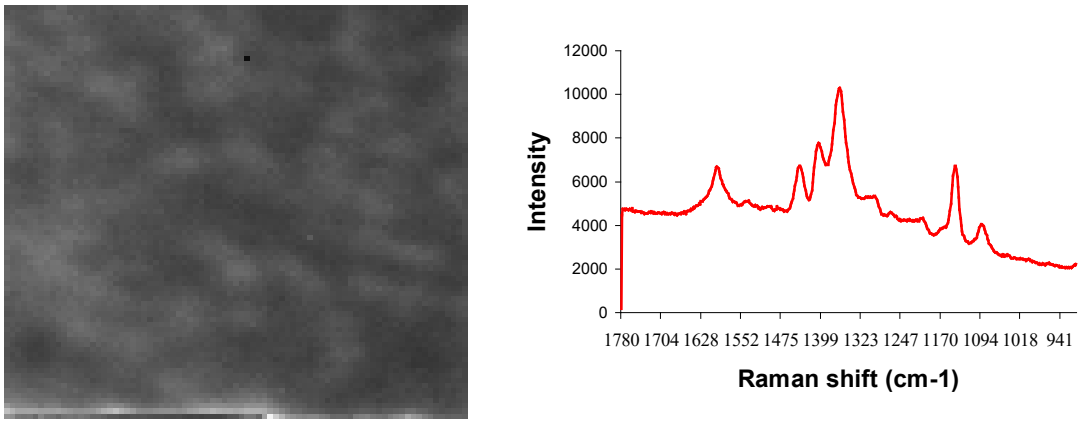

B)

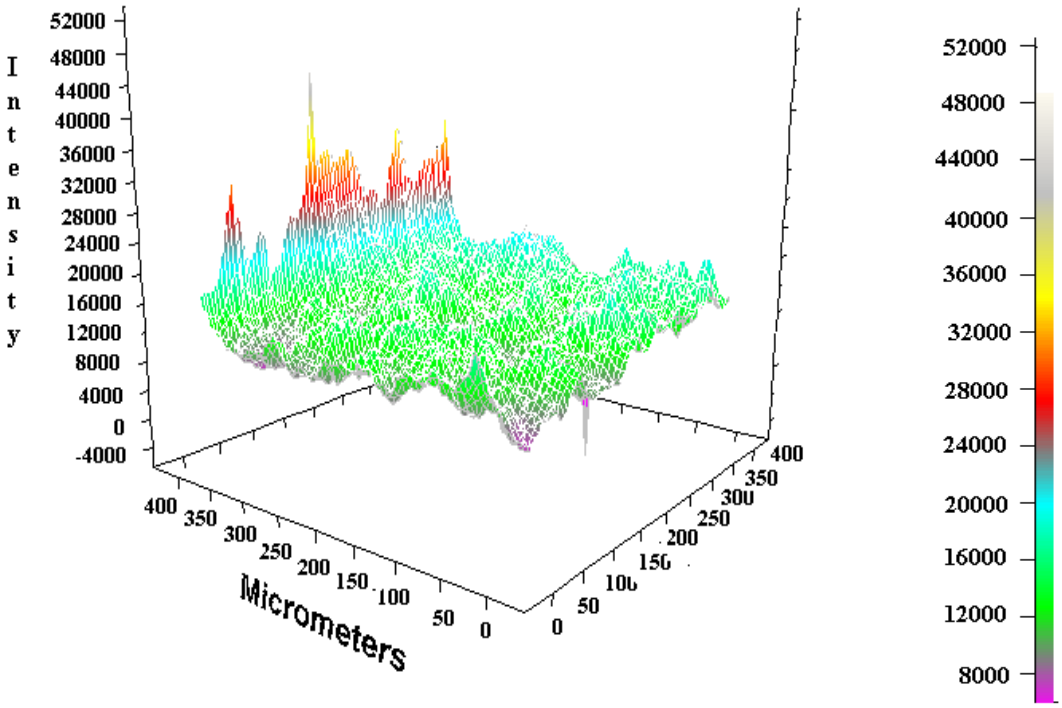

Figure 3.5. The grey scale surface mapping image (A) and the 3D representation (B) of the PVA surface with adsorbed dye maleimide **10**.

The reproducibility of the SERRS signals was estimated by analysis of five different samples of PVA films and measuring SERRS at five different positions on each sample.

All the samples were prepared at the same time using the spin coating system. The percentage relative standard deviations (%RSD) are given below in Table 3.1.

Table 3.1. SERRS intensities (average of five replicates) and % RSD values at different sampling points on one PVA –Ag sample and on five separate samples.

	SERRS (one sample)		**SERRS (5 samples)**	
ν	**I (1380 cm-^{1})**	**I (1143cm^{-1})**	**I (1380cm^{-1})**	**I (1145 cm^{-1})**
Average	44545	18919	43583	15836
St. Deviation	4237	1242	6153	2821
%RSD	10%	6.5%	20%	18%

As can be seen from Table 3.1., reasonably low RSD values were obtained for SERRS analysis from one sample, indicating that SERRS scattering efficiency is relatively similar over the same disc. However, the increase in RSD for different samples showed a poorer reproducibility. Thus, the SERRS efficiency is relatively evenly distributed within one sample but there is a greater discrepancy between films. The reason for this is likely to be the method of film preparation, as the thickness of the silver will vary from film to film. Methods of improving the reproducibility of the film production are currently been investigated by others at Strathclyde.

TiO_2–Ag discs were also investigated. They are prepared by depositing silver onto a glass slip coated with TiO_2 containing sol-gel. It is thought that TiO_2, being a semi conducting material, may provide additional electrons to contribute to the surface plasmon thus increasing the electromagnetic enhancement necessary to obtain good SERRS signals.

The AFM images of TiO_2 substrates together with cold deposited films, colloid immobilised on a grid and PVA-Ag disc (Fig. 3.6) were obtained to get an insight into the surface roughness and specific surface features. Colloid deposited on the grid showed the same features as seen already in TEM images (Fig. 3.1). Clusters of silver particles of different sizes were observed as well as a few nanorods. Silver particles of the cold deposited films are evenly distributed over the area and are rough enough to produce excellent SERRS.[116]

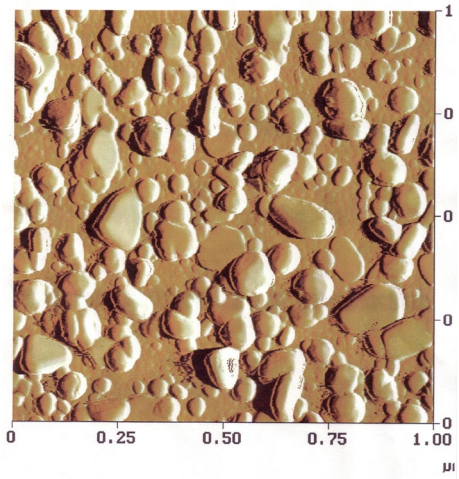

TiO_2 - silver

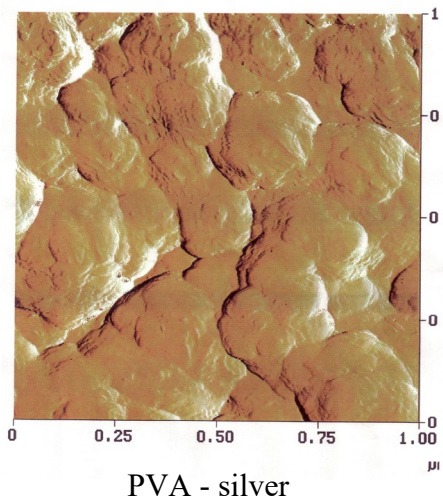

PVA - silver

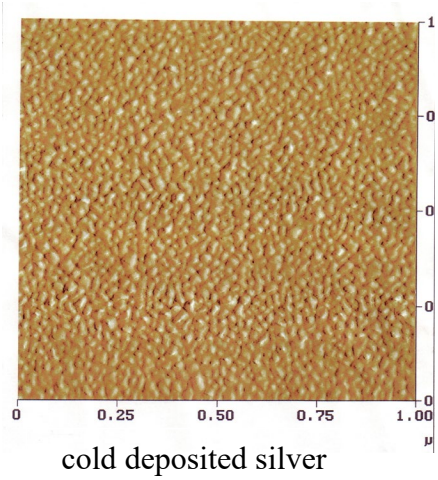

cold deposited silver

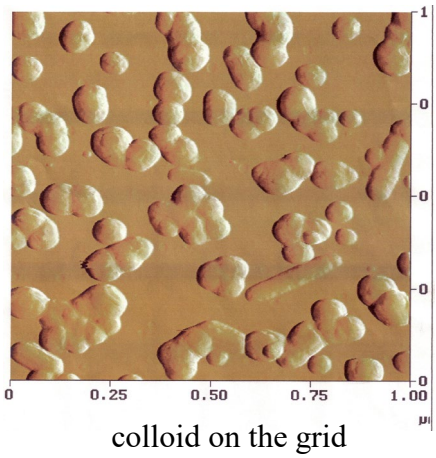

colloid on the grid

Figure 3.6. The AFM images of 4 studied substrates.

TiO_2 particles of random sizes covered with silver make up the TiO_2 substrate, while the features of PVA-silver disc are masked by a polymer, which is covering the surface.

The SERRS spectra and the scattering intensity for TiO_2 –Ag and PVA -Ag discs were compared using dye maleimide **10**. The intensity of the spectrum from the TiO_2-Ag disc was lower than that from PVA-Ag disc (Figure 3.7), but the reproducibility as indicated by the RSD values was better (Table 3.2).

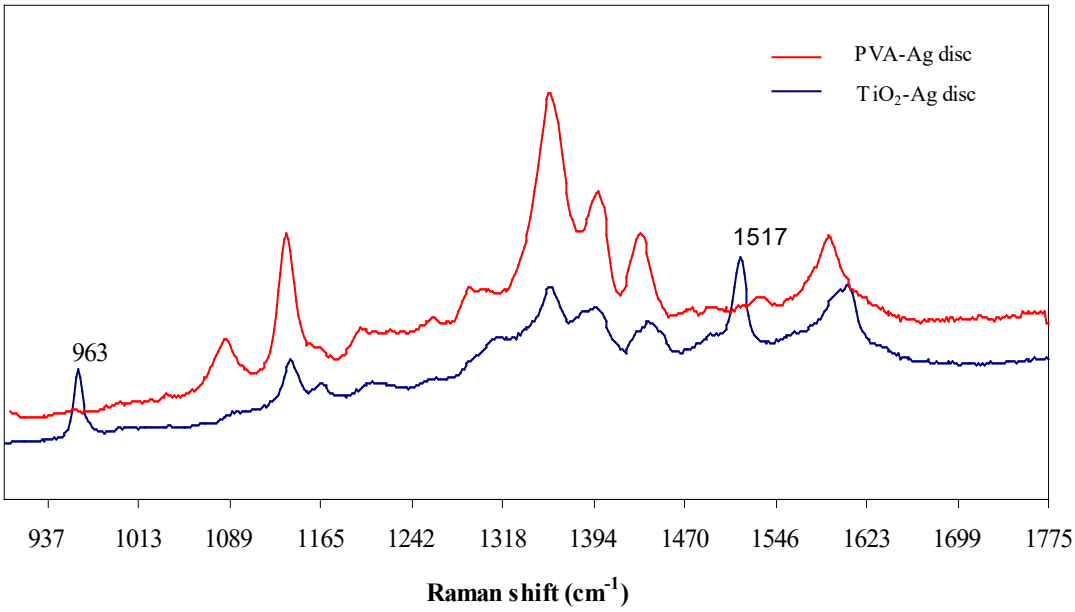

Figure 3.7. The comparison of the spectra of dye maleimide **10** taken using PVA Ag and TiO_2-Ag substrates. The peaks at 963 and 1517 cm^{-1} are attributed to the substrate itself and are not related to the dye.

Table 3.2 SERRS intensities (average of five replicates) and % RSD values at different sampling points on one TiO_2 –Ag sample and on five separate samples.

	SERRS (one sample)	**SERRS (5 samples)**
ν	**I (1358 cm^{-1})**	**I (1358 cm^{-1})**
Average	11442	12245
St. Deviation	994	1859
%RSD	8.7%	15.2%

Although the reproducibility is improved compared to PVA-Ag discs, the surface of the TiO_2-Ag discs is such that dye spreads rapidly over it. It is difficult to achieve the adsorption of the dye by pippeting the small volumes on the surface. Thus, the disc was dipped in the solution of the dye and more than 30 min is necessary for adsorption to be achieved. For comparison, dipping was not necessary for PVA-Ag discs and the adsorption of the dye is achieved in 10 minutes simply by pippeting the desired volume onto the surface. Therefore, PVA-Ag discs are more

suitable for the DNA experiments and could be useful in production of DNA arrays, since the adsorption will be achieved rapidly and the printing or spotting of the labelled DNA would be easier and faster.

3.3.2. Electron microprobe analysis of PVA-Ag discs

Both X-ray fluorescence and secondary electron (SE) measurements were carried out on PVA-Ag disc. The SE image (Figure 3.8) represents the surface of the PVA-Ag disc indicating its topography and roughness.

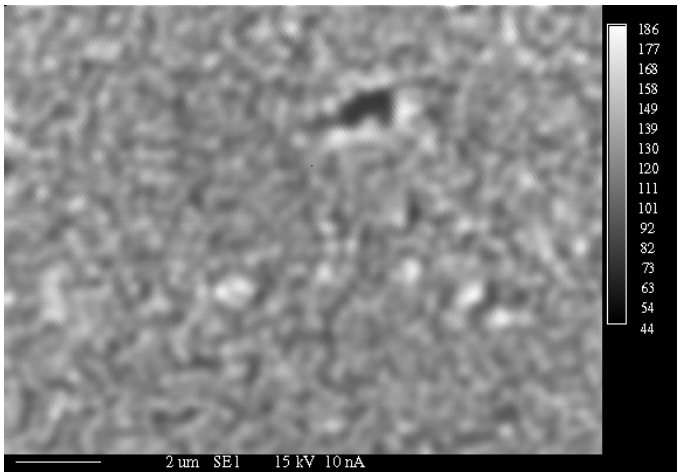

Figure 3.8: The secondary electron image of the PVA-Ag surface. The white and grey areas represent silver.

X-ray fluorescence measurements were taken mainly because there was concern over the possible existence of iron (III) salts, following the reduction of the silver ions with iron (II) sulphate, which could contaminate the surface and possibly interfere with the SERRS measurements. Iron was not found on the surface. Additionally the maps of silver and oxygen from PVA were obtained (Figure 3.9). It can be seen that the maps are complementary to each other showing the distribution of silver and oxygen on the surface.

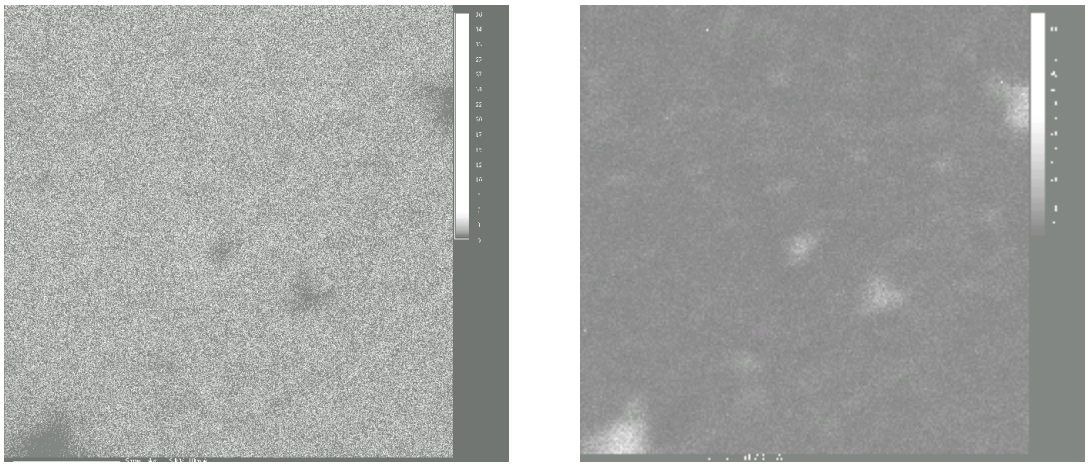

a) b)

Figure 3.9: The silver (a) (white spots) and corresponding oxygen (b) maps of the PVA-Ag surface. Dark patches on a) and bright on b) are the damages on the disc.

When the SERRS map of the investigated disc, which was covered with dye **10,** was recorded, there was no SERRS scattering where the disc was damaged by the electron beam (Fig. 3.10).

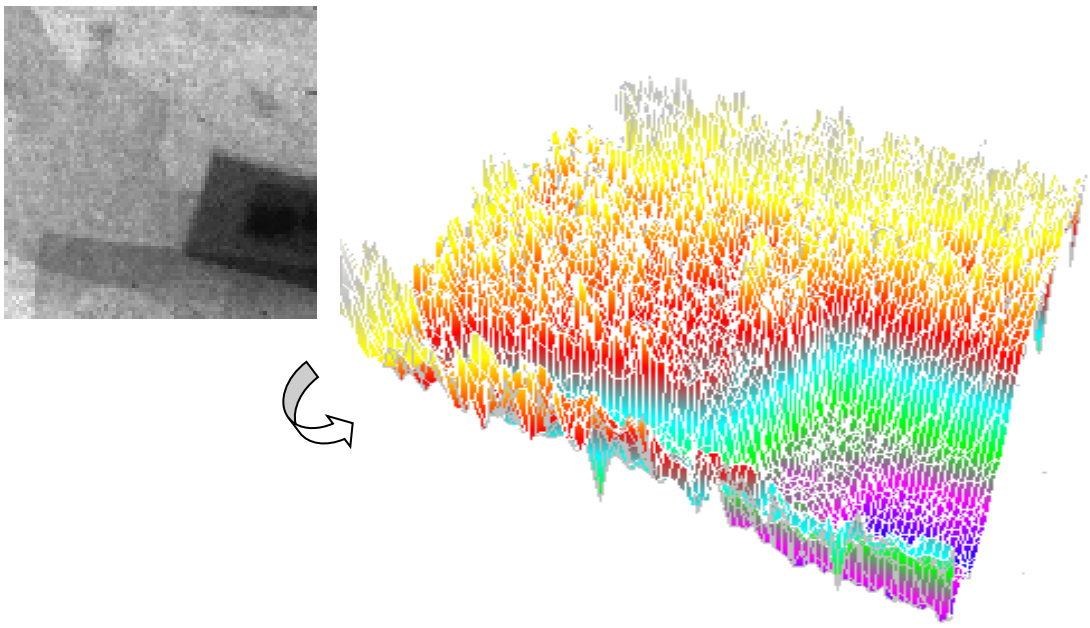

Figure 3.10. The SERRS map of the disc deposited with dye **10** after electron microprobe measurements.

The map shows that there is a great potential of SERRS surface mapping in the investigation of the coverage and distribution of the dyes on the substrate surface. It can be foreseen that in the future special masks can be made to enable the production of SERRS arrays and mapping will be a useful tool in determining the position of the desired species on the surface. For now, SERRS mapping can be used to describe the behaviour and distribution of biomolecules, like DNA or proteins, on the SERRS surface.

Taking into account all the data gathered in the investigation of the substrates, PVA-Ag discs definitely fulfilled most of the requirements for effective SERRS substrates and they were used, along with silver colloid, in the further investigation of labelled oligonucleotides. Results and discussion on oligonucleotide labelling are presented in *Chapter 5*.

Chapter 4

Surface enhanced resonance Raman scattering (SERRS) of the benzotriazole dyes and dye maleimides

4.1. Introduction

SERRS can provide enhancement factors of up to 10^{14} over normal Raman scattering (see *Chapter 1*) and it proved to be an extremely sensitive and selective technique for the detection and identification of suitable molecules, including labelled DNA.[119] As mentioned previously, for a compound to be SERRS active it must adsorb onto the metal surface used to provide the surface enhancement and have an electronic transition at the frequency close to the excitation frequency. An additional advantage of SERRS is that energy transfer can occur from excited states of the molecule to the surface causing fluorescence quenching[65], thus enabling use of a range of chromophores. Although surface enhancement can be obtained by adsorbing a dye onto the metal surface by electrostatic attraction, it is preferable to complex the dye directly to the metal particles. A range of benzotriazole dyes was previously synthesised[88, 120] enabling the covalent attachment of the SERRS active dyes to the surface through benzotriazole. However, their primary amine were difficult to derivatise due to extensive electron delocalisation.[102] This lack of reactivity was disadvantageous when additional chemical modifications of the dyes were desired e.g. to bond them to non SERRS active compounds to act as label.

A new group of more reactive SERRS active dyes was synthesised and explained in detail in *Chapter 2*. The spectroscopic properties of these dyes were investigated to assess their sensitivity for the further use in oligonucleotide labelling and the results are presented here.

4.2. Experimental

A Renishaw 2000 Raman spectrometer with 514.5 nm laser excitation was used for SERRS measurements. The spectra were recorded using 3 accumulations of 3 s, if not stated otherwise. Silver colloid was prepared using modified Lee Meisel method and sodium chloride was used as aggregating agent. PVA-Ag discs were prepared as described in *Chapter 8*. SERRS spectra were recorded using 4×10^{-7} mol dm^{-3} methanol-water solution and any differences in concentration are being referred to at the appropriate place in the discussion. Normal Raman scattering was obtained from solid sample presented as fine powders on glass slides.

4.3. Results and discussion

4.3.1. UV/Vis and SERRS spectra of synthesised dyes

To be SERRS active, a dye has to be adsorbed onto a suitable metal surface and have a chromophore with an electronic transition close in frequency to the laser. [Ref] The maximum absorbance wavelengths and the values of extinction coefficients for investigated dyes are given in Table 4.1.

Table 4.1. UV/Vis data for synthesised dyes.

Dye	λ_{max}/nm	ε / dm^3 $mol^{-1}cm^{-1}$
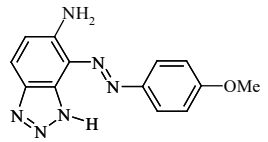 **1**	443.2 (MeOH-H_2O)	16036
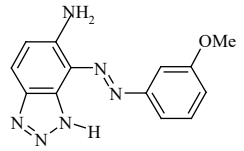 **2**	438.0 (MeOH-H_2O)	12036
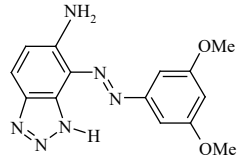 **3**	439.0 (MeOH-H_2O)	13667
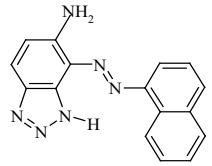 **4**	462.0 (MeOH-H_2O)	14314
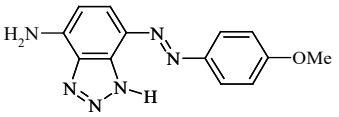 **5**	425.0 (MeOH-H_2O)	29813
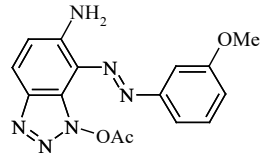 **13**	442.0 (MeOH-H_2O)	1015

Table 4.1 (continued): UV/Vis data for synthesised dyes

Dye	λ_{max}/nm	ε / dm^3 $mol^{-1}cm^{-1}$
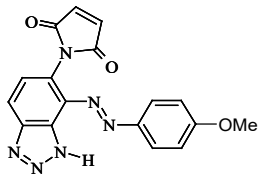 **10**	386.0 (MeOH-H_2O)	17353
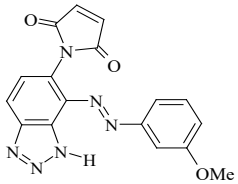 **12**	354.0 (MeOH-H_2O)	11583
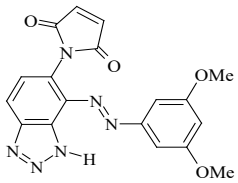 **14**	362.0 (MeOH-H_2O)	13370
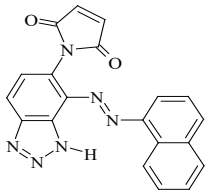 **15**	400 (MeOH-H_2O)	9389

It was expected that dye **4,** with a λ_{max} equal to 462 nm and therefore closer to the wavelength of the laser source (514.5 nm) than the other dyes, would give the most intense SERRS because of the resonance effect. However, this was not the case. In fact, dye **5** with a λ_{max} of 425 nm gave the most intense spectra at $4x10^{-7}$ mol dm^{-3} (Fig. 4.1) with a dominant azo stretch at 1376 cm^{-1}.

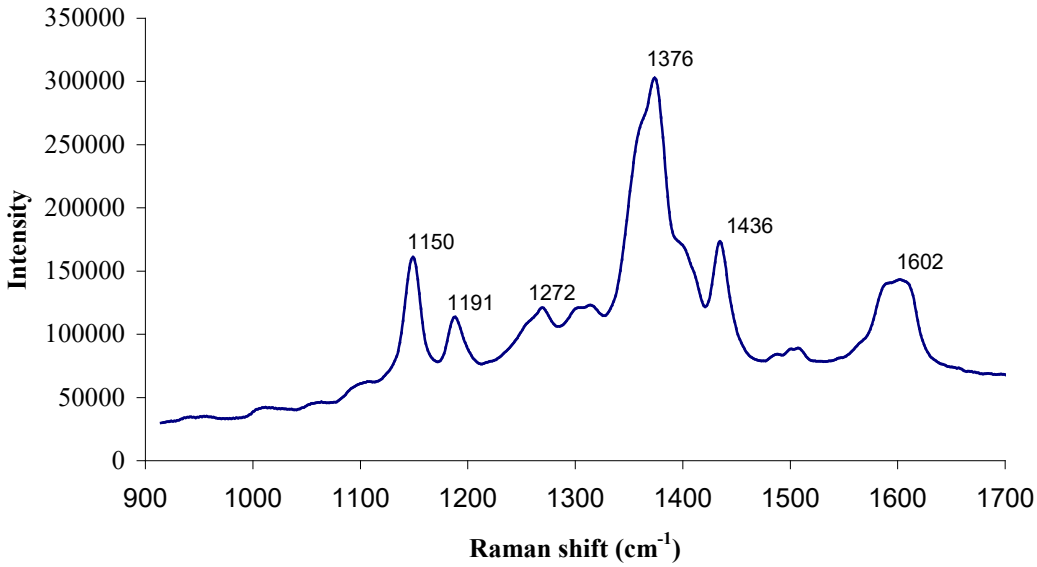

Figure 4.1. SERRS spectra of dye **5** taken in silver colloid.

When the UV-Vis data for all synthesised dyes were compared to the intensity of their azo band in the spectra an interesting correlation was observed. The SERRS intensity increased with the excitations coefficient of the dye (Table 4.2).

Table 4.2. Comparison of the extinction coefficient values (ε) to intensity of the most intense peak in SERRS spectra of the dyes.

Dye	ε (at λ_{max}) / dm^3 $mol^{-1}cm^{-1}$	Intensity of the azo peak
5	29813	305 503
1	16036	188 513
4	14314	154592
3	13667	120932
2	12036	80082
13	1015	3536

We believe that the reason for such behaviour lies in the interaction of the dyes with the surface plasmon at 514.5 nm. The coupling of the surface plasmon and the dyes is more efficient if the energy absorbing transitions in dyes are more allowed. The higher the coefficient, the more allowed are the transitions and therefore coupling with the surface plasmon is more efficient. That leads to more intense SERRS.

However, there are small deviations from linearity (Fig 4.2), which might be explained by other phenomena contributing to SERRS. The biggest deviation is shown by dye **4,** which has λ_{max} close to the laser excitation and therefore may have a larger molecular resonance contribution to the SERRS effect. Because of this additional contribution of the resonance effect, the intensity of SERRS of dye **4** is slightly higher than expected if only the extinction coefficient is taken into account. The linear correlation between extinction coefficient and SERRS intensity has not been observed before. In the future there could be a simple way of determining the SERRS activity of the benzotriazole dye by checking its extinction coefficient.

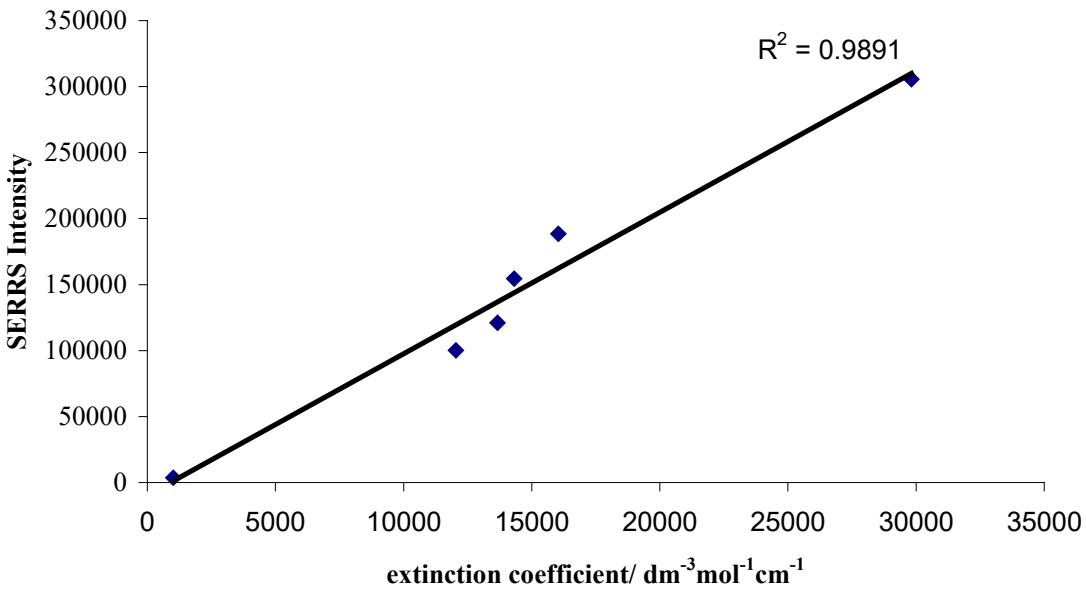

Figure 4.2. Relationship between extinction coefficient and SERRS intensity of six BT dyes.

The same relationship between extinction coefficient and SERRS intensity is not observed for dye maleimides. The λ_{max} of these dyes is shifted towards wavelengths lower than surface plasmon wavelength of the silver colloid (402 nm). Therefore the surface plasmon resonance contribution from these dyes to SERRS enhancement is less. There are additional experiments currently under way to provide a more complete explanation of this phenomenon.

4.3.2. Assignment of the SERRS spectra of BT dyes

To assign the observed bands for azo dyes (Fig. 4.3) and dye maleimides (Fig. 4.4), DFT calculations were performed on dye **10** and Raman and IR spectra of solid dyes were recorded. The DFT calculated values for the dye are given in the Appendix as well as Raman and IR spectra. Published data for other similar compounds *e.g.* benzotriazole[121] and azo dyes [88] were used in assignment of the bands.

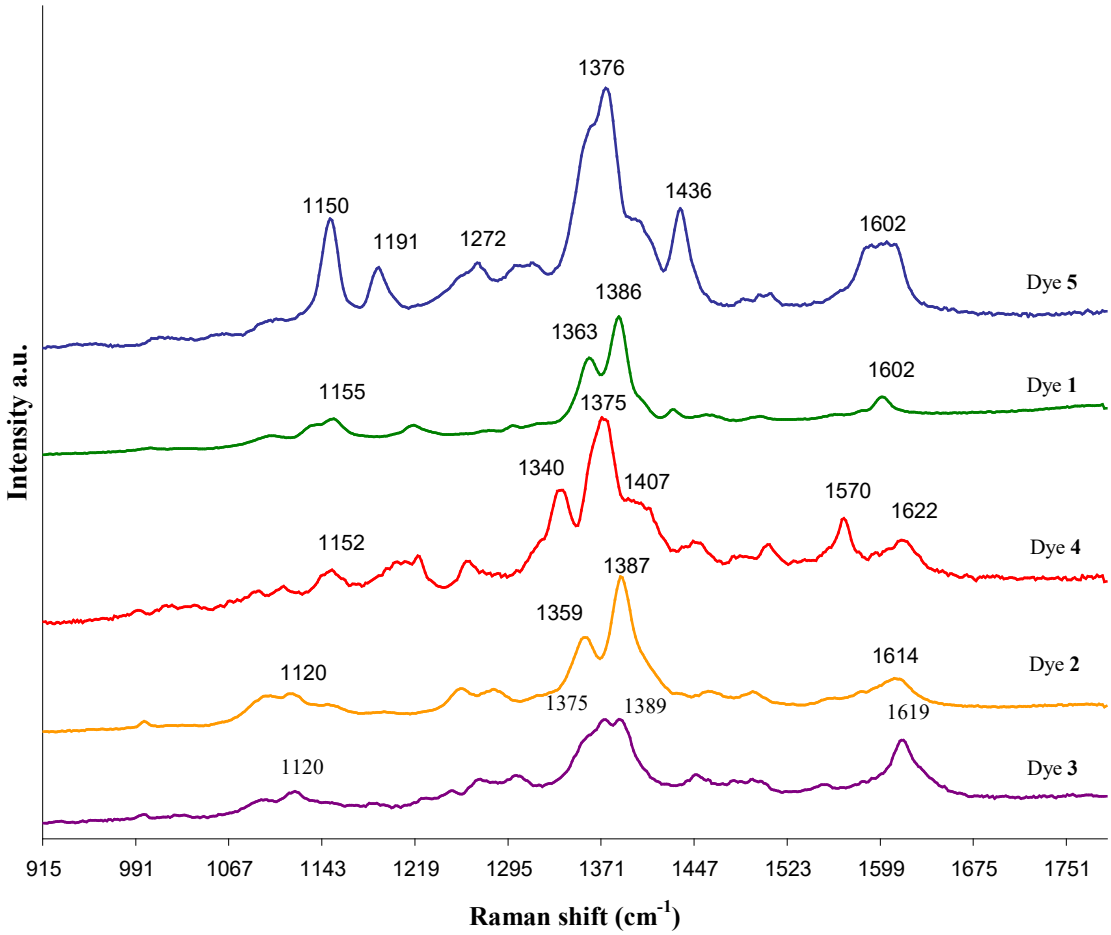

Figure 4.3. SERRS spectra of benzotriazole dyes at 514.5 nm using silver colloid. For display purpose only the strongest bands are labelled. The spectra are displayed with decreasing intensity at the same concentration.

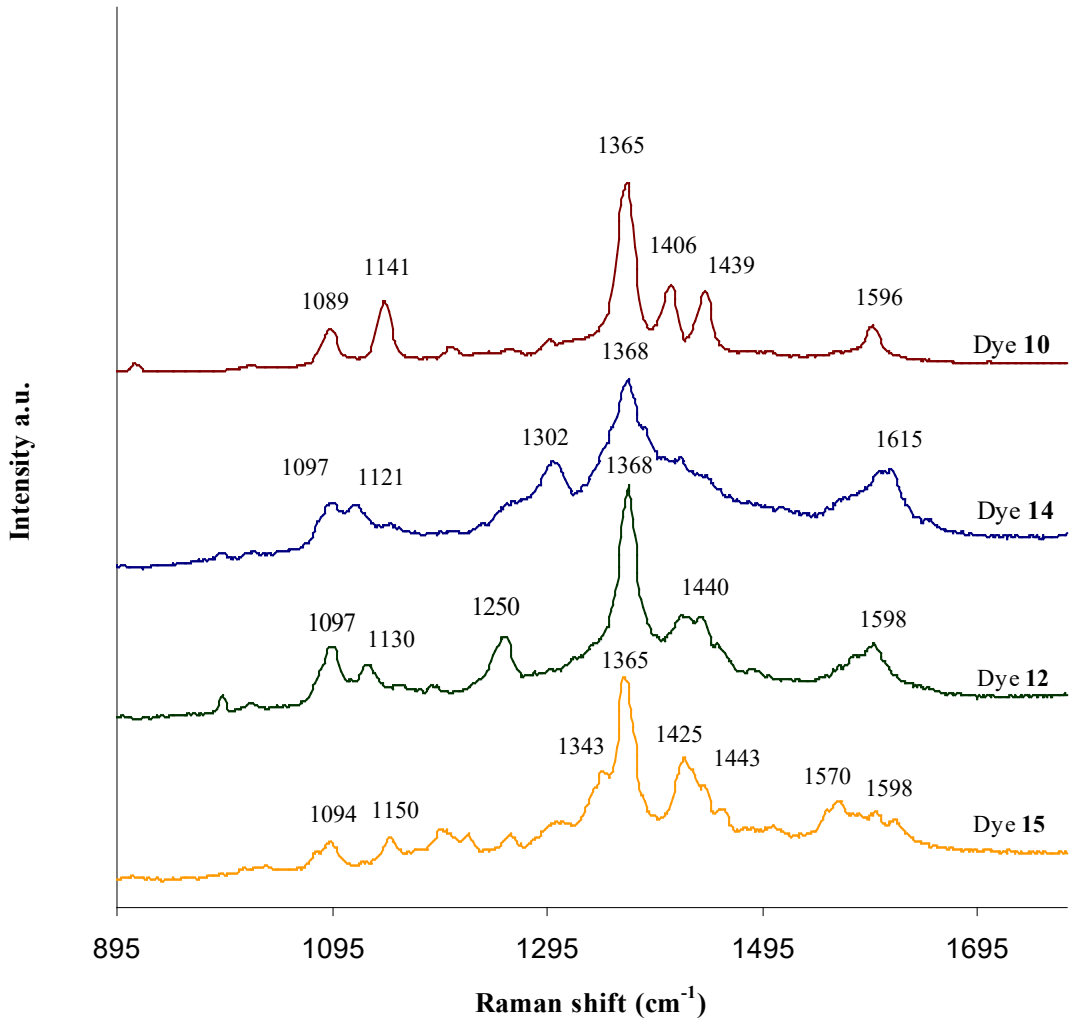

Figure 4.4. SERRS spectra of benzotriazole dye maleimides ($1x10^{-6}$ mol dm^{-3}) taken in silver colloid at 514.5 nm. The spectra are scaled for display purposes.

Several bands were observed that were common to all azo dyes investigated. The band with the highest intensity in all spectra was observed in the 1379-1390 cm^{-1} range and is shown by DFT calculation for dye **10** to be the azo stretch. The following diagrams (Fig.4.5) show DFT results for the main bands of dye **10**.

1) Quadrant stretch with associated azo displacement predicted at 1598 cm^{-1} (1592 cm^{-1} for solid dye)

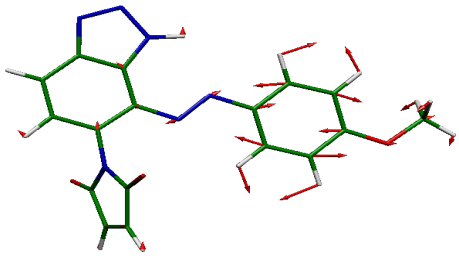

2) Aromatic ring stretches with associated azo stretch predicted at 1434 cm^{-1} (1445 cm^{-1} for solid dye)

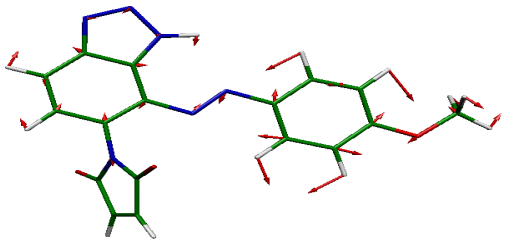

3) Benzotriazole ring and attached phenyl ring stretches predicted at 1421 cm^{-1} (1415 cm^{-1} for solid dye)

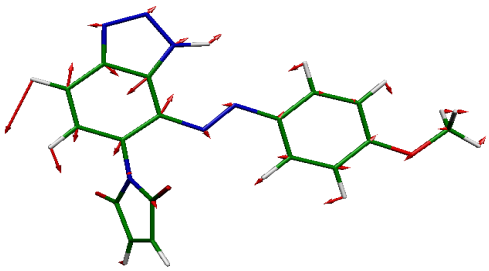

4) Azo stretch with C-C and C-H stretches of aromatic rings predicted at 1378 cm^{-1} (1370 cm^{-1} for solid dye)

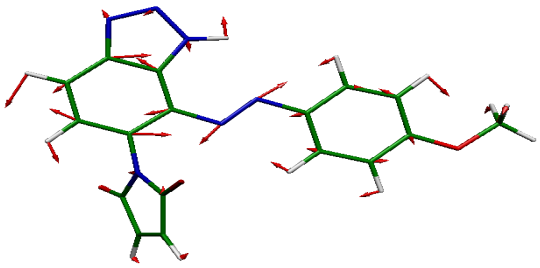

5) C-N and C-H vibrations of maleimide ring with C-H displacements of phenyl rings predicted at 1192 cm^{-1} (1204 cm^{-1} for solid dye)

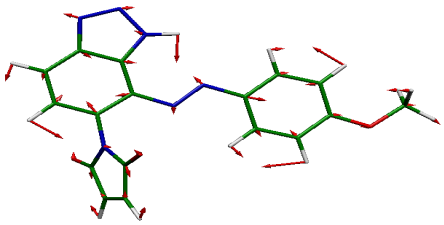

Figure 4.5. Diagrams of vibrational vectors for the significant modes of the dye maleimide **10.** The vibrational modes were predicted by DFT calculation (BLYP/6-31G(d,p)) and compared to the experimental Raman spectra.

Aromatic ring stretches associated with azo displacements appear between 1597-1603 cm^{-1} and 1443-1445 cm^{-1} as strong bands. Benzotriazole ring vibrations are also present in all spectra; the strong band at 1145-1155 cm^{-1} is associated with the combination of skeletal vibrations of benzotriazole ring with in plane C-H bending. A strong band at 1420-1425 cm^{-1} represents the C-C stretch of triazole-phenyl ring system. Additionally, when the spectrum of dye **2** was compared to the spectrum of its

acetylated form, dye **13** (Fig. 4.6)**,** a change in the 1285 cm^{-1} band was observed. That indicates that this strong band also corresponds to the benzotriazole ring vibration with N-H bending**.**

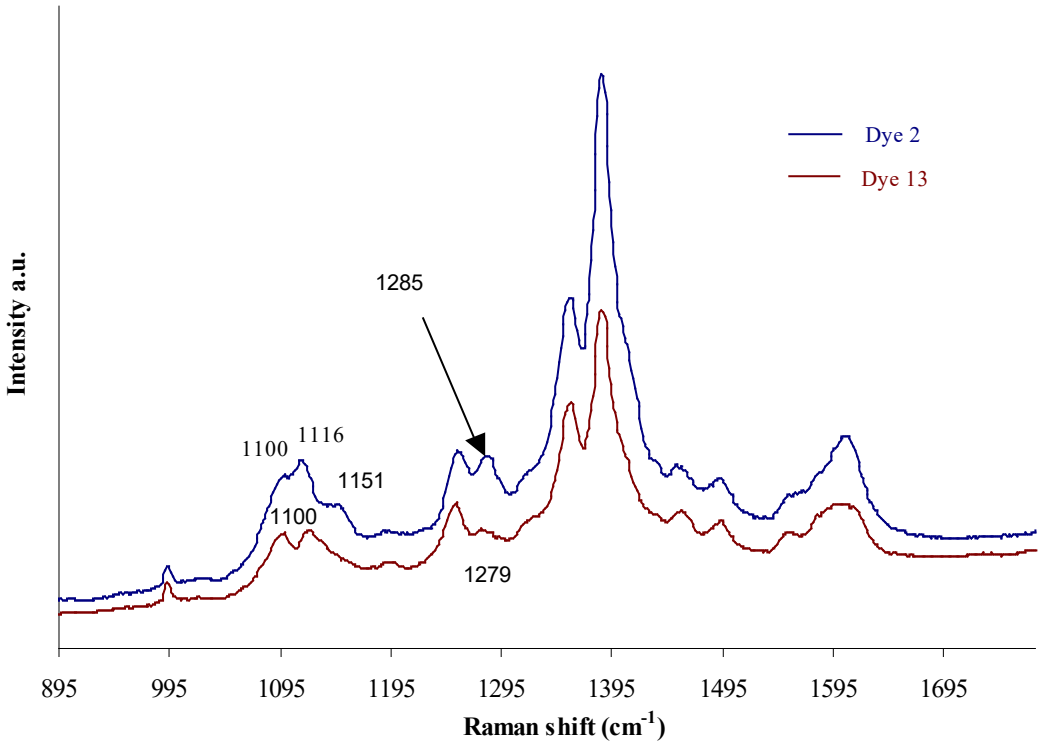

Figure 4.6. The comparison of SERRS spectra of dye **2** and dye **13** taken at 514.5 nm in silver colloid. The spectra are scaled for display purposes.

The vibration observed at 1120 cm^{-1} appears only in the spectra of dyes **2** and **3** which have methoxy groups in meta position and are described as C-H wagging and quadrant C-C stretch of methoxy groups attached to the ring. The bands appearing between 1614 and 1620 cm^{-1} are assigned to the N-H bending of the primary amine and they are observed in all dyes except for the maleimides in which the primary amine is derivatised.

Dye maleimides have weak bands at 1200-1205 cm^{-1} which are not observed in other synthesised dyes and can be assigned to the stretching of the C=C bond and C-N bond of maleimide. The band between 1090 and 1097 cm^{-1} is attributed to the combination of quadrant stretches and C-N vibrations.

The most distinct feature in the spectra of dye maleimides, compared to those of the dyes from which they were synthesised, is the shift of the azo peak to lower wavelengths. The hydrogen bond formed between primary amine and azo nitrogen (Fig 2.8, *Chapter 2*) influences the frequency of the azo vibration, which differs from the frequency in dye maleimides, where the formation of the hydrogen bond is prevented.

4.3.3. The concentration study of BT dyes

Concentration studies were carried out using both silver colloid and PVA-Ag discs as substrates to investigate the limits of detection for every dye. As seen in Fig. 4.7., the spectra of dye **1** taken using silver colloid as substrate changes significantly as the concentration decreases.

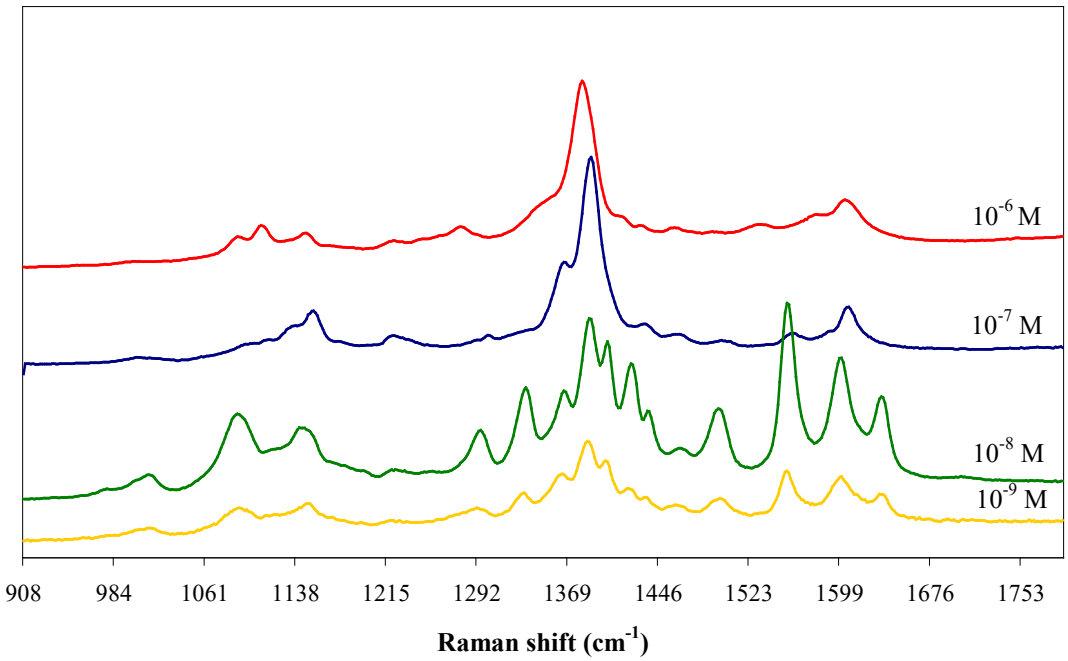

Figure 4.7. Changes in SERRS spectra of dye **1** with concentration. Silver colloid was used as a SERRS substrate for the measurements.

Several new bands appear in the 1290-1600 cm^{-1} region of the spectra at $1x10^{-8}$ mol dm^{-3}, some of which are very intense. Jones *et al.*[122] observed similar changes in the spectra of dye Blue74 and attributed it to the difference in the interaction of the

molecules on the silver surface. Two explanations could give account for the observed differences. First, dye **1** may adopt a different orientation on the metal surface depending on concentration. However, although the bands enhanced in SERS are dependent upon the orientation of the molecule of the surface, this effect is diminished with SERRS.[123] A comparison of resonance Raman and SERRS spectra at 514.5 nm excitation of dye **1** was attempted. Unfortunately, it was not possible to obtain good quality resonance Raman spectrum of solid dye **1** due to the high fluorescence background. Therefore, dye **5**, which gives an excellent resonance Raman spectrum at 514.5 nm was used for comparison (Fig. 4.8). There were three new bands in the SERRS spectrum and some changes in the position of the bands compared to the resonance spectrum. This indicates that orientation of the dye on the metal surface may be responsible for differences between the resonance Raman and the SERRS spectrum.

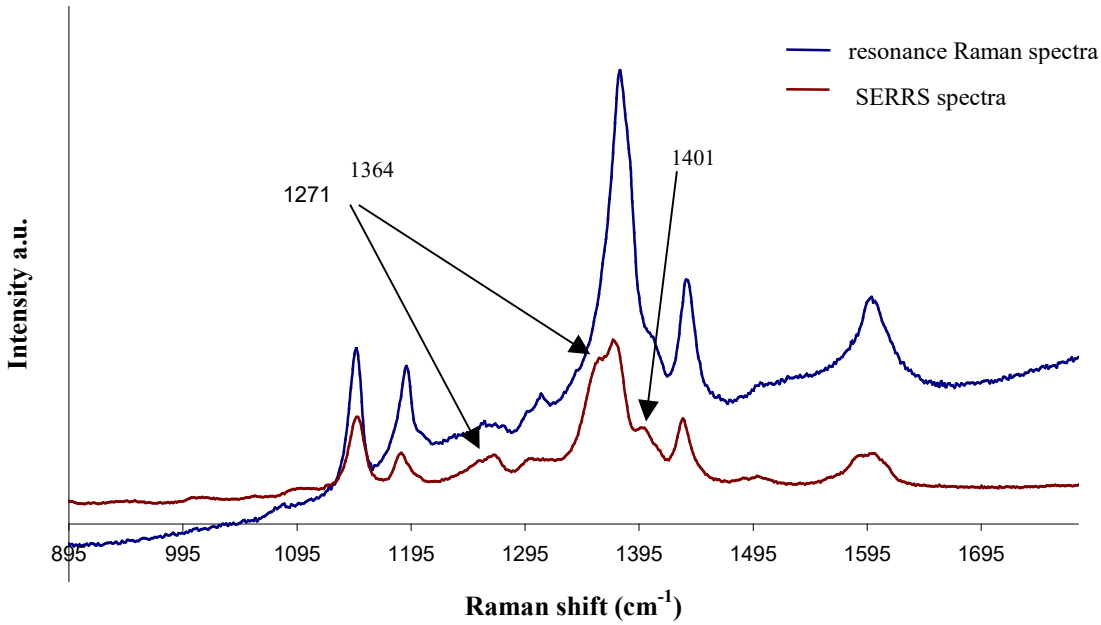

Figure 4.8. Resonance Raman and SERRS spectra of dye **5** at 514.5 nm. The spectra are scaled for display purposes. Three peaks that account for the Arrows indicate differences in spectra.

However, differences in orientation are unlikely to account for the changes that are observed in the spectra of BT dyes as concentration decreases. The reason may be that a change in orientation has led to the difference in metal complexing

between silver and dye molecules. Dye **1** appears to be a pure azo at higher concentrations with a clear azo stretch at 1384 cm^{-1}. However, at lower concentrations the clear azo band is lost as indicated by the appearance of new bands. The changes with the concentration occur only with the dyes that have primary amino group ortho to azo bond (dyes **1**, **2**, **3**, **4**). We believe that these changes occur due to additional silver metal complexing through the primary amino group and the azo bond. This would cause the loss of the pure azo character observed in the spectra at low concentrations. If that were the case, acetylated dye or dye maleimides, where the primary amine is derivatised, would not behave in the same way and this was indeed observed. The SERRS spectra of acetylated dye **13** at different concentrations are shown in Fig. 4.9.

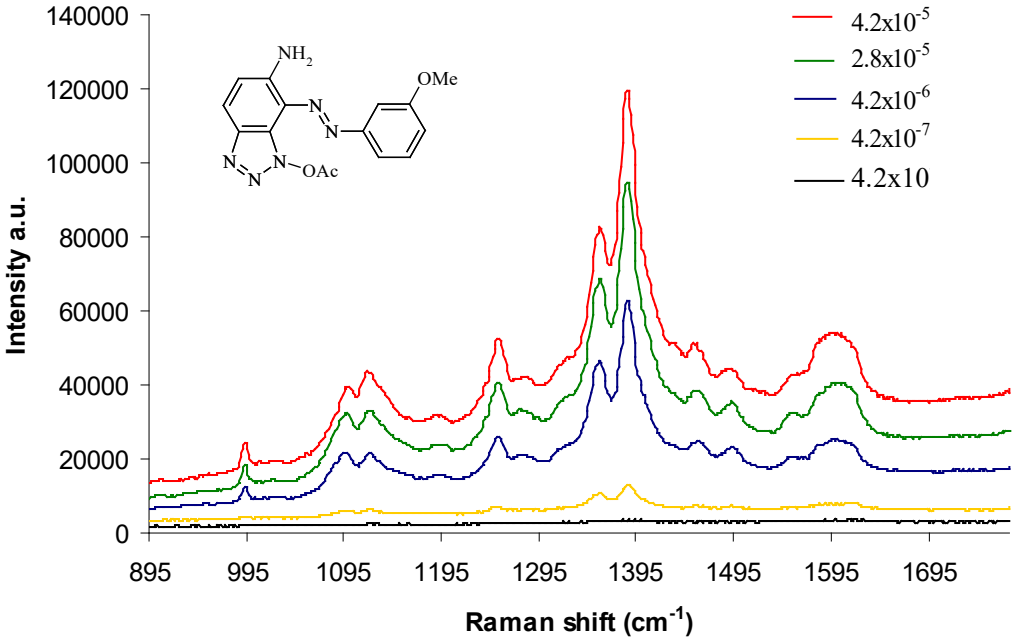

Figure 4.9. SERRS spectra of acetylated dye **13** in silver colloid at different concentrations in mol dm^{-3}.

The benzotriazole nitrogen of dye **13** is acetylated and not accessible for metal complexing and there are no changes in SERRS spectra at different concentrations. Furthermore, when spectra of benzotriazole maleimide dyes are recorded, there are also no changes with concentration. Maleimide dyes are derived from amino benzotriazole dyes and their amino group is replaced with a maleimido group, which does not complex to the silver.

When PVA silver discs were used as the metal surface, the spectra of the dyes were similar to those obtained with colloid but did not change with concentration. This might be due to the polymer film that is coating silver particles and restrains the orientation of the dye molecules and movement of the silver nanoparticles within the substrate. Hence, the metal complexing of the dye does not change with concentration.

4.3.4. Mulitiplexing by SERRS

4.3.4.a) Dye maleimides in a mixture

Preliminary studies were conducted to investigate the potential of the synthesised SERRS dyes to distinguish individual species in a mixture of labelled species (multiplexing). This is particularly important in biotechnology where the identification of certain genetic diseases is simplified by finding individual DNA suquences in a mixture.

The most widely used technique for multiplexing today is fluorescence. However, the number of possible labels, which can be identified in the same mixture is limited due to the overlapping emission spectra of individual labels. That limits the sensitivity and as well the number of possible fluorophores to be used. On the other hand, SERRS multiplexing enables the identification of many labells *in situ*. Previously, work has been done in distinguishing different commercial fluorophores used in DNA labelling in a mixture by SERRS.[124] To investigate the multiplexing potential of three SERRS dye maleimides, the individual spectra were recorded and compared to the mixture (Fig. 4.10.). The spectrum of the mixture shows the features from each of the individual dyes allowing the identification of the components.

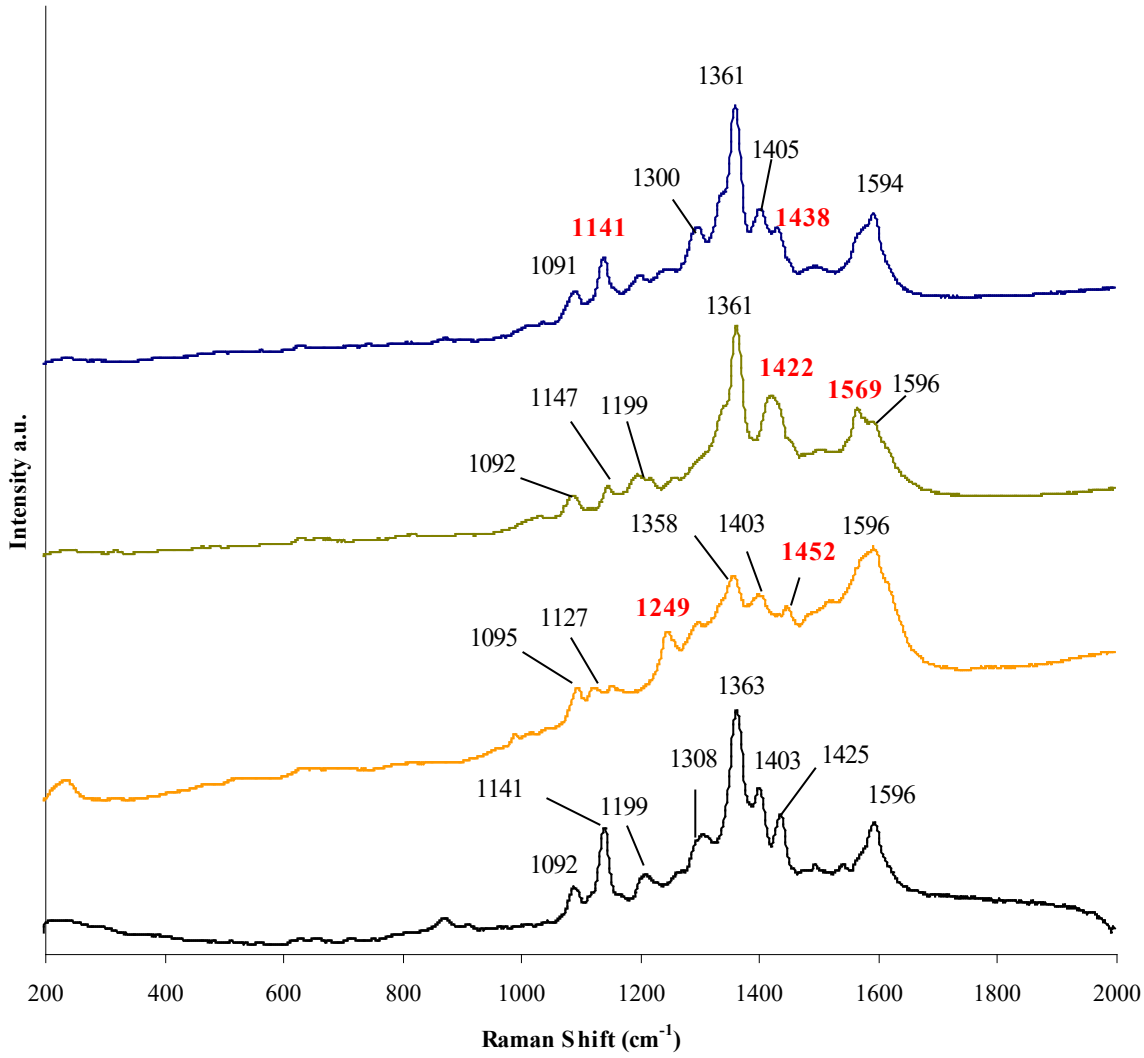

Figure 4.10. SERRS spectra of three dye maleimides and their mixture on PVA silver disc. Concentration of each maleimide dye individually and in the mixture was $1x10^{-6}$ mol dm^{-3}. The spectra are scaled for display purposes and fingerprint peaks are marked red.

Maleimides studied have unique peaks that can be used as fingerprints (Table 4.3).

Table 4.3. Raman shifts of fingerprint peaks for three different dye maleimides.

Dye **10**	Dye **12**	Dye **15**
1438 cm^{-1}	1452 cm^{-1}	1422 cm^{-1}
1141cm^{-1}	1249 cm^{-1}	1569 cm^{-1}

SERRS maps were recorded to provide additional information. 10 µL of each maleimide **10**, **12** and **15** were individually spotted on to the PVA- Ag disc and allowed to mix and adsorb on the surface for 20 min. The spectra over a randomly selected area of the disc were recorded and maps produced using the fingerprint peaks for each maleimide (Figure 4.11).

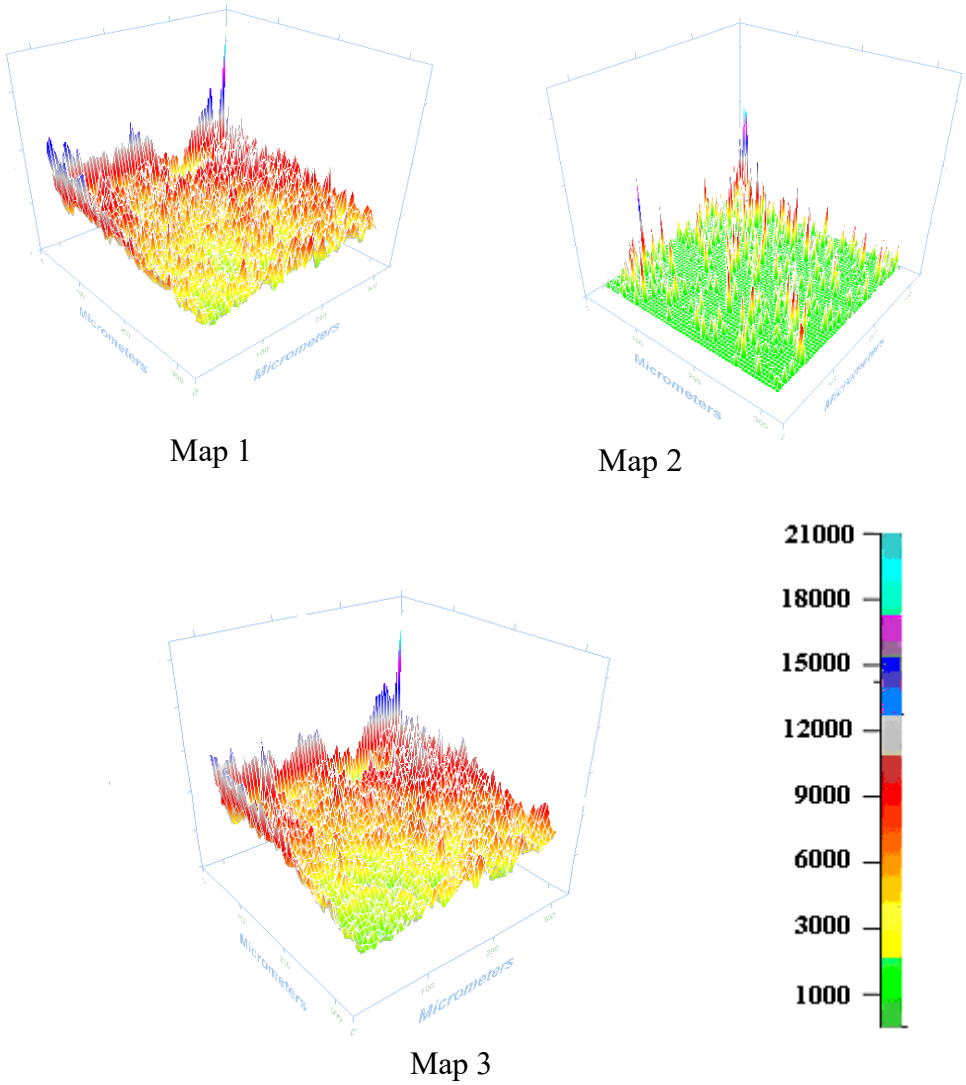

Figure 4.11. SERRS maps created with respect to fingerprint peaks of each studied dye maleimides. Map 1 corresponds to dye **15**, map 2 to dye **12** and map 3 to dye **10**. Spectra were accumulated over 400x400 µm area. Red region of the map represents the highest and the green the lowest intensity of the recorded spectra. The concentration of each dye was $1x10^{-6}$ mol dm^{-3}.

Map 1 was created from the intensity of 1422 cm^{-1} peak characteristic for dye **15** and it showed high intensity and dense distribution on the surface (indicated by red – yellow areas). When map 2 of 1249 cm^{-1} peak (dye **12** fingerprint) was obtained, it showed just a few peaks indicating that dye **12** is not present on the whole mapped area in significant amounts. Map 3 obtained by using 1141 cm^{-1} fingerprint peak for dye **10** the distribution was similar to that of map 1 although the green area in the bottom corner means that the distribution of dye **10** at that region is very low. From the presented maps it can be concluded that only dye **10** and **15** are present on the mapped area in significant amounts, while there is an absence of dye **12**.

These preliminary studies show the huge potential of SERRS mapping for discrimination of labels in the mixture, but further research is under way taking into account the relative intensities and concentration of investigated dyes.

4.3.4.b) Dye maleimide 10 and Diels Alder cycloadducts in the mixture

To investigate further the potential of benzotriazole dye maleimides and SERRS for DNA labelling, the spectra of dye **10** and two different Diels Alder cycloadducts of it were studied. The main advantage of using Diels Alder chemistry in labelling and detection with SERRS is the formation of a new distinct molecular species during the addition of the label (see *Chapter 1*). A range of dienes with benzotriazole maleimide as dienophile was previously examined and the differences between the starting material and cycloadduct were observed in the SERRS spectra.[100] Seven different dienes were used and each cycloadduct gave unique spectra different from the spectra of benzotriazole maleimide. A similar approach was taken with dye maleimide **10**. Two different cycloadducts were synthesised and their SERRS spectra compared to the spectrum of the starting dye (Fig. 4.12.).

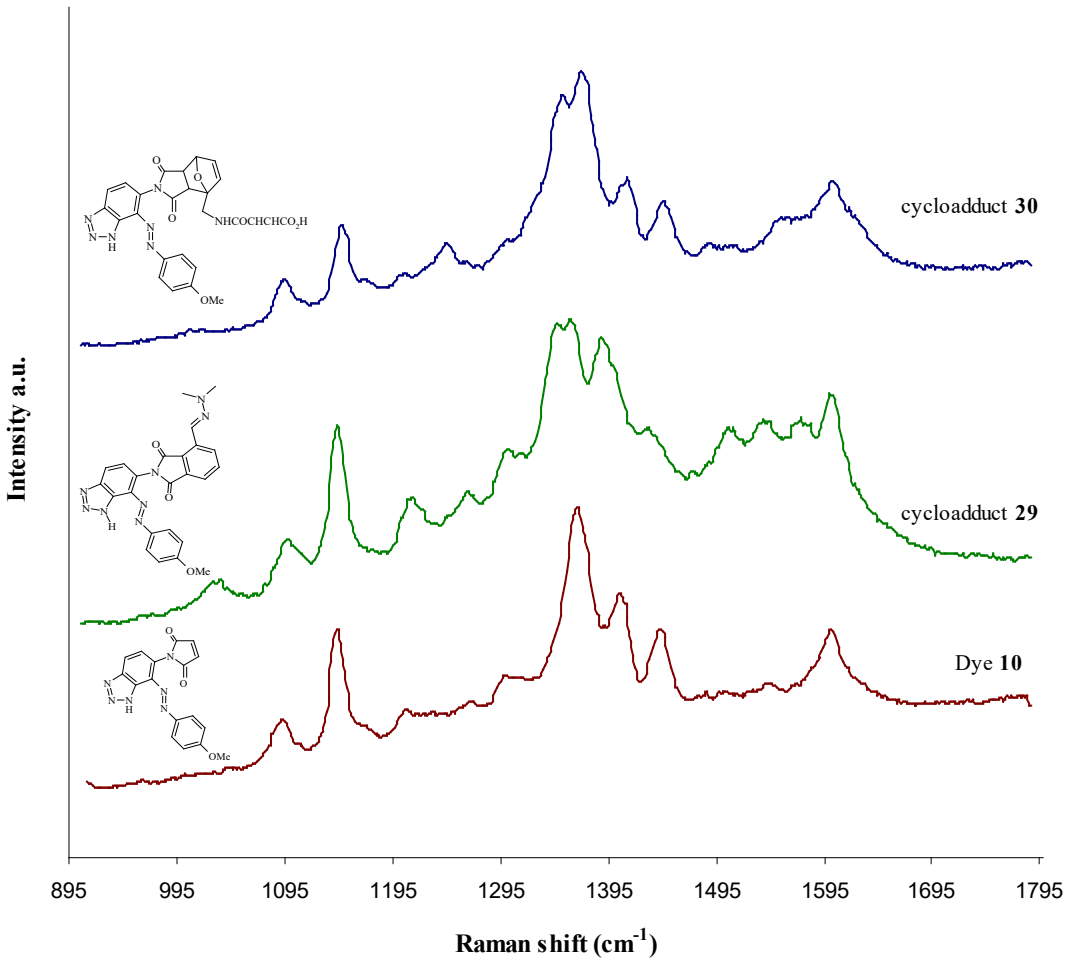

Figure 4.12: SERRS spectra of maleimide cycloadducts **29** and **30** and dye maleimide **10**. All spectra are taken on PVA silver disc using 514.2 nm laser. The spectra are scaled for display purposes.

The spectra of cycloadducts show that there are clear differences between the starting material and cycloadducts (Table 4.4). There are changes in the position and the intensity of the peaks in the 1200-1300 cm^{-1} region where maleimide ring vibrations occur. This is expected because of the formation of the cycloadducts, which changes the structure of the molecules and therefore influences the vibrations. The most striking difference is the appearance of the new peaks in both cycloadducts at 1345- 1350 cm^{-1} and 1542 cm^{-1}. In this region, the peaks are usually assigned to azo peak stretches and quadrant stretches of phenyl rings in combination with azo displacements. The formation of new peaks indicates that the bulky groups present in cycloadducts influence the azo vibrations.

Table 4.4. Comparison of the Raman shifts (cm^{-1}) of the characteristic bands of dye maleimide **10** and its cycloadducts. The biggest differences are marked red.

Dye maleimide **10**	Cycloadduct **29**	Cycloadduct **30**
n.o.	1029 (w)	n.o.
1089(m)	1093 (m)	1090 (m)
1141 (s)	1143 (s)	1142 (s)
1204 (vw)	1209 (s)	n.o.
n.o.	n.o	1241 (w)
n.o.	1267 (w)	n.o.
1300 (w)	1298 (s)	n.o.
n.o	1345 (vs)	1350 (vs)
1361 (vs)	1359 (vs)	1363 (vs)
1405 (s)	1396(s)	1405 (m)
1438 (m)	1430 (vw)	1438 (m)
n.o.	1503 (m)	n.o.
n.o.	1542(m)	1544 (w)
n.o.	1571(m)	n.o
1595 (s)	1598 (s)	1599 (s)

(vw) very weak; (w) weak; (m) medium; (s) strong; (vs) very strong; (no) not observed.

Observed changes in spectra of the Diels Alder products are big enough to enable detection of cycloadducts in the presence of the starting material. Therefore there is no need for separation of the starting material from cyloadducts prior to SERRS detection. These results are used further in developing the novel DNA labelling chemistry and detection by SERRS, which is described in the following chapters.

Chapter 5

Oligonucleotide labelling and detection using Diels Alder cycloaddition and SERRS

5.1. Introduction

A number of methods for detecting specific DNA sequences have been used to provide data for the diagnosis of diseases and examination of gene expression. The most widely used methods rely on either mass spectrometry[125] or fluorescence detection[126] after specific molecular biological event occured. Advanced fluorescence techniques such as Taqman (see *Chapter 1*, page 24) and Molecular Beacons dominate the field of fluorescence detection of DNA and are able to provide real time data in PCR experiments. However, the addition of fluorescent labels to oligonucleotides to enable the detection is disadvantageous since most labels have appreciable biological activity if they associate with DNA in non covalent fashion.[16] Furthermore, the synthesis of suitable labels is often complex and expensive.

SERRS offers improved sensitivity and the ability to identify the components in a mixture without separation. Initially, fluorescent labels were used in the detection of DNA by SERRS as some fluorophores can be excellent SERRS labels due to the efficient fluorescence quenching ability of metal.[65] Therefore, suitable fluorescence labels may be used for SERRS, as well as specifically designed SERRS dyes, if the requirement of the adsorption to the metal surface is fulfilled.

SERRS has been successfully used in the detection of femtomolar concentrations of fluorescently labelled DNA and in multiplex genotyping.[127] In an effort to make use of the great detection potential of SERRS and increase the range of labels for detection, a new approach to labelling based on Diels Alder chemistry was developed. Diels Alder cycloadditon was chosen as a labelling method because it is a fast, high yielding reaction, which occurs in aqueous solutions.[128a,b] Therefore it is particularly suitable for reactions involving biologically important molecules.

The method for using the Diels Alder cycloaddition to generate SERRS active oligonucleotides involves the addition of a small diene tag to the 5' end of the oligonucleotide. The diene oligonucleotide can then be used for cycloadditions with a range of dienophiles. Both fluorescent and SERRS dienophiles can be used to label DNA in this way for either fluorescence or SERRS detection. The main advantage of using cycloaddition with SERRS is that a new distinct molecular species is produced after the addition of the label. Benzotriazole maleimide dyes were successfully synthesised (*Chapter 2*) and their application in DNA labelling using Diels Alder

chemistry is described in this chapter. The principle of Diels Alder was further proven using a range of commercially available fluorophore maleimides as dienophiles.

The stability of modified oligonucleotides was assessed by determining the melting temperature. The melting temperature (T_m) is defined as the temperature at which 50% of the DNA exists as a duplex and 50% as single strands. Accurate measurement of T_m is obtained by conducting UV melting experiments. The UV absorbance of single stranded DNA is higher than the absorbance of duplex DNA. This is due to a property known as hypochromicity and arises from the coupling of transition dipoles between neighbouring stacked bases. The melting curve is obtained by measuring the change in UV absorbance as the temperature increases and plotting a graph of temperature *vs* absorbance. The first derivative of this curve is used to calculate a value for T_m, and can be used to describe duplex stability. This is an important factor in antisense therapy, PCR and gene recognition and to indicate any changes in stability upon the modification of the single strands.

5.2. Experimental

Oligonucleotides were synthesised using an Expedite 8909 oligonucleotide synthesiser and purified by reverse phase HPLC (experimental details are given in *Chapter 8*). SERRS spectra were taken using a Renishaw Raman spectrometer with 514.5 excitation laser and silver colloids and PVA-Ag discs as substrates. A Cary Eclipse fluorimeter was used to measure the fluorescence at different excitation wavelengths.

5.3. Results and Discussion

5.3.1. Synthesis of modified oligonucleotides for Diels Alder cycloaddition

5.3.1. a) Furan modification

The study of the cycloaddition of benzotriazole maleimides with different dienes indicated that furan was a suitable diene to use.[100] It readily undergoes the Diels Alder cyloaddition. Therefore it was decided to add a furan moiety to the 5' end of synthetic oligonucleotides. Two different 12 base long single stranded oligonucleotides (probe 1: 5'-TCT-CAA-CTC-GTA-3' and probe 2: 5'CGC-ATT-CAG-GAT-3') were synthesised using an automatic synthesiser and in the final step a commercially available amino phosphoramidite linker added to the 5'end. Furan derivative **29** was made by reacting 2-furfuryl amine with succinic anhydride using 1,1–carbonyldiimidazole as a coupling agent. A solution of the furan carboxylic acid was then added to a solid phase synthesis column containing the amino oligonucleotide bound to a solid support (Scheme 5.1).

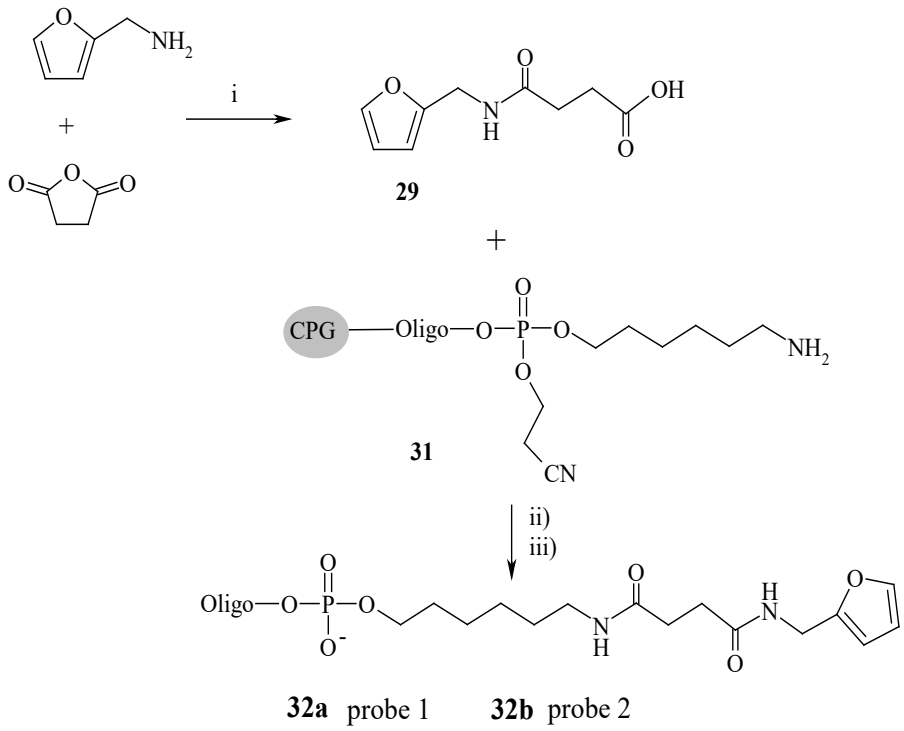

Scheme 5.1. Addition of the furan to the 5' terminus of the oligonucleotide: i) DCM, 4h, ii) CDI, DMF, 40°C, 3h iii) NH_4OH, 55°C, 12h.

The modified oligonucleotides were cleaved from the solid support and the protecting groups removed in one step by heating in concentrated ammonia. Finally, they were purified by reverse phase HPLC. Efficiency of coupling was estimated by comparing the intensity of the last failure oligonucleotide sequence and the furan modified oligonucleotide and was found to be greater than 95% (Fig. 5.1.). MALDI mass spectra of probe 2 furan **32b** showed only one peak at 4025.40, which confirmed that the oligonucleotides were successfully modified with furan.

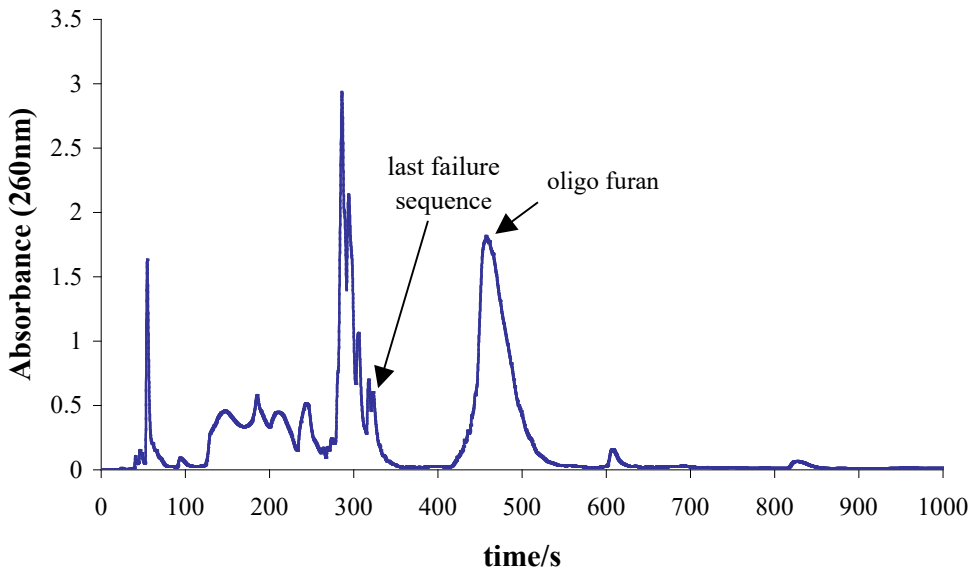

Figure 5.1. Reverse phase HPLC trace for the purification of furan modified oligonucleotide **32a** using method 1 and a C-18 Chromolith column.

5.3.1. b) Butadiene modification

Butadiene phosphoramidite was synthesised by David Robson and used to improve the addition of the diene moiety to the oligonucleotide and to widen the range of dienes used. Butadiene phosphoramidite was added to 5' end of oligonucleotide during automated synthesis allowing 30 min coupling time. Modified probe **33** was purified by reverse phase HPLC (Fig. 5.2.).

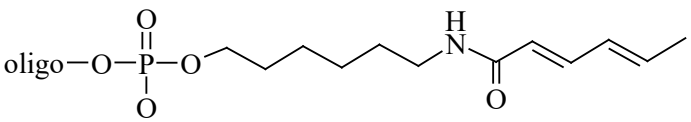

33

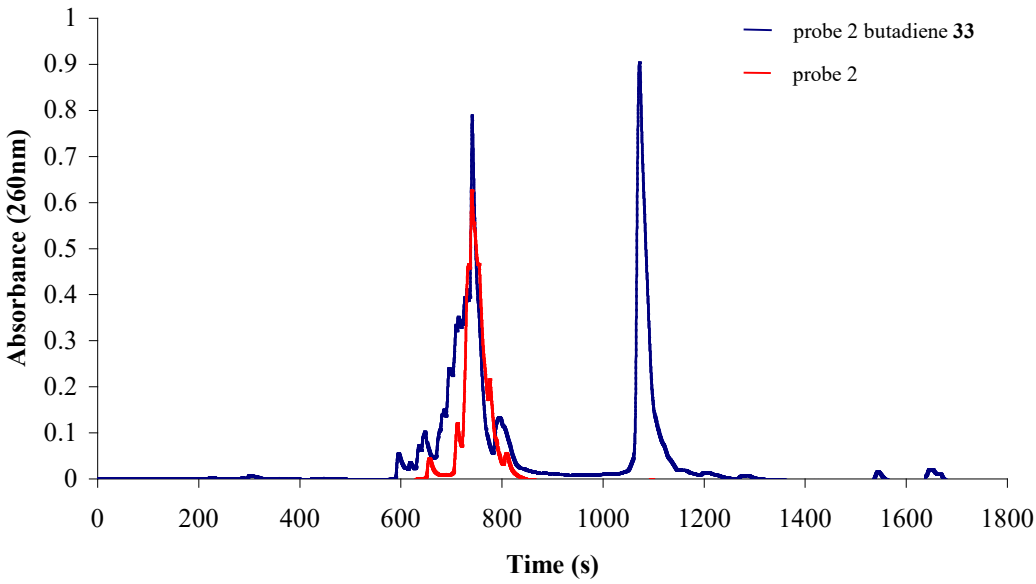

Figure 5.2. HPLC trace of probe 2 butadiene **33** compared to unmodified probe 2 using method 3 and a C-18 column. Estimated coupling efficiency was more than 96%.

.

5.3.2. Labelling of diene modified oligonucleotides with SERRS active dyes

A variety of conditions were examined for Diels Alder cycloaddition using the benzotriazole maleimide dye **10** and furan modified oligonucleotide **32a**. The optimal conditions were found to be similar to those reported by Hill *et al.*[129] Furan modified probe **32a** was dissolved in 25 mM phosphate buffer at pH 5.5 and mixed with a threefold excess of maleimide dye **10**. Acetonitrile was added to obtain 30:70 ratio of organic solvent to water. The mixture was then heated to 40°C and progress of the cycloaddition followed by HPLC showing the completion of the reaction in less than 2.5 hours (Fig. 5.3.).

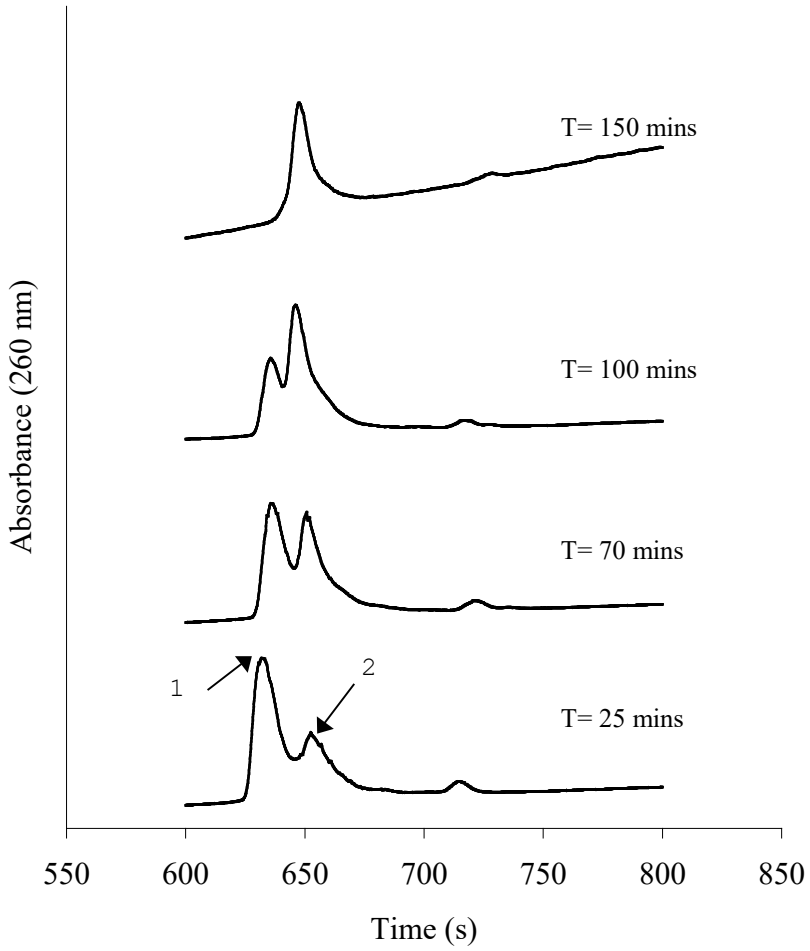

Figure 5.3. HPLC trace of probe 1 furan **33a** and dye **10** cycloaddition obtained using method 2 and a C-18 Chromolith column. Peak 1 = furan oligonucleotide **33a**, peak 2 = oligonucleotide cycloadduct.

The amount of sample analysed by HPLC was 50μL of 4.0×10^{-6} mol dm^{-3} solution, which equates to 0.1 nanomoles and was the lowest observable amount using UV-detection at 260 nm.

Cycloaddition of the maleimide dye **10** to oligonucleotide butadiene required longer reaction time and the reaction mixture was heated overnight at 40°C.

Both probe **33a** and probe **33b** required the same conditions and reaction time to undergo the cycloaddition, which proved that the reaction was not sequence dependant.

The stability of the furan modified oligonucleotides and the cycloadducts compared to unmodified oligonucleotide was assessed using UV melting data to obtain the melting temperatures T_m (Table 5.1).

Table 5.1. Melting temperature for unmodified and modified probe 1 and probe 2. Concentration of all probes was 1.0×10^{-6} mol dm^{-3}

Oligonucleotide	T_m/°C
probe 1	43.3
probe 1 furan **33a**	42.6
probe 2	43.0
probe 2 furan **33b**	42.8
probe 2 cycloadduct with dye **10**	44.2

Values of T_m indicate that there in no significant destabilising effect on the duplex formation when oligonucleotides are modified with a furan moiety or when the cycloadduct is formed. This is important, as it is vital that this type of chemistry did not interrupt a duplex if it was to be useful in practical applications.

5.3.3. SERRS detection of the oligonucleotide cycloadducts

Progress of the cycloadditon was also followed by SERRS at a concentration lower than could be detected by the UV-HPLC system to evaluate the sensitivity of the technique. Equimolar amounts of furan oligonucleotide and maleimide dye were used and copper (II) nitrate added as a catalyst. Salts like sodium chloride or copper nitrate are known to accelerate the rates of Diels Alder reactions.[130]

10 µl of an equimolar reaction mixture of furan **33a** and dye **10** was added to PVA-Ag disc after different reaction times, allowed to adsorb for 10 min and washed well with water. Excellent spectra were obtained using 514.5 nm excitation (Fig. 5.4.).

Distinct differences are observed in the spectra of the cycloadduct oligonucleotide compared to the spectra of maleimide dye **10**. New bands are observed at 1204, 1236 and 1387 cm^{-1} and the changes in relative intensity of bands at 1300 and 1434 cm^{-1} occur. Surprisingly, the signal to noise ratio of the

oligonucleotide cycloadduct is significantly better than that of the cycloadduct itself. This may be attributed to the presence of the oligonucleotide, which may cause the orientation of the dye on the surface to change in a favourable manner. The sensitivity of this SERRS measurement was excellent. The excitation light is focused onto a small area of the film (x50 objective was used, area under objective is estimated to 20 pm^2) and the actual number of moles under examination is estimated to be in the region of 10 attomoles.

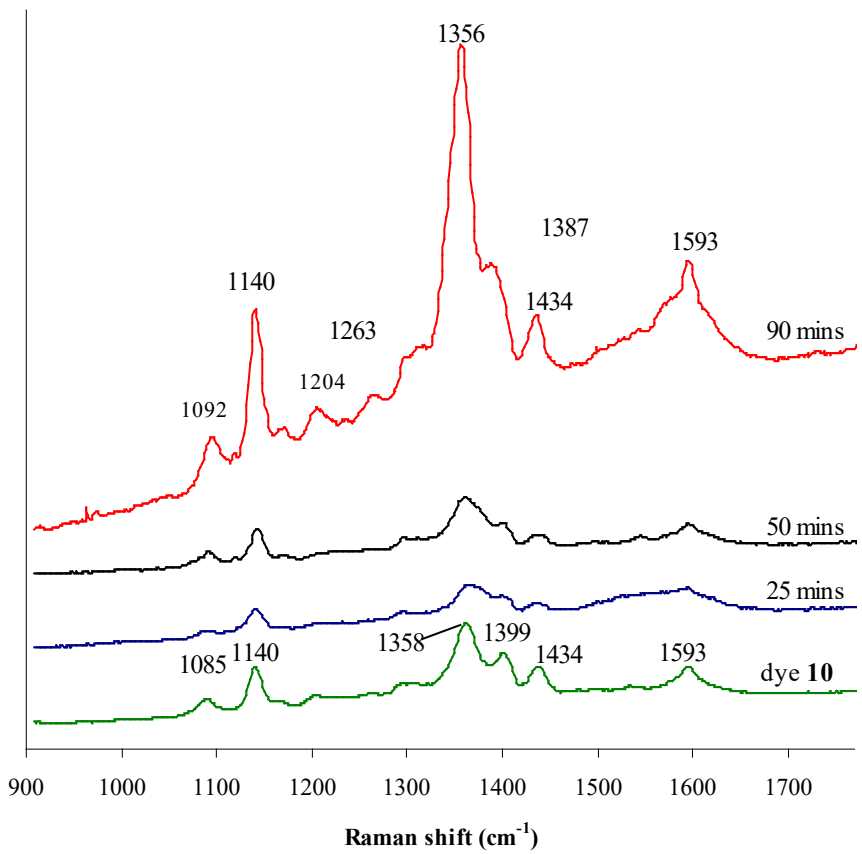

Figure 5.4. SERRS of the cycloadditon from PVA-Ag disc. The concentration of the cycloadduct was 6.3×10^{-8} $moldm^{-3}$.

The oligonucleotide cycloadduct was also investigated using silver colloid as a substrate. When the silver colloid was used, direct addition of the oligonucleotides to the suspension resulted in very poor signals. However, as found previously for oligonucleotides, addition of spermine improves surface adsorption.[131] Therefore spermine was added to the oligonucleotide cycloadduct in colloid and the resulting spectra was similar to those obtained from PVA surfaces (Figure 5.5).

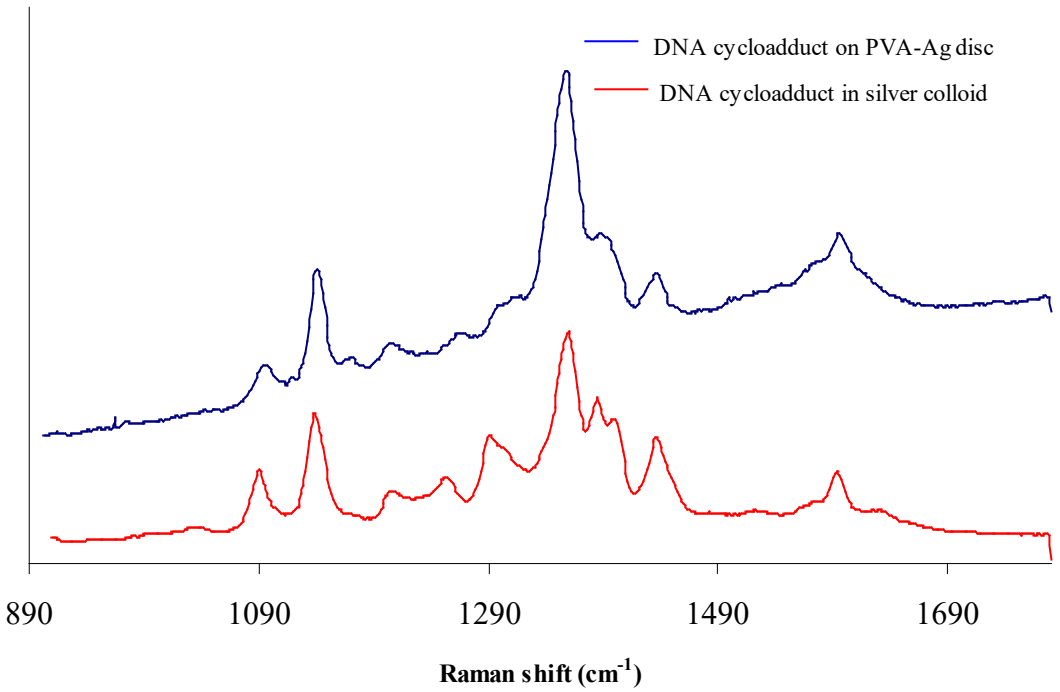

Figure 5.5. SERRS spectra of oligonucleotide cycloadduct using silver colloid and PVA-Ag disc. Concentration of the cycloadduct was $1x10^{-7}$ mol dm^{-3}. The spectra are scaled for display purposes.

The differences in the 1400-1350 cm^{-1} region can be explained by the difference in relative coverage of the silver substrate surface. In approximation, the number of cycloadduct molecules per surface area of the disc is 1000 times larger than that calculated for colloid indicating that multilayers of the cycloadduct are formed on PVA-Ag. In that case the complex interaction between molecules in different layers is possible, leading to a differences in orientation of the molecules, which then in turn causes observed changes in the spectra.

To demonstrate the selective nature of SERRS, three other benzotriazole maleimide dyes were also added to oligonucleotide furan **32b**. The spectra of oligonucleotide cycloadducts with dye **12**, **14** and **15** are shown in Fig. 5.6. Each cycloadduct shows clear differences from each other and also from the starting benzotriazole dye maleimide.

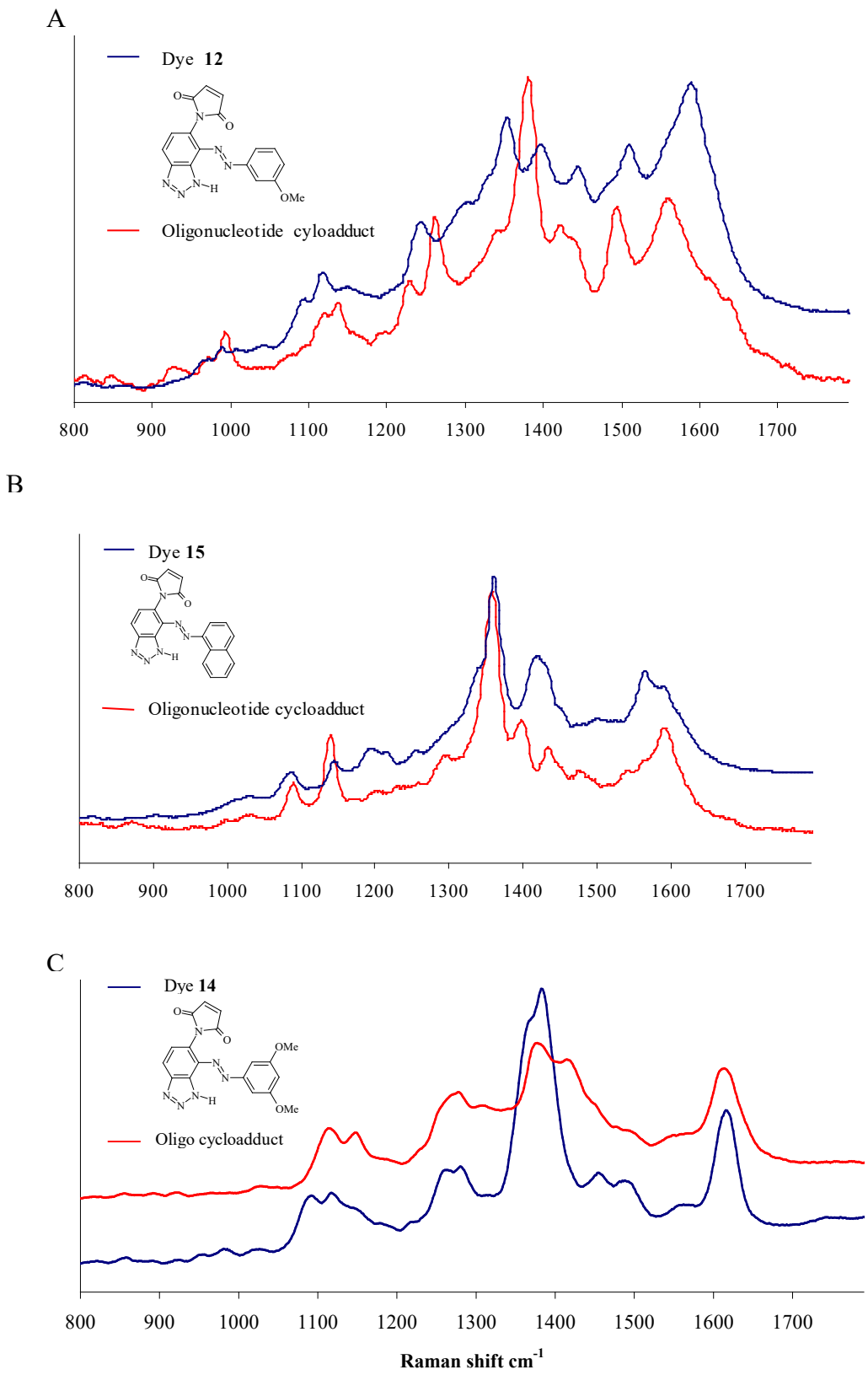

Figure 5.6. SERRS spectra of the benzotriazole dye maleimides with cycloadducts formed using probe 2 furan **32b** ($1x10^{-7}$ mol dm^{-3}). A) Dye **12**, B) dye **15** and C) dye **14**. The spectra have been scaled for display purposes.

Additionally, the SERRS spectra from a butadiene cycloadduct formed with dye **10** was compared to the SERRS spectra of a furan cycloadduct of the same dye and the differences observed (Fig. 5.7.).

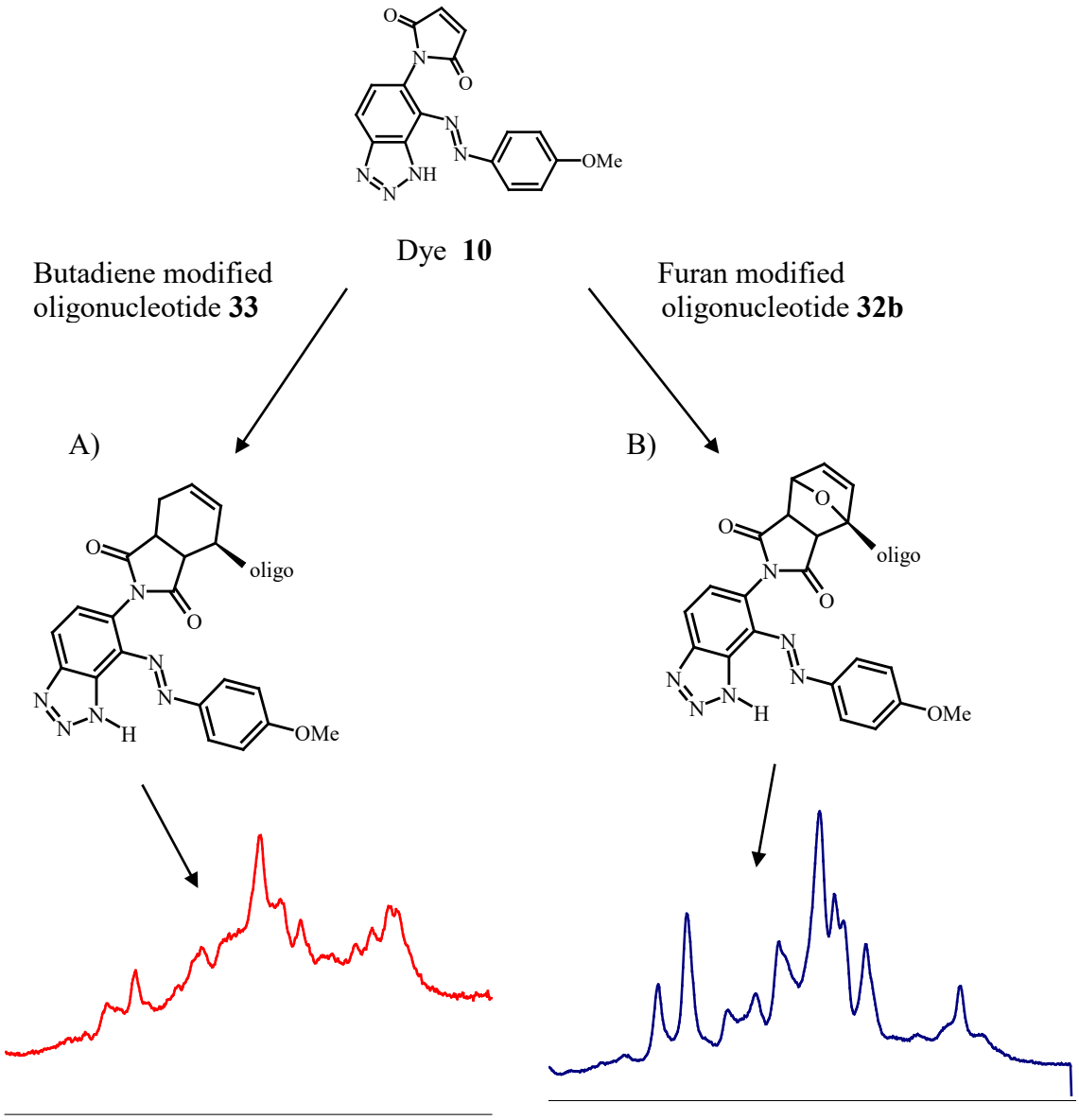

Figure 5.7. SERRS spectra of the cyloadduct of dye maleimide **10** with two different modified oligonucleotides. A) Cycloadduct synthesised with butadiene **33** and B) with furan **32b**.

It can be concluded that there is a clear potential for SERRS to be used in oligonucleotide multiplexing. Oligonucleotide cyloadducts with different dyes gave distinctly different spectra. Therefore, cyloaddition with dye dienophiles can be used

to label different sequences and benzotriazole maleimide dyes can be very good reporter dyes. Moreover, SERRS spectra differ with the oligonucleotide diene used for cycloadditions, which additionally increases the number of possible combinations.

5.3.4. Oligonucleotide labelling with fluorophores

Commercially available fluorophores were added to the 5' end of the furan modified oligonucleotide **32a** using Diels Alder cycloadditions. Nine commercially available fluorophore maleimides were used in cycloaddition reactions under optimal conditions (described in section 5.4). The only exception were two rhodamine (TAMRA) isomers, which were not heated at 40°C but allowed to undergo reaction overnight at room temperature. The reason for the change in procedure in the case of TAMRA maleimide is its thermal instability.[28.] The two isomers of TAMRA, 5 and 6, were examined to see if the different isomers affected the cycloaddition but this was not the case. The HPLC traces show clear differences between the furan oligonucleotide peak and the cycloadduct peak (Fig. 5.8) indicating that the cycloadduct has formed in excellent yield.

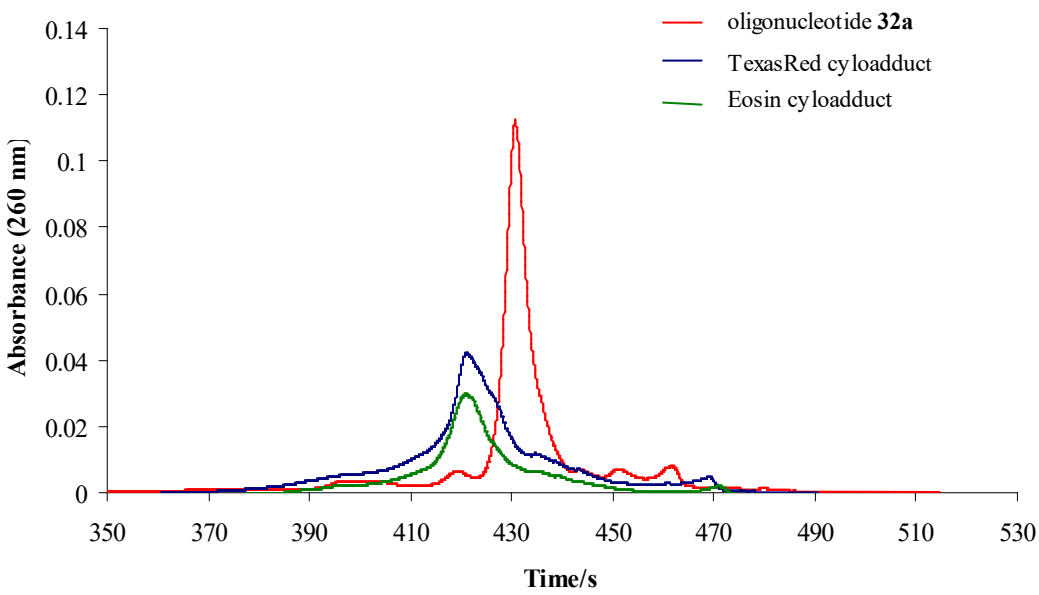

Figure 5.8. HPLC trace of oligonucleotide diene **32a** and two different fluorophore cyloadducts (with TexasRed and Eosin maleimide) obtained using method 2 and a C-18 Chromolith column.

All of the cycloadducts displayed a reduced retention time due to the increased polarity of the conjugated oligonucleotides. Purified oligonucleotide cycloadducts were desalted using standard procedures with a Sephadex column[132] and dissolved in water. Aqueous solutions were then examined for fluorescence. The emission wavelengths observed for the oligonucleotides differed slightly from those quoted. This is presumed to be due to the use of aqueous solutions for measurements as opposed to methanol. Table 5.2 shows the retention times (t_r) of the modified furan oligonucleotide and cycloadducts as well as corresponding fluorescence data.

Table 5.2. Retention times (t_r) and fluorescence emission data **(λ_{em})** for oligonucleotide furan **25a** and fluorophore cycloadducts.

Oligonucleotide	**t_r /s**	**λ_{em}/ nm**	**λ_{em}/ nm (literature values)**
Furan **32a**	430.7	none	none
FAM cycloadduct*	420.5	513	515(MeOH)
TAMRA 5 cycloadduct	424.0	569	567 (MeOH)
TAMRA 6 cycloadduct	427.0	566	567 (MeOH)
AlexaFluor 532 cycloadduct	427.2	549	552(MeOH)
TexasRed cycloadduct	420.7	619	600 (MeOH)
Coumarin cycloadduct	418.0	400	463 (MeOH)
Eosin cycloadduct	421.2	537	545 (MeOH)
Pyrenyl cycloadduct	422.1	368	375 (MeOH)
Cy3 cycloadduct	426.4	560	565 (MeOH)

* the structures of fluorophores are given in the Appendix

Fluorescence data proved that the oligonucleotides were fluorescent and that the cycloadditon does not interfere with the fluorescence emission.

Finally, it can be concluded that the Diels Alder cycloaddition used for 5' end labelling of DNA is fast, simple and high yielding. Use of benzotriazole maleimide dyes as labels and subsequent detection of labelled oligonucleotides by SERRS shows excellent promise in terms of selectivity, sensitivity and simplicity. The cycloadduct produced is a distinctive species and there is no need for separation from the starting material prior to analysis. Moreover, it was shown that oligonucleotides can be detected by SERRS in attomolar quantities. The various fluorophore maleimides used

to label oligonucleotides additionally demonstrated the versatility of the Diels Alder approach and the selectivity of the procedure.

This new method of labelling of biomolecules and the use of SERRS for detection can be effective for many other targets, one of which is discussed in the following chapter.

Chapter 6

Principle and design of SERRS Beacons

6.1. Introduction

The ability to detect specific DNA sequences or individual DNA bases within a sequenced genome is key to evaluation and diagnosis of specific illnesses. In recent years, a number of methods have been developed for detecting specific sequences of DNA utilising the high specificity of DNA hybridisation. Probes based on fluorescence detection during PCR amplification, which include Molecular Beacons[57], Taqman[53] or Scorpion[56] probes are routinely used in laboratories. The advantage of fluorescence detection is that the labels and many probes are commercially available and the instrumentation is easily accessible. However, due to the detection limits, a large number of PCR cycles are required to guarantee accurate analysis of the target DNA. Moreover, the multiplexing ability of fluorescence is limited by the use of optical filters to discriminate between fluorophores.[54]

Molecular beacons, which will be discussed further in this chapter, are ingeniously designed probes with a stem-loop structure. They employ the principle of fluorescence quenching to detect target DNA (see *Chapter 1*).

One of the main challenges in the use of molecular beacons is the background fluorescence due to inefficient quenching. This often leads to decreased sensitivity. Moreover, the number of available quencher- fluorophore pairs is limited leading to decreased multiplexing ability. Therefore, there is a constant need for new, efficient quenchers. Recently, Dubertet *et al.* attached gold nanoparticle to the 3' end of a Beacon and fluorescein to the 5' end.[66] The quenching was improved due to the presence of gold nanoparticles, which acted as highly efficient quenchers.

Taking into account the results of SERRS detection of oligonucleotides presented in Chapter 5 and the known ability of silver nanoparticles to quench fluorescence[65], a new class of molecular probes based on the SERRS detection and molecular beacons principle was designed and is presented here.

6.2. Experimental

SERRS spectra were taken using a Renishaw Raman 2000 spectrometer with 514.5 nm excitation. All fluorescence data were obtained using a Cary Eclipse fluorimeter. Experimental details are given in *Chapter 8*.

6.3. Quenching potential of benzotriazole dyes

The Stern Volmer equation (Eq. 6.1) is commonly used to describe fluorescence quenching:

Equation 6.1. $\phi_f/\phi_{f+q} = K_{sv}C_q + 1$

where ϕ_f is the quantum yield of unquenched fluorophore

ϕ_{f+q} is the quantum yield of quenched fluorophore

K_{sv} is the Stern –Volmer constant

and C_q is the concentration of the quencher

The Stern Volmer constant serves as a direct measure of the efficiency of the quenching and it is usually quoted together with the percentage of quenching to describe the qualities of quencher. Our synthesized BT dyes are structurally similar to DABCYL, which is the most widely used quencher in molecular beacons[57](Fig. 6.1).

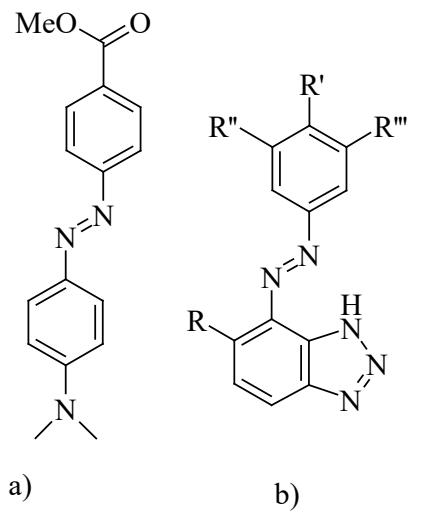

Figure 6.1. Structures of a) DABCYL and b) BT dyes.

Therefore, the quenching ability of all the dyes synthesised within the laboratory was tested with fluorescein, which is the most commonly used fluorophore in the design of molecular probes. The decrease of fluorescence was monitored at different concentrations as quencher dye was added to the fluorophore solution. The quantum yields of fluorophore solution, which are required for determination of the Stern Volmer constant, were estimated using following relationship[133] :

Equation 6.2. $\phi_f = (A_s/ A_f)\cdot(F_f/F_s)\cdot(n_f/n_s)^2\cdot\phi_s$

where ϕ is the fluorescence quantum yield

A is the absorbance at the excitation wavelength

F is the area under emission curve

n is the refractive index of the solvents used

Subscripts f and s refer to unknown and the standard respectively.

In equation 6.2. absorbance A accounts for the number of absorbed photons and area F accounts for the number of emitted photons. When the light passes from one medium to another, part of it is lost because of reflection, which depends upon the difference between the refractive indices of the two media. Therefore, a correction for the refractive indices has to be introduced when unknown and standard are used in different solvents. The standard used in determination of quantum yield is 1.0 mol dm^{-3} solution of quinine sulphate in sulphuric acid with know quantum yield of 0.55. Graphs of the ratio of quantum yields in presence and absence of quenchers *vs* concentration of quencher were plotted (Fig. 6.2.).

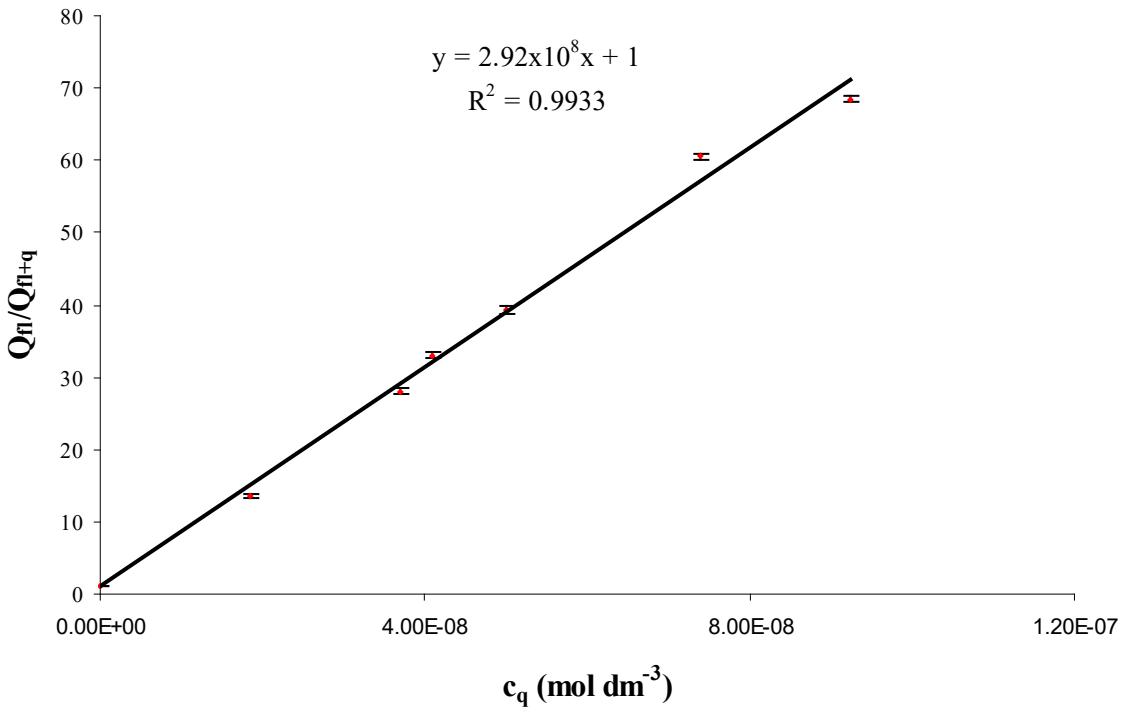

Figure 6.2. Concentration of the quencher dye **1** plot *vs* ratio of quantum yields (fluorophore/fluorophore+quencher). Fluorescein was the fluorophore used. Quinine sulphate was used as standard to determine the quantum yields.

The slope of the straight line obtained corresponds to the Stern Volmer constant for investigated quenchers.

Efficiency of quenching is commonly referred to as percentage of quenching. The percentage can be easily determined using Eq.6.3.

Equation 6.3. % quenching = $[(\phi_f-\phi_{f+q})/\ \phi_f]\cdot 100$

The values of both K_{sv} and % quenching of fluorescence quenching of fluorescein for dyes studied are shown in table 6.1.

Table 6.1. Stern Volmer constants (K_{sv}) and percentage quenching of fluorescein fluorescence using different BT dyes as quenchers.

Quencher dye	K_s mol^{-1}dm^3	%quenching
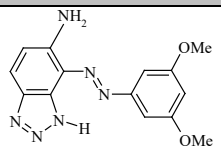 **3**	$1.32\cdot 10^9$	98.3
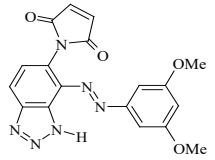 **14**	$9.82\cdot 10^8$	97.7
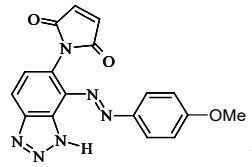 **10**	$5.76\cdot 10^8$	96.7
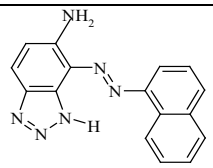 **4**	$4.73\cdot 10^8$	95.9
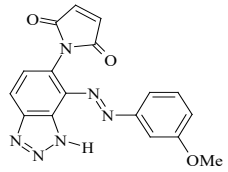 **12**	$3.59\cdot 10^8$	94.3
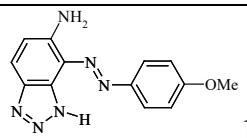 **1**	$2.92\cdot 10^8$	93.5

Quencher dye	K_s mol^{-1}dm^3	%quenching
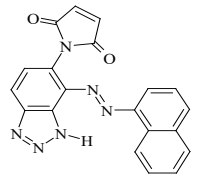 **15**	$2.06 \cdot 10^8$	90.9
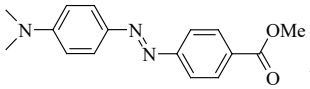 **DABCYL**	$1.83 \cdot 10^8$	87.9
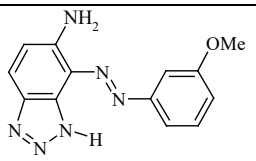 **2**	$1.06 \cdot 10^8$	83.4

It can be seen from the table that all dyes apart from dye **2** are more efficient fluorescein quenchers than the widely used DABCYL. The most interesting are dye maleimides, which are successfully used for DNA labelling (*Chapter 5*). They are excellent quenchers and have great potential to be used as quenchers in stem-loop molecular probes.

6.4. Fluorescence quenching of fluorescein labelled oligonucleotide

The quenching ability of some of the benzotriazole dyes was further investigated using a fluorescein labelled oligonucleotide. Furan oligonucleotide **33b** was labelled with dyes **10** and **14** using Diels Alder cycloaddition as described in *Chapter 5*. A complementary oligonucleotide sequence was synthesised using fluorescein CPG to add the fluorophore to the 3' end. It was shown previously by Marras *et al*. that hybridisation of the quencher labelled oligonucleotide to its complementary sequences labelled with fluorophore brings fluorophore and quencher in proximity and causes the quenching of the fluorescence.[64] A solution of fluorescein oligonucleotide in hybridisation buffer (4nM $MgCl_2$, 15 mM KCl, 10 mM Tris-HCl, pH 8) was made. To it 5 equivalents of complementary sequence labelled with BT dye was added and allowed to hybridise. The fluorescence of both control (fluorescein oligonucleotide with non labelled complementary sequence) and fluorescein

oligonucleotide with two quencher labelled complementary sequences was measured using 495 nm excitation. The results are shown in Fig. 6.3. To test if the addition of silver colloid and aggregating agent have any effect on the fluorescence quenching, the solutions, one with added colloid (500 μL) and other containing colloid and aggregating agent spermine (500 μL and 10 μL respectively) with hybridised fluorophore and quencher labelled oligonucleotides were made.

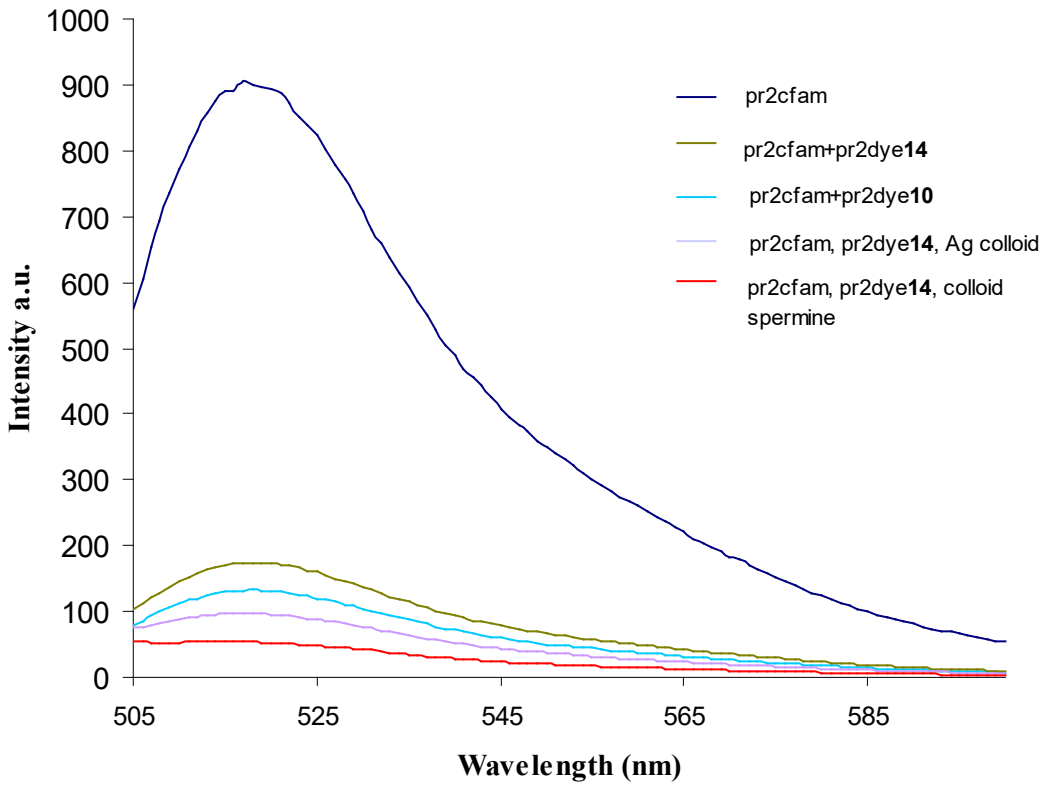

Figure 6.3. Fluorescence quenching of fluorescein labelled oligonucleotide using two different benzotriazole labelled oligonucleotides, silver colloid and spermine. The concentration of fluorescein oligonucleotide was 1.0×10^{-7} mol dm^{-3}.

Quenching efficiency was determined by dividing the fluorescence intensity of the hybrid by the fluorescence intensity of the fluorophore labelled oligonucleotide, multiplying the result by 100 and then subtracting the result from 100.[64] Oligonucleotide labelled with dye **14**, which was found to be the best quencher in the study of the quenching properties of the dyes, was hybridised to the fluorescein oligonucleotide, 85 % of quenching was observed. The quenching efficiency of the

dye **10** labelled oligonucleotide was slightly better (87%). However, addition of the Ag colloid increased the quenching efficiency further to 91 % and addition of spermine to the colloid caused the efficiency to increase to 95%. As expected, silver nanoparticles caused additional quenching of the fluorescence. Aggregating agents, such as spermine contributed to the further increase in quenching. Spermine is commonly used for aggregation of silver colloids in SERRS detection of oligonucleotides and is also an excellent neutraliser of the DNA phosphate backbone. That enables the oligonucleotides to get closer to the silver nanoparticles and interact with the fluorophore causing an additional decrease in fluoresecence. This data gave further insight in the quenching ability of the benzotriazole dye and silver colloid and lead to the design of novel type of stem –loop molecular probe.

6.5. SERRS Beacon

6.5.1. Design of SERRS Beacon

It was shown in previous chapters that SERRS is a powerful technique for DNA detection. Furthermore, a simple and effective method for DNA labelling based on Diels Alder chemistry was developed. All of these results were used to design a biomolecular probe, known as a SERRS Beacon. The quenching ability of benzotriazole dyes is utilised together with the detection potential of SERRS in a molecular probe to detect single base mismatches at ultra low concentrations.

A SERRS Beacon combines SERRS with fluorescence in one format and exploits the advantages of both techniques. The Beacon was synthesised using a 3'-fluorescein solid support and adding butadiene phosphoramidite to the 5' end during solid phase synthesis. The loop sequence was complementary to a gene section encoding the polymorphic form of the human cytokine receptor.[134] Benzotriazole maleimide dye **10** was added to the butadiene residue *via* Diels Alder cycloaddition (Scheme 6.1.).

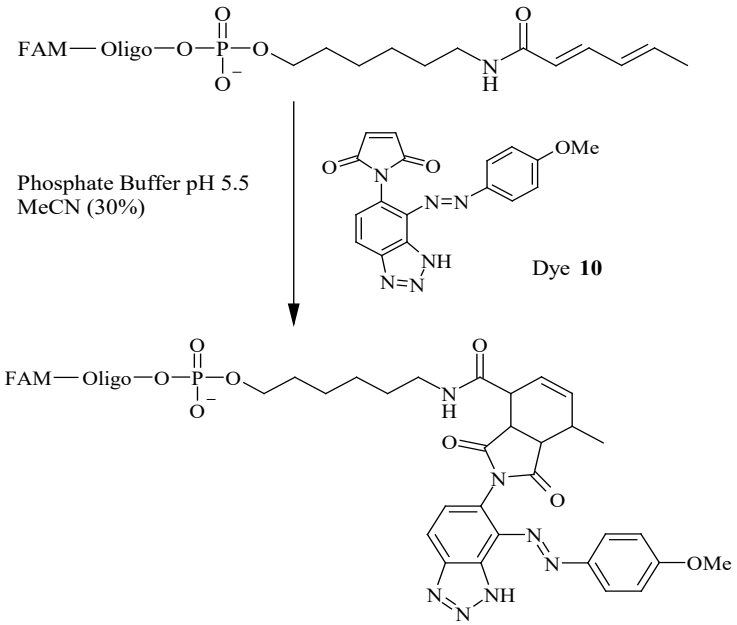

Scheme 6.1. The synthesis of a SERRS Beacon. A benzotriazole azo maleimide dye was added to the oligonucleotide *via* Diels Alder cycloaddition using standard conditions as described in Chapter 5.

Dye **10** is found to be an excellent fluorescence quencher. Additionally it has benzotriazole moiety for attachment to silver nanoparticles and hence, enabling SERRS measurements. Furthermore, silver additionally quenches the fluorescence, thus decreasing the background fluorescence when the beacon is in the closed form (Fig. 6.4).

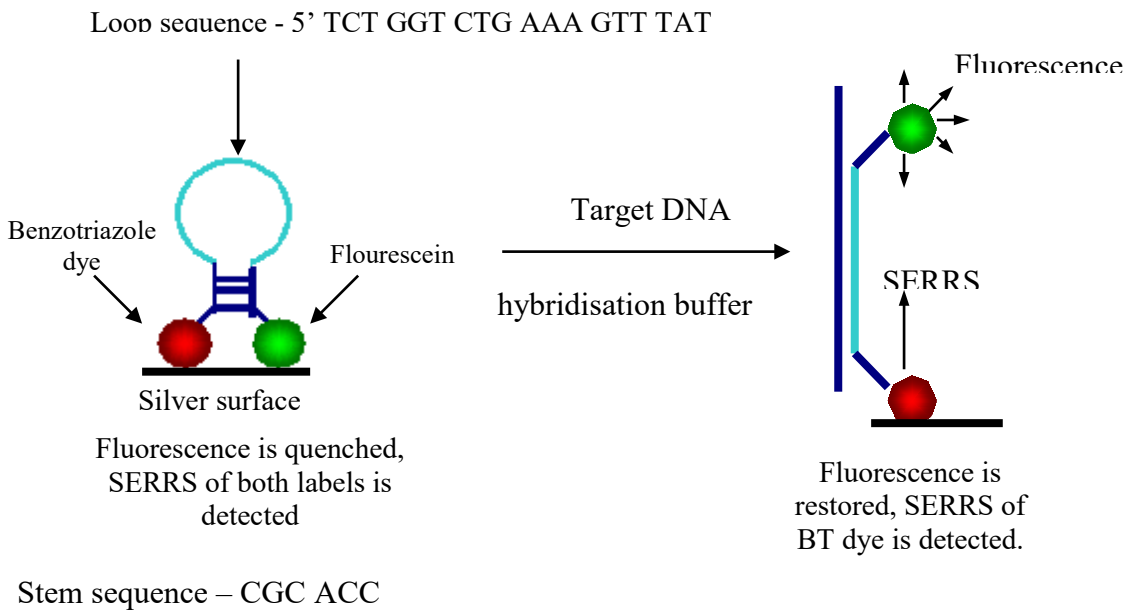

Figure 6.4. The concept of SERRS Beacon.

Two different formats for SERRS measurements were used to evaluate sensitivity and specificity of the SERRS Beacon, namely silver colloid and a PVA-silver disc.

6.5.2. Detection of target DNA using silver colloid as a SERRS substrate

Detection of the target DNA was first attempted using silver colloid as a substrate and spermine as an aggegating agent. When the target DNA is not present, the SERRS beacon remains in its closed form. Benzotrizole dye **10** attached to the 5'end of the Beacon immobilises the probe on the silver nanoparticles and forces fluorescein to be close to the surface and produce SERRS. When the spectrum of the closed SERRS Beacon is compared to the Beacon probe without benzotriazole dye attached on the 5'end, the immobilising effect of the dye can clearly be seen (Fig 6.5.).

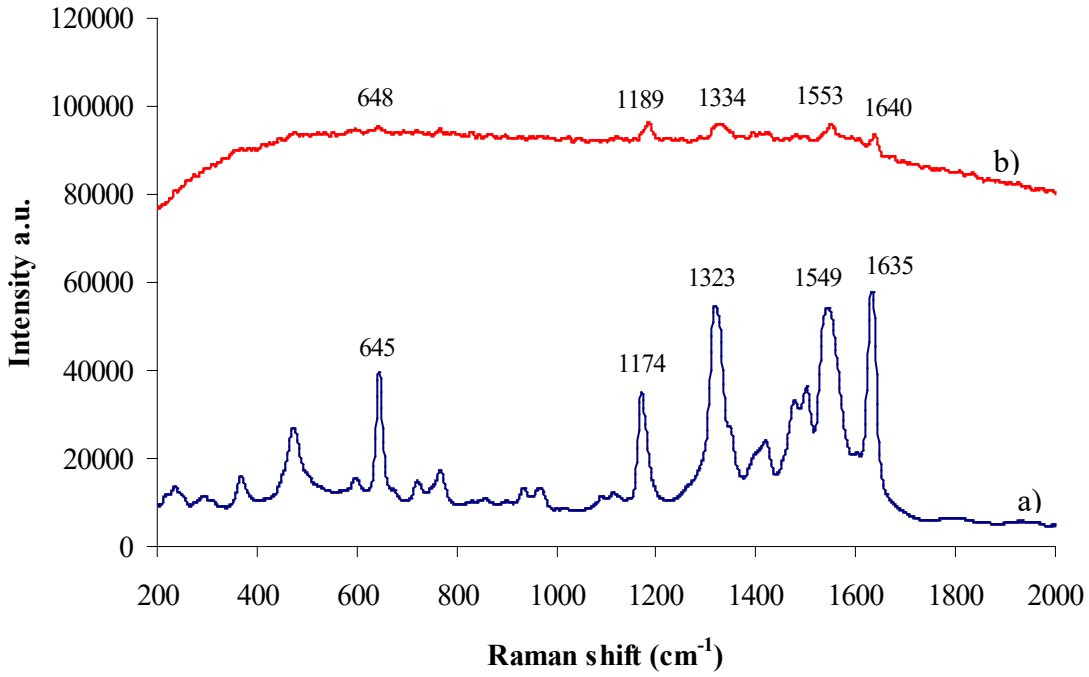

Figure 6.5. SERRS spectra of a) SERRS beacon with dye **10** attached on the 5' end and b) molecular beacon with butadiene on the 5' end. Fluorescein is used as a fluorophore on 3' end. Silver colloid was used as SERRS substrate with spermine as aggregating agent. The concentration of both

probes was 3.7×10^{-8} mol dm^{-3}.

The Beacon with fluoresceine and butadiene only on the opposite ends (Fig. 6.5.b) gives very poor SERRS spectra with a large fluorescence background. However, the closed SERRS Beacon, which has dye 10 on the 5' end, of the same concentration gives excellent fluroescein SERRS spectrum. Additionally, there is no fluorescence background observed indicating that the benzotriazole dye has both immobilising and the quenching effect on fluorescein.

In the absence of the target DNA, there was no fluorescence detected in the solution of the SERRS beacon using a Cary Eclipse fluorimeter, a Stratagene MX4000 fluorescence plate reader and Renishaw Raman spectrometer. However, when the SERRS was examined, the fluorescein SERRS spectrum dominates as fluorescein gives stronger signals than dye **10** by approximately two orders of magnitude. When target DNA, with sequence complementary to the loop part of the beacon, was added to the SERRS beacon, a change in spectra was recorded. Fluorescence is restored, which is indicated by the broad band with maximum around 550 cm^{-1}, but strong fluorescein SERRS signals remained (Fig. 6.6.).

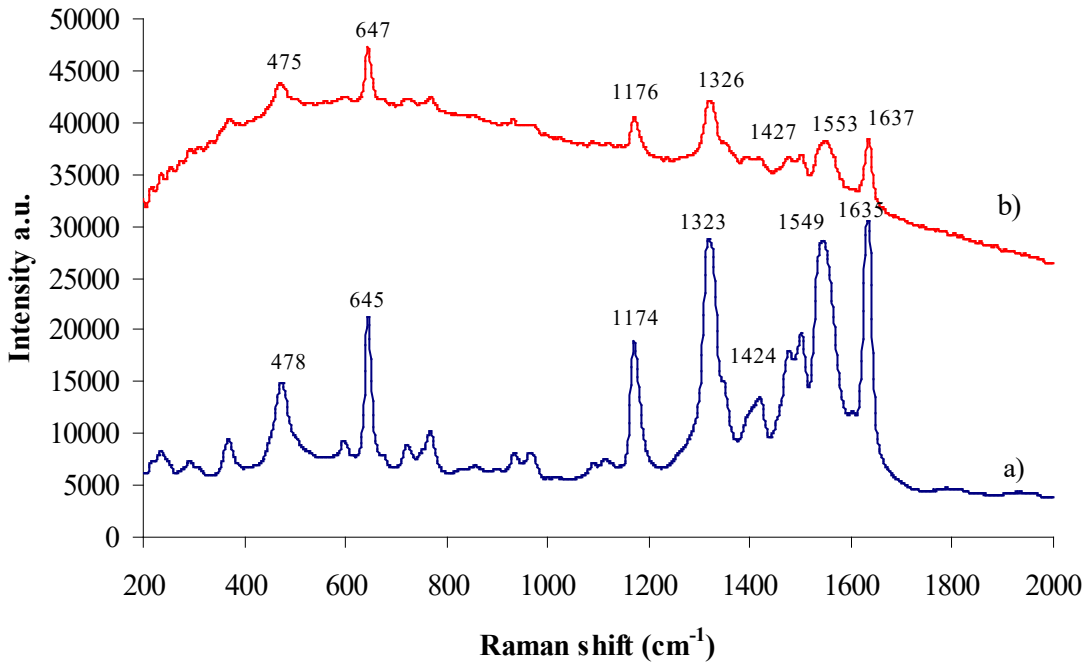

Figure 6.6. SERRS spectra in silver colloid of a) closed SERRS beacon and b) open SERRS beacon in the presence of target DNA. The concentration of both was 3.4×10^{-8} mol dm^{-3}.

Although it can be seen from the spectra that upon the addition of target DNA, the SERRS Beacon opens up and fluorescence is restored, it was still not possible to detect the benzotriazole dye cycloadduct immobilised on the silver surface. It was thought that this was due to the use of spermine, which caused the overaggregation of the silver nanoparticles and masking of the signal from the benzotriazole dye cycloadduct. Additionally, fluorescein gives excellent SERRS when close to the silver nanoparticles surface even in the open form of the Beacon. Therefore, another approach was taken. First, the spermine was not used to aggregate silver colloid prior to SERRS measurements and second, the amount of silver nanoparticles in the colloid was reduced by dilution. It was thought that reducing the number of silver nanoparticles could decrease the probability of the fluorescein molecule to interact with silver when the SERRS beacon opens up.

The SERRS spectra of the closed beacon, beacon with added target DNA, with single base mismatch sequence and nonsense control were recorded using silver colloid without added spermine (Fig. 6.7.). There are differences in these spectra when compared to the spectra of the Beacon when spermine is used as an aggregating agent.

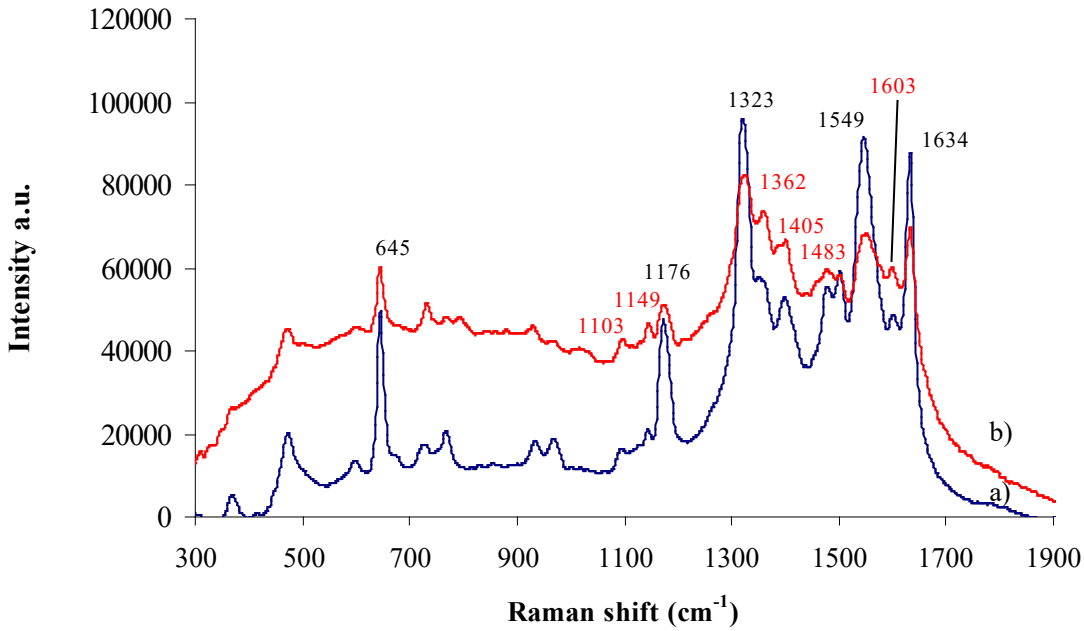

Figure 6.7. SERRS spectra in silver colloid without addition of spermine of a) closed SERRS beacon and b) SERRS beacon in the presence of the target DNA. The concentration of the both probes was 3.4×10^{-8} mol dm^{-3}. Benzotriazole dye **10** cycloadduct peaks are marked red.

Both SERRS bands from benzotriazole dye **10** cycloadduct and fluorescein can be observed in the closed beacon, although cycloadduct bands are significantly less intense. When exact complementary sequence is added, the fluorescence is restored and the intensity of the SERRS bands of the cycloadduct is increased. Complementary sequence with single base mismatch and control nonsense sequence were also added to the SERRS Beacon to investigate its specificity. The spectra obtained showed that there are no changes from the spectra of the SERRS Beacon indicating that the Beacon remained closed (Fig.6.8.).

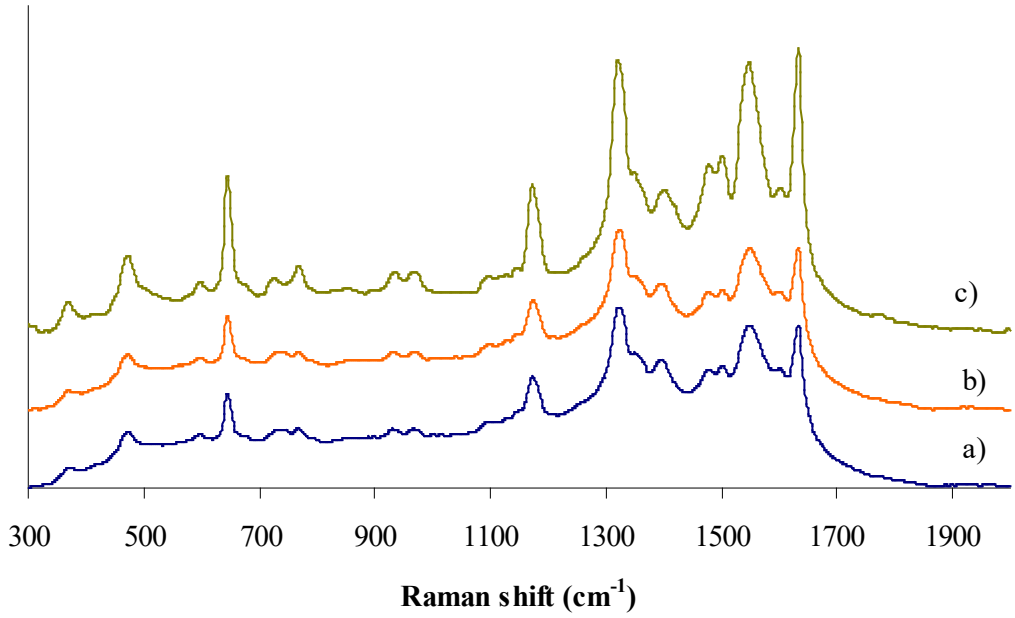

Figure 6.8. SERRS spectra of a) closed SERRS beacon, b) SERRS beacon with single base mismatch sequence added and c) with nonsense control using silver colloid without spermine. Concentration of SERRS beacon was 3.4×10^{-8} mol dm^{-3}. The spectra have been scaled for display purposes.

To obtain more intense spectra of the benzotriazole dye cycloadduct and to decrease the intensity of fluorescein SERRS in open beacon form, a range of experiments with diluted colloids was performed. 50 and 25 % colloids were prepared by diluting the stock colloid solution with 50 or 75% of distilled water respectively. SERRS spectra were first obtained without using spermine for aggregation. The recorded spectra of SERRS beacon with added target DNA, using both diluted colloids, changed significantly compared to the spectrum taken form the stock silver colloid (Fig. 6.9 i) and ii)).

i)

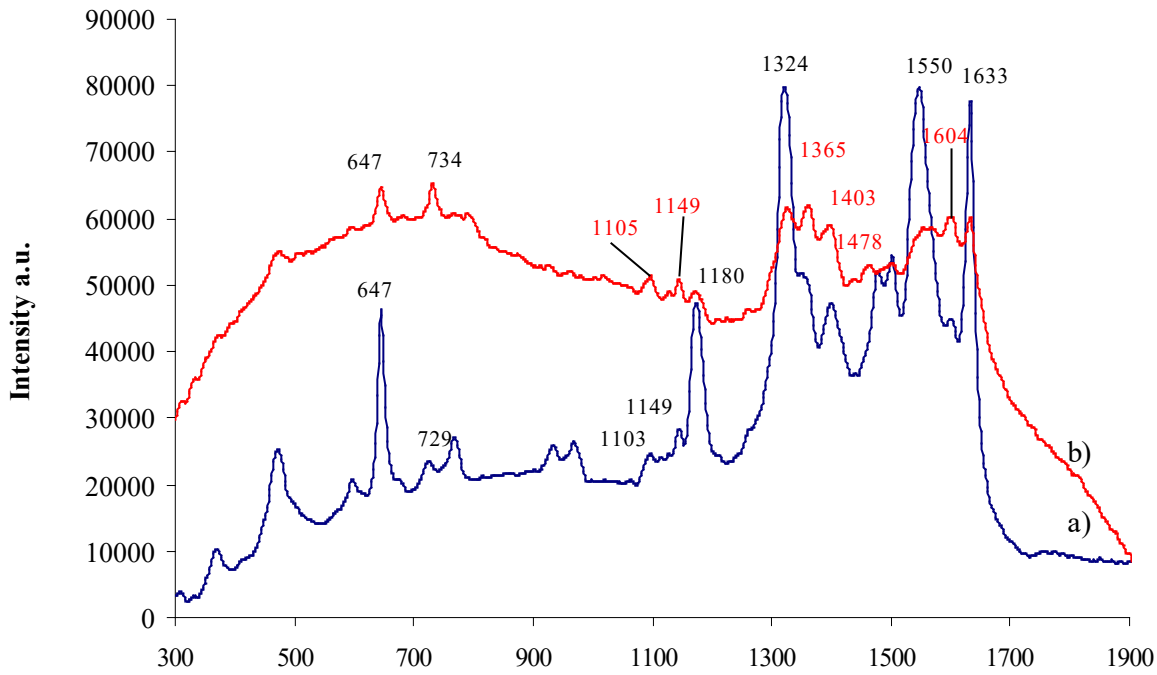

ii)

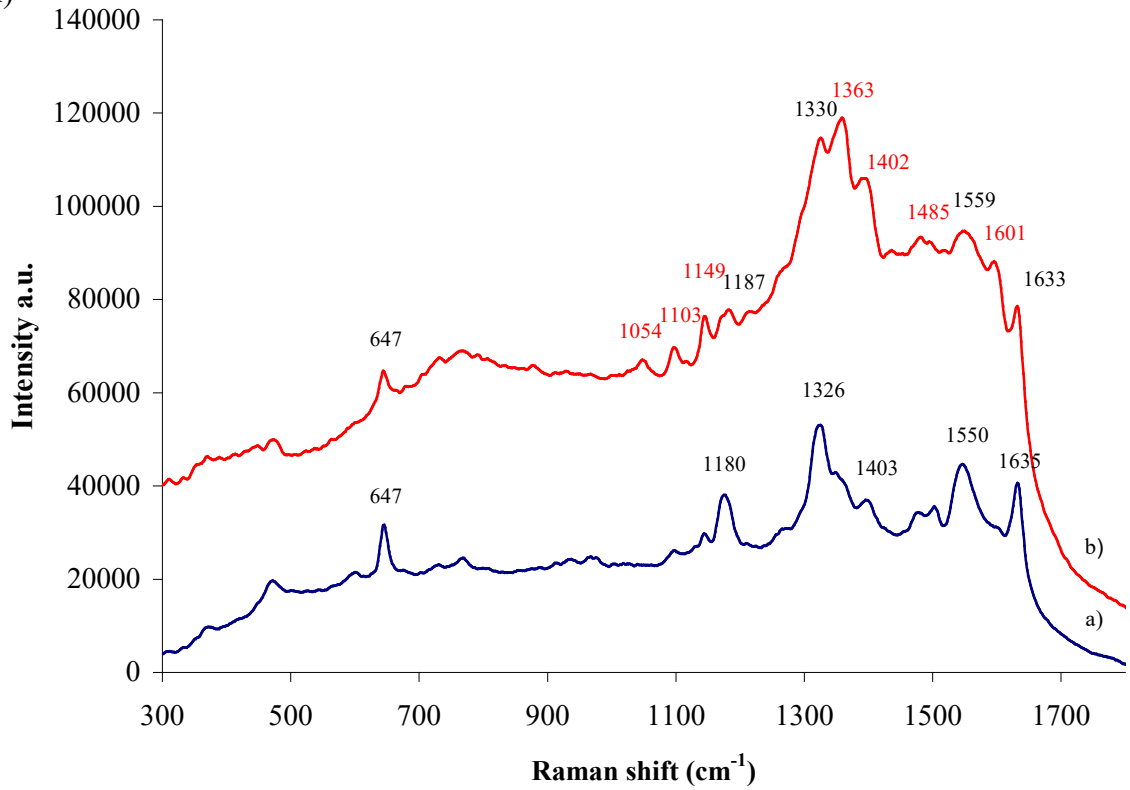

Figure 6.9. SERRS spectra of a) closed beacon and b) beacon in the presence of target DNA using i) 50% and ii) 25% silver colloid without spermine. Concentration of SERRS beacon was 3.4×10^{-8} mol dm^{-3}.

When 50 % colloid was used as the SERRS substrate, both benzotriaozle dye cyloadduct and fluorescein peaks can be observed in the opened form of the beacon. However, the intensity of the bands has changed compared to the spectra taken in stock solution. The benzotriazole dye cycloadduct bands were increased and the fluorescein decreased. Additionally, fluorescence is restored when target is added indicating that the conformation of the Beacon has changed.

Even more remarkable differences are observed when 25% colloid is used. The SERRS of benzotriazole dye cycloadduct dominates the spectrum with only few fluorescein peaks at 647, 1330, 1559 and 1635 cm^{-1} present. The change in the Beacon conformation upon the addition of the target DNA is clearly indicated by the change in the SERRS spectrum. When single base mismatched sequence and nonsense control were added, there were no changes from the spectrum of the closed Beacon observed indicating that SERRS beacon does not open up.

When spermine was used to aggregate the 50 % colloid before taking SERRS spectra, there were only changes in fluorescence upon adding a target (Fig. 6.10.i)). However, when 25% colloid was used, weak SERRS bands of benzotriazole cycloadduct can be observed when the Beacon is opened (Fig. 6.10 ii)). The fluorescein SERRS bands dominate in both colloids in the closed Beacon form.

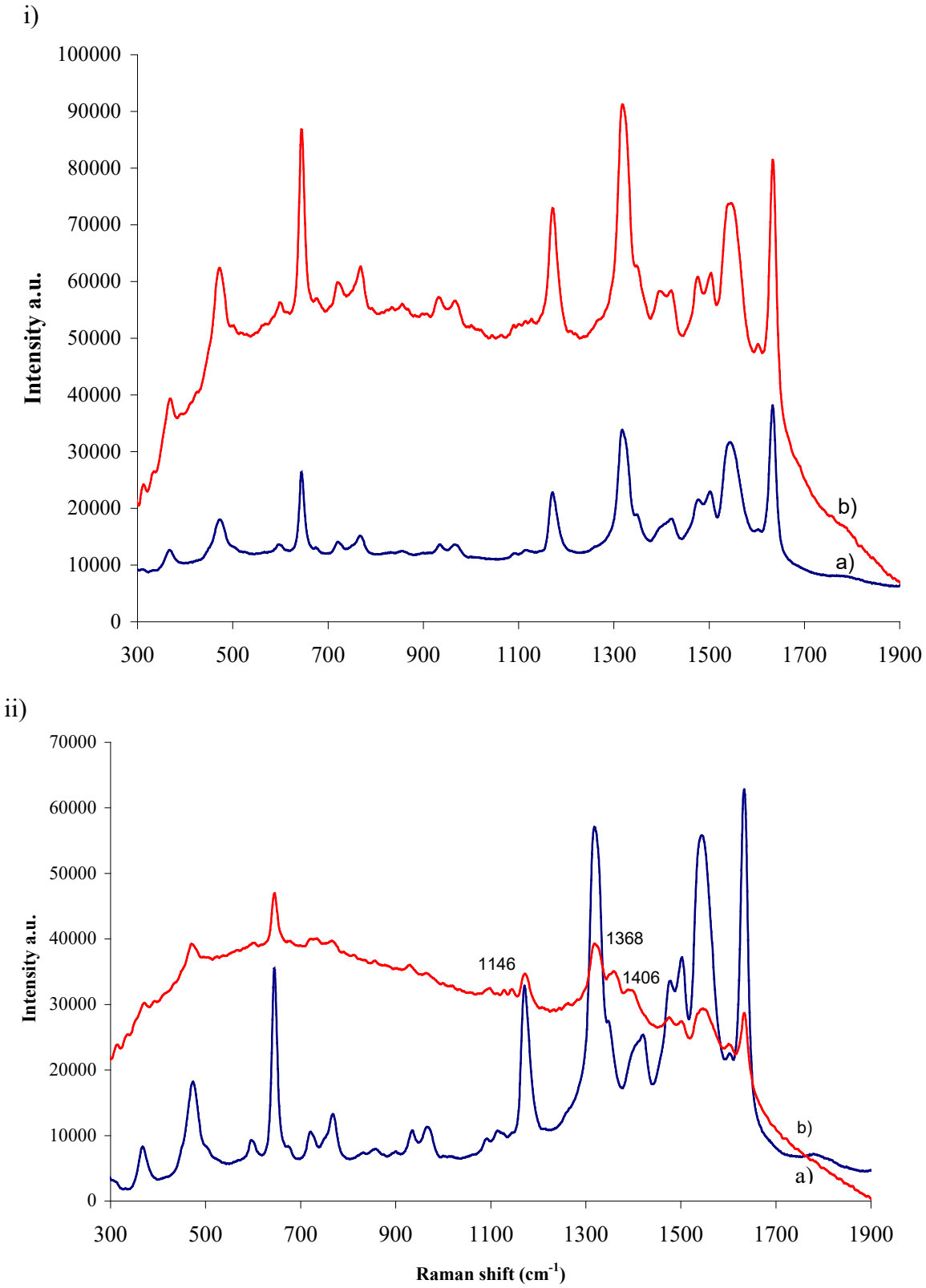

Figure 6.10. SERRS spectra of a) closed Beacon and b) open Beacon in i) 50 and ii) 25 % of silver colloid with spermine as aggregating agent. Concentration of SERRS beacon was 3.4×10^{-8} mol dm^{-3}. The benzotriazole dye cycloadduct peaks are marked in ii).

The study of SERRS Beacon using silver colloids showed that aggregating agent as well as number of silver nanoparticles in the colloid influence the appearance of the SERRS spectra. Since fluorescein is a good SERRS dye when it is close to the silver surface, it is masking the SERRS bands of the benzotriazole dye **10** cycloadduct attached on the 5'end. However, if the amount of silver is reduced and spectra taken without aggregating the colloid with spermine, spectra of the open Beacon in the presence of the target DNA change significantly compared to the closed Beacon. Additionally, there are no changes when a single mismatched sequence is used indicating the high specificity of the SERRS Beacon.

6.5.3. Detection of target DNA using PVA-Ag disc as a SERRS substrate

To investigate different formats that could be used with the SERRS Beacon, a PVA-silver disc was used as the substrate to provide additional quenching by silver and to generate the SERRS. PVA-silver discs are robust, easily handled and allow accurate spotting for the SERRS Beacon due to the hydrophilic nature of the PVA surface preventing uncontrollable spreading of the spot.

SERRS Beacon was added to the surface in a buffered solution and left for 20 minutes prior to washing with water several times. The same experiments as in the case of silver colloid were repeated and the spectra acquired. When the exact complementary sequence was added to the SERRS beacon, very distinct changes in the SERRS spectrum were observed (Fig 6.11.).

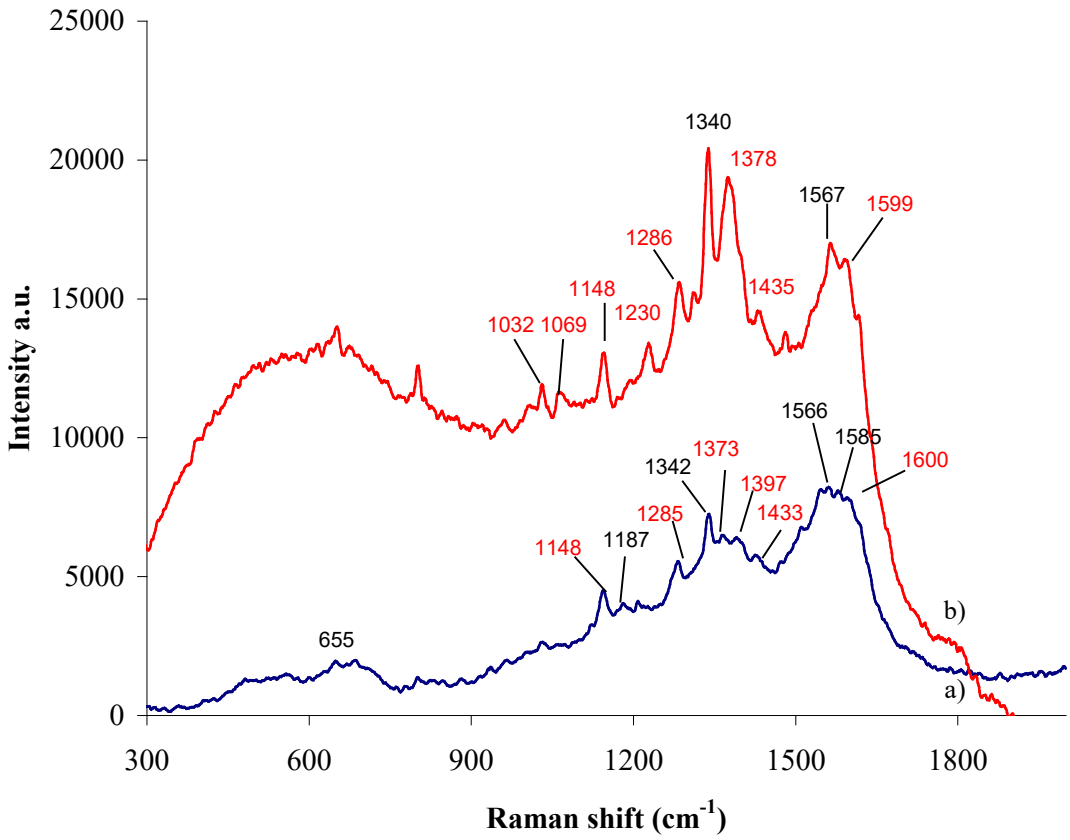

Figure 6.11. SERRS spectra of a) closed and b) opened Beacon on PVA-Ag disc. Concentration of the SERRS Beacon was 4.7×10^{-7}. Benzotriazole dye cycloadduct bands are marked red.

The SERRS spectra have changed as expected from the data collected in silver colloid, which indicates that different forms of beacon exist in the solution when complementary sequence is added. The single base mismatch sequence and the nonsense control showed some changes in the intensity of 1373 and 1187 cm^{-1} bands in the spectra when compared to the spectrum of closed Beacon (Fig. 6.12.). However, the fluorescence was not restored nor there were significant differences in the appearance and intensity of other peaks. The relative intensity changes in the two mentioned peaks are due to the orientation of the Beacon on the surface, not the conformational change and the Beacon still remains closed.

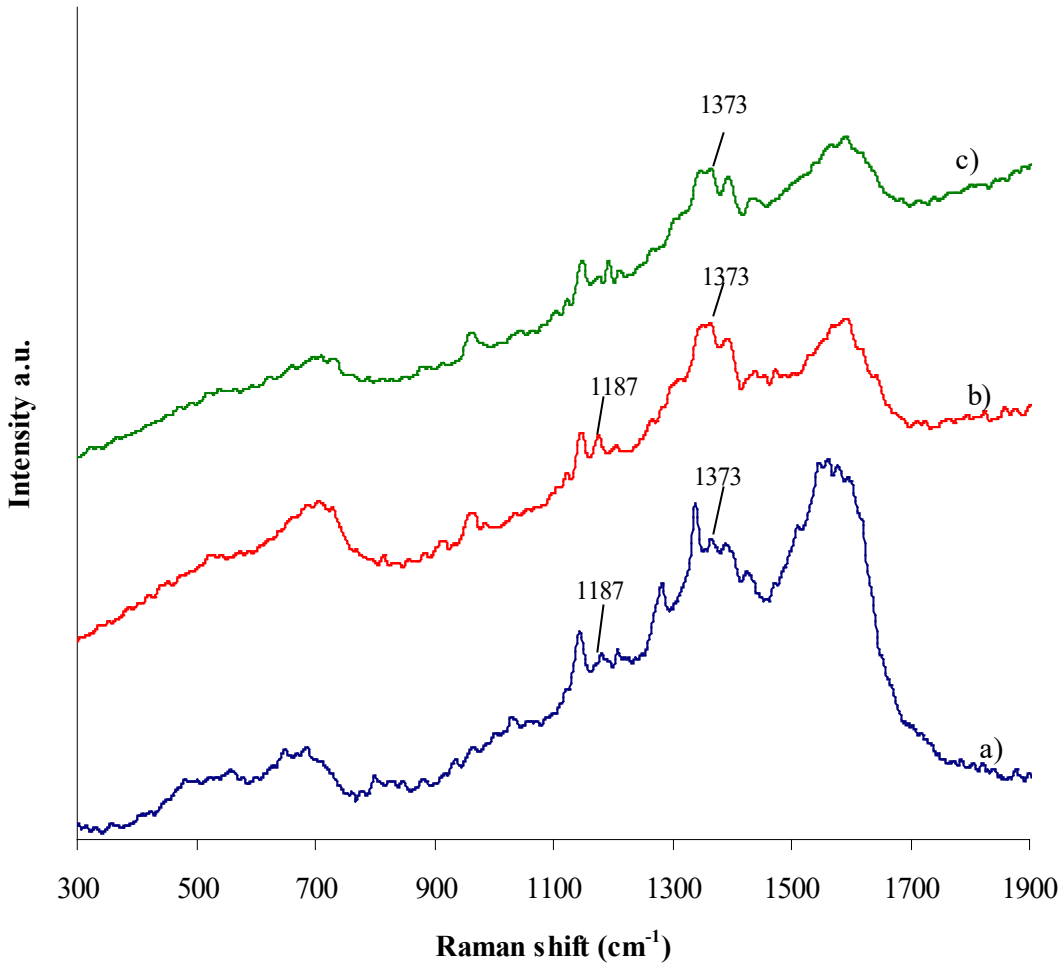

Figure 6.12. SERRS spectra of a) closed SERRS beacon, b) with single base mismatch sequence and c) nonsense control using PVA-Ag disc. Concentration of the Beacon was 4.7×10^{-7} mol dm^{-3}.

In this example a 3' fluorescein was used in combination with one benzotriazole maleimide dye. The nature of the 5'-labelling means that once the diene modified Beacon sequence has been synthesised, a range of different maleimide dye quenchers can be added to the 5' end. That can lead to the increase in the multiplexing capacity of the SERRS Beacons due to the different SERRS signals from structurally similar dyes. A further degree of multiplexing can be obtained by changing the diene used to generate a different cycloadduct with the range of dye maleimides. Cycloadducts made from either different dyes and the same diene or different dienes and the same maleimide give distinctly different SERRS signals (*Chapter 5*) thus allowing a high degree of multiplexing by using only the one

fluorescent dye. Obviously changing the identity of the fluorescent dye can increase this degree of multiplexing further as this also gives different SERRS codes. Additionally, the SERRS Beacons can be used as either solution state probes or in a surface array. Each approach is under further investigation but this initial enabling study clearly demonstrates the high potential that SERRS Beacons have as a new class of molecular reporter.

Chapter 7

Conclusions

A range of novel benzotriazole dyes with a primary amino group, which are excellent SERRS dyes, was successfully synthesised. They were further derivatised with the maleimide group that acted as a dienophile in Diels Alder cycloaddition. Cobalt naphthenate was found to be the best reagent for maleimide formation with maximum yield around 60% depending on the dye used as a starting reagent (Scheme 7.1).

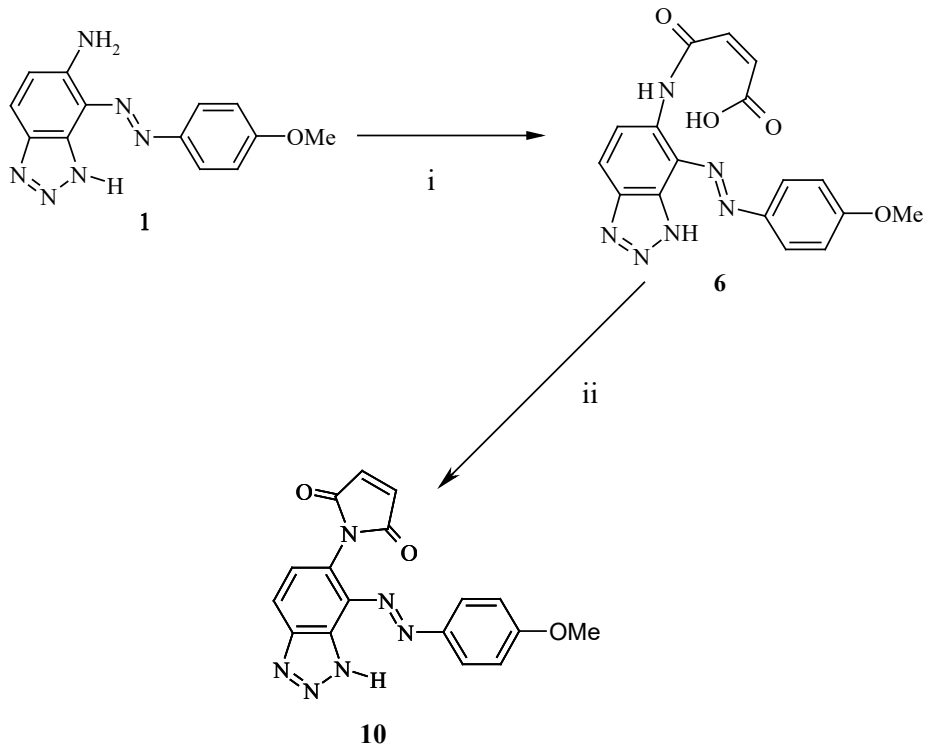

Scheme 7.1. Formation of maleimide ring using cobalt naphthenate as illustrated using dye **1**. (i) Maleic acid anydride, DCM and (ii) Co(II) naphthenate, Ac_2O.

During the investigation of different methodologies for maleimide ring formation using a variety of phenylamines, isomaleimide side product was isolated. A range of aromatic isomaleimides and maleimides was formed and imide – isoimide rearrangement studied. The effect of substituents on the maleimide was determined. It was found that the presence of an electron-donating group favours the isomaleimide and an electron withdrawing the maleimide formation. This information is useful in designing the synthesis of new maleimides for use in a range of applications including biological labelling using Diels Alder chemistry.

Two different oligonucleotides were successfully labelled with SERRS active dye maleimides using Dielas Alder cycloadditions. Both furan and butadiene modified oligonucleotides readily undergo cyloaddition reaction although with different reaction times (Scheme 7.2.).

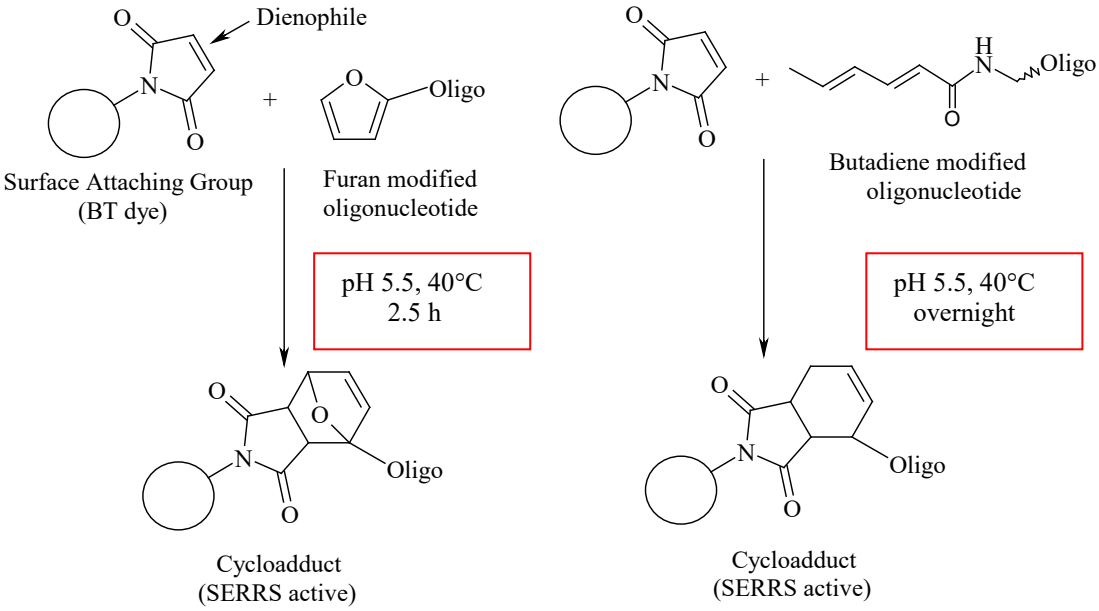

Scheme 7.2. Labelling of diene modified oligonucleotides with SERRS active dye maleimides.

Furan oligonucleotide showed the completion of the reaction in less than 2.5 hours at 40°C in pH 5.5. buffer. Butadiene oligonucleotide reacted with benzotriazole maleimide overnight. The oligonucleotide labelled with dye **10** was detected at level of 10^{-17} moles using SERRS and PVA-Ag discs as a SERRS active surface. PVA-Ag discs and TiO_2 –Ag discs were investigated for their potential as SERRS substrates. PVA-Ag fulfilled most of the requirements for an effective SERRS substrate and was used together with silver colloid in the investigation of labelled oligonucleotides.

SERRS spectra of the dye maleimides used in oligonucleotide labelling differ from the SERRS spectra of oligonucleotide cycloadducts. This enables the analysis of oligonucleotides *in situ* and in the presence of starting material. Moreover, the spectra of cycloadducts made using furan differ from the ones made with butadiene indicating the multiplexing potential of this system.

Fluorescence quenching ability of benzotriazole dyes was investigated using fluorescein as a fluorophore. Most of the dyes were found to be better quenchers than commercially available DABCYL.

Finally, SERRS beacons were designed using one of the benzotriazole dye maleimides and fluorescein (Fig. 7.1)

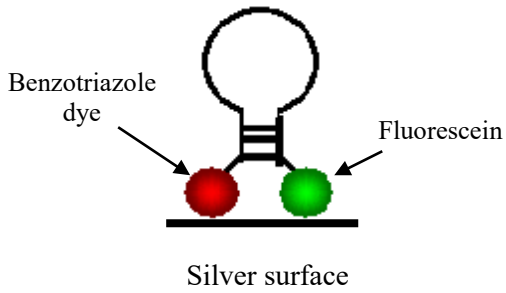

Figure 7.1. SERRS Beacon.

SERRS Beacons are new class of biomolecular probe, which combines the detection technique of fluorescence and SERRS to provide an ultra sensitive probe. The SERRS spectra of this type of probe changes dramatically with addition of complementary sequence, while there are no changes when single base mismatch or nonsense oligonucleotide controls are added. Therefore, the SERRS beacons have required specificity and sensitivity for single base resolution.

In final conclusion, Diels Alder cyloaddition can be used as a new approach to biological labelling and shows excellent promise in terms of selectivity, sensitivity and simplicity. Four specifically designed reagents were synthesised to react with diene modified oligonucleotides in an aqueous environment and produce distinctive species as determined by SERRS. This approach to labelling was successful in the design of SERRS beacons and can be effective for many other targets.

Chapter 8

Experimental data and procedures

8.1. Synthesis and properties of benzotriazole dyes and dye maleimides

8.1.1. General

All chemicals were purchased from Aldrich Ltd. except for 5-aminobenzotriazole (Lancaster Synthesis Ltd), cobalt naphthenate (Fluka). ^{1}H NMR spectra were recorded on a Brücker 400 (400 MHz) instrument. Mass spectra were recorded on a JEOL AX505 spectrometer using chemical ionization (CI) or Fast Atom Bombardment (FAB) in a 3-nitrobenzyl alcohol matrix. Flash chromatography was carried out using silica gel 60 (Merck) or Biotage prepacked silica columns when automatic Biotage flash chromatography apparatus was used. Thin layer chromatography was carried out on aluminium sheets, coated with silica gel 60 F_{254}, 0.2 mm layer (Merck) (A) EtOAc-hexane (1:1); (B) DCM-MEOH (9:1); (C) EtOAc-hexane 1:1.5. UV/Vis absorption spectra were measured using a Cary Bio300 UV-Vis spectrometer using quartz glass cuvettes with path length 10 mm. Melting points were measured using a Buchi melting point B-545 apparatus and are uncorrected.

8.1.2. Synthesis of benzotriazole dyes

4- (4'-Methoxy-phenylazo)-3*H*-benzotriazole-5-yl amine [1]

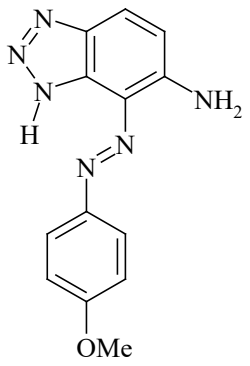

p-Anisidine (2.50 g, 20.0 mmol) was dissolved in HCl (50:50, 6 ml) and diazotised by dropwise addition of sodium nitrite (1.67 g, 24.0 mmol, in 15 ml H_2O) at 0ºC. An excess of nitrous acid was detected using starch-potassium iodide paper. 5-Aminobenzotriazole (2.44 g, 0.018 mol) was dissolved in sodium acetate buffer (pH

6, 80 ml) and methanol and the diazonium solution added dropwise to the coupling agent at room temperature to form a brown precipitate. After filtration the residue was washed with distilled water and then dried to yield the title compound as a brown powder (4.54 g , 85 %): R_f (A) 0.41; mp 218.0 °C; ^{1}H NMR δ_H(acetone-d_6): 3.87 (3H, s, C*H*$_3$); 6.60 (2H, br s, N*H*$_2$), 6.94 (2H, d, J8.9, H-4), 7.05 (2H, d, *J*8.3, Ar-H), 7.82 (1H, d, *J*8.9, H-5), 8.15 (2H, d, *J*8.5, Ar-H), 14.51 (1H, br s, N*H*); λ_{max} (MeOH-H_2O)/nm: 443.2 (ε/dm^3 mol^{-1} cm^{-1}16036); *m/z* (CI) 269.11562 [$C_{13}N_6OH_{13}$ $(M+H)^+$ < 2 ppm]; Anal. Calc. for $C_{13}H_{12}N_6O$: C, 58.20; H, 4.51; N, 31.33. Found: C, 57.71; H, 4.07; N, 30.81.

4- (3'-Methoxy-phenylazo)-3*H*-benzotriazole-5-yl amine [2]

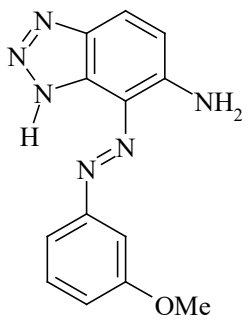

Following the same procedure as for the synthesis of **1**, *m*-anisidine (1.50 g, 12 mmol) and 5-aminobenzotriazole (1.60g, 10 mmol) afforded the title compound as a brownish-orange powder (2.62 g, 81%); R_f (A) 0.39; mp 205.6 °C; ^{1}H NMR δ_H(acetone-d_6): 3.83 (3H, s, C*H*$_3$), 6.80 (2H, br s, N*H*$_2$), 7.02 (2H, m, Ar-H), 7.42 (1H, d, *J*8.3, H-4), 7.75 (2H, m, Ar-H), 7.83 (1H, d, *J*8.5, H-5), 14.47 (1H, br s, N*H*); λ_{max} (MeOH-H_2O)/nm: 438.0 (ε/dm^3 mol^{-1} cm^{-1} 12036); *m/z* (CI) 269.11589 [$C_{13}N_6OH_{13}$ $(M+H)^+$< 3 ppm] ; Anal. Calcd. for $C_{13}H_{12}N_6O$: C, 58.20; H,4.51; N, 31.33. Found: C, 58.58; H, 4.45; N, 28.83.

4- (3',5'-Dimethoxy-phenylazo)-3*H*-benzotriazole-5-yl amine [3]

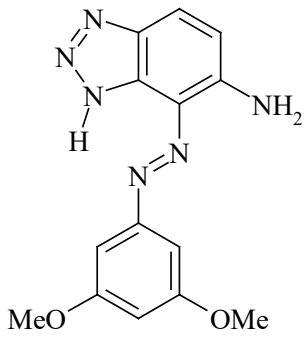

Following the same procedure as for the synthesis of **1**, 3,5 -dimethoxyaniline (0.50 g, 4.0 mmol) and 5-aminobenzotriazole (0.40g, 3.0 mmol) afforded the title compound as an orange powder (0.61 g, 62%): R_f (A) 0.45; mp 193-195 (decomp.); ^{1}H NMR δ_H(acetone-d$_6$): 3.84 (6H, s, 2xCH_3), 6.57 (1H, m, Ar-H), 6.80 (2H, br s, NH_2), 7.03 (1H, d, *J*8.9, H-4), 7.41 (2H, s, Ar-H), 7.84 (1H, d, *J*9.0, H-5), 14.53 (1H, br s, N*H*), λ_{max} (MeOH-H_2O)/nm: 439.0 (ε/dm^3 mol^{-1} cm^{-1} 13667); *m/z* (CI) 298.11782 [$C_{14}H_{15}N_6O_2$ $(M+H)^+$< 0.1ppm) Anal. Calcd. for $C_{14}H_{14}N_6O_2$: C, 54.45 ; H, 4.93; N, 29.34. Found: C, 54.72; H, 5.08; N, 30,05.

4- (Naphthalen-1-ylazo)-3*H*-benzotriazole-5-yl amine [4]

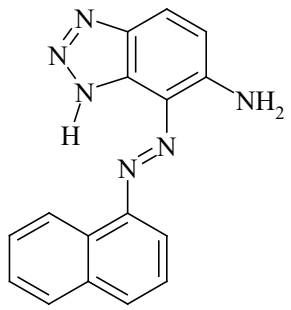

Following the same procedure as for the synthesis of **1**, α-aminonaphthalene (1.20 g, 8.0 mmol) and 5-aminobenzotriazole (1.02 g, 7.0 mmol) afforded the title compound as a red powder (0.96 g, 51%): R_f (A) 0.47; mp 194.0 °C; ^{1}H NMR δ_H(acetone-d$_6$): 7.00 (2H, br s, NH_2), 7.64 (4H, m, Ar-H), 7.85 (1H, m, Ar-H), 7.90

(1H, d, *J*8.9, H-4), 8.0 (2H, m, Ar-H), 8.86 (1H, d, *J*8.9, H-5), 14.57 (1H, br s, N*H*), λ_{max} (MeOH-H_2O)/nm: 462.0 (ε/dm^3 mol^{-1} cm^{-1} 14314); *m/z* (CI) 289.11885 [$C_{16}H_{13}N_6$ $(M+H)^+$ < 3.0 ppm ; Anal. Calcd. for $C_{16}H_{12}N_6$: C, 66.66; H, 4.20; N, 29.15. Found: C, 67.03; H, 4.32; N, 27.12.

7-(4'- Methoxy - phenylazo) –1*H*-benzotriazole-4-yl amine [5]

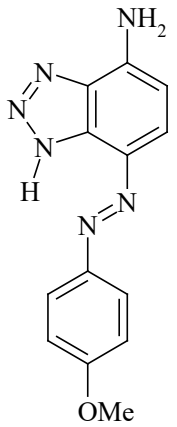

Following the same procedure as for the synthesis of **1**, *p*-anisidine (0.70, 9.0 mol) and 4-aminobenzotriazole (0.84 g, 6.0 mol) afforded the title compound as an olive green powder (1.26 g, 75% yield): R_f (A) 0.34; mp 203.4 °C; ^{1}H NMR δ_H (acetone-d_6): 3.82 (3H, s, C*H*$_3$), 6.51 (2H, br s, N*H*$_2$), 6.67 (1H, d, *J*8.2, H-5), 7.00 (2H, d, *J*9.0, Ar-H), 7.87 (1H, d, *J*8.2, H-6), 8.86 (2H, d, *J*9.0,Ar-H); λ_{max} (MeOH-H_2O)/nm: 425.0 (ε/dm^3 mol^{-1} cm^{-1} 29813); *m/z* (CI) 269.11506 [$C_{13}H_{13}N_6O$ $(M+H)^+$ < 0.1 ppm]; Anal. Calc. for $C_{13}H_{12}N_6O$: C, 58.20; H, 4.51; N, 31.33. Found: C, 57.57; H, 4.98; N, 30.92.

8.1.3 Synthesis of the maleamic acids

3-[4-(4'-methoxy –phenylazo)-3*H*-benzotriazol-5-ylcarbamoyl] acrylic acid [6]

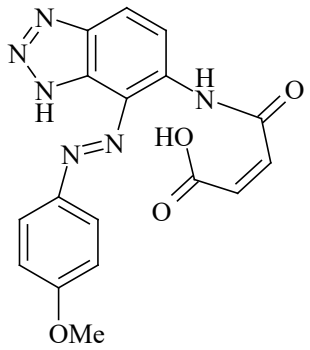

BT dye **1** (2.68 g, 10.0 mmol) was partially dissolved in DCM (40 ml) and maleic acid anhydride (1.92 g, 20.0 mmol in 10 ml DCM) was added portionwise over half hour. The reaction mixture was stirred at room temperature overnight to produce a brown precipitate, which was collected by filtration, washed with DCM and dried. (3.00 g, 82% yield): R_f (B) 0.10; mp 193°C (decomp.); ^{1}H NMR δ_H (DMSO-d_6): 3.90 (3H, s, C*H*$_3$), 6.43 (1H, d, *J*12, C*H*CHCO$_2$H), 6.72 (1H, d, *J*12, CHC*H*CO$_2$H), 7.17 (2H, d, *J*9.0, Ar-H), 8.23 (1H, d, *J*8.8, H-4), 8.33 (1H, d, *J*8.8, H-5), 8.43 (2H, d, *J*9.0, Ar-H), 10.93 (1H, br s, N*H*CO), 11.00 (1H, br s, CO$_2$*H*), 15.74 (1H, br s, N*H*); *m/z* (FAB) 367.11534 [C_{17} $H_{15}N_6O_4$ $(M+H)^+$ < 0.4 ppm]; Anal. Calcd. for $C_{17}H_{14}N_6O_4$: C, 55.74; H, 3.85; N, 22.94. Found: C, 54.96; H, 3.61; N, 22.21.

3-[4-(3'-Methoxy-phenylazo)-3*H*-benzotriazole-5-ylcarbamoyl) acrylic acid [7]

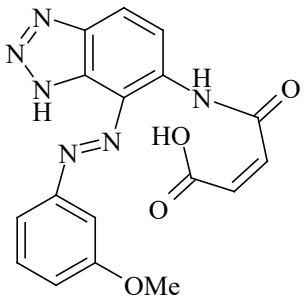

Following the same procedure as for the preparation of **6**, BT dye **2** (1.00 g, 3.0 mmol in 40 ml DCM) and maleic acid anhydride (0.73 g, 7.0 mmol in 10 ml DCM) afforded 0.87 g of a light brown powder (yield 67%) identified as the title

compound: R_f (B) 0.12; decomposes at 196°C; ^{1}H NMR δ_H (DMSO-d_6): 3.93 (3H, s, C*H*$_3$), 6.43 (1H, d, *J*12, C*H*CHCO$_2$H), 6.373 (1H, d, *J*12, CHC*H*CO$_2$H), 7.10 (1H, m, Ar-*H*), 7.51 (1H, m, Ar-H), 8.03 (2H, m, Ar-*H*), 8,25 (1H, d, *J*9.0, *H*-4), 7.92 (1H, d, *J*9.0, *H*-5), 10.55 (1H, br s, N*H*CO), 12.98 (1H, be s, -CO$_2$*H*), 15.36 (1H, br s, N*H*); *m/z* (FAB) 367.11456 [$C_{17}H_{15}N_6O_4$ $(M+H)^+$ < 2.5 ppm]; Anal. Calcd. for $C_{17}H_{14}N_6O_4$: C, 55.74; H, 3.85; N, 22.94. Found: C, 54.82; H, 3.99; N, 22.51.

3-[4-(3,5'-Dimethoxy-phenylazo)-3*H*-benzotriazole-5-ylcarbamoyl] acrylic acid [8]

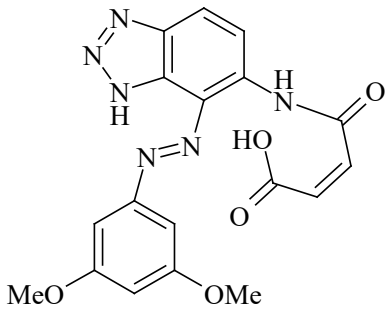

Following the same procedure as for the preparation of **6**, BT dye **3** (3.00 g, 10.0 mmol in 40 ml DCM) and maleic acid anhydride (2.00 g, 20.0 mmol in 10 ml DCM) afforded 3.15 g of a dark brown powder (yield 80%) identified as the title compound: R_f (B) 0.10; decomposes between 196-199°C; ^{1}H NMR δ_H(DMSO-d_6): 3.91 (6H, s, 2xC*H*$_3$), 6.43 (1H, d, *J*12, C*H*CHCO$_2$H), 6.73 (1H, d, *J*12, CHC*H*CO$_2$H), 6.77 (1H, s, Ar-*H*), 7.70 (2H, s, Ar-H), 8.29 (1H, d, *J*9.0, *H*-4), 8.35 (1H, d, *J*9.0, H-5), 11.01 (1H, br s, N*H*CO), 13.05 (1H, br s, -CO$_2$*H*), 15.76(1H, br s, N*H*); *m/z* (FAB) 397.12604 [$C_{18}H_{17}N_6O_5$ $(M+H)^+$ < 2.6 ppm].

3-[4- (Naphtalen-1-ylazo)-3*H*-benzotriazole-5-ylcarbamoyl] acrylic acid amine [9]

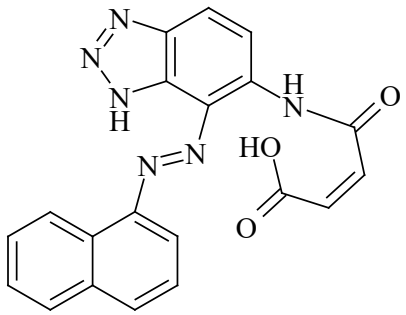

The same procedure was followed as for the synthesis of **6.** Dye **4** (0.25 g, 9.0 mmol) and maleic acid anhydride (0.17g, 2.0 mmol in 5 ml DCM) afforded the title compound as a dark orange powder (0.25 g, yield 75%): R_f (B) 0.12; mp 202°C; ^{1}H NMR δ_H (DMSO-d_6): 6.43 (1H, d, *J*12, C*H*CHCO$_2$H), 6.72 (1H, d, *J*12, CHC*H*CO$_2$H), 7.00 (3H, m, Ar-H), 7.80 (2H, m, Ar-*H*), 8.16 (2H, m, Ar-*H*), 8.34 (1H, d, *J*8.2, *H*-4), 8.87 (1H, d, *J*8.1,H-5), 11.00 (1H, br s, N*H*CO), 12.97 (1H, br s, -CO$_2$*H*), 15.82 (1H, br s, N*H*); *m/z* (FAB) 387.12109 [$C_{20}H_{15}N_6O_3$ $(M+1)^+$ < 1.4 ppm]; Anal. Calcd. for $C_{20}H_{14}N_6O_3$: C, 62.17; H, 3.65; N, 21.76. Found: C, 60.81; H, 3.41; N, 21.14.

.

8.1.4. Synthesis of the dye maleimides from maleamic acid

1-[4-(4'-Methoxy-phenylazo)-3*H*-benzotriazole-5-yl]-pyrrole–2,5-dione [10]

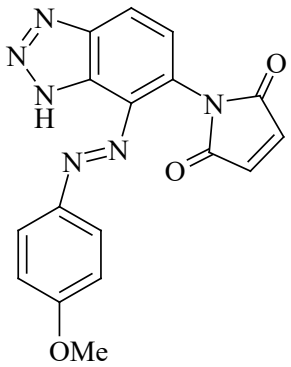

Method 1. A solution of dye **1** (0.50g, 2.0 mmol) in DMA (5 ml) was added dropwise to a stirred solution of maleic anhydride (0.18g, 2.0 mmol) in DMA (2ml). Then cobalt naphthenate solution (0.02 ml cobalt naphthenate in 10 ml DMA) was added followed by acetic anhydride (0.40, 4.0 mmol) and the solution was warmed to 75ºC, stirred for 1 hour under nitrogen then cooled and diluted with water. The resulting precipitate was collected and washed thoroughly with water, then dissolved in DCM and filtered again to remove a dark brown insoluble precipitate. DCM was removed under reduced pressure and the brownish red solid purified by column chromatography using ethyl acetate/hexane (1:1.5) as an eluent. The resulting dark orange powder was identified as title compound (0.24g, 0.007 mol, 35% of yield): R_f (C) 0.57; ^{1}H NMR δ_H (DMSO-d_6): 3.90 (3H, s, C*H*$_3$), 7.14 (2H, d, *J*9.0, Ar-H), 7.32 (2H, s, C*H*=C*H*), 7.58 (1H, d, *J*8.7, H-4), 8.10 (2H, d, *J*8.8, Ar-H), 8.39 (1H, d, *J*8.7, H-5), 16.05 (1H, br s, N*H*): λ_{max} (MeOH-H_2O)/nm: 386.0 (ε/dm^3 mol^{-1} cm^{-1} 17353); *m/z* (CI) 349.10450 [$C_{17}H_{13}N_6O_3$ $(M+H)^+$<1.2 ppm]; Anal. Calc. for $C_{17}H_{12}N_6O_3$: C, 58.64; H, 3.47; N, 24.14. Found: C, 58.41; H, 3.68; N, 22.97.

The maleimide was crystallized from MeOH/H_2O mixture giving orange needles. The melting point was not determined because the compound decomposes before it melts.

Method 2.To a solution of dye acid derivative **6** (0.30g, 1.0 mmol) in DMA (2 ml), cobalt naphthanete solution (0.01 ml in 10ml DMA) was added under nitrogen and heated to 40º C. Acetic acid anhydride (0.16 ml, 1.6 mmol) was then added and the reaction mixture warmed to 70-80ºC and stirred for 1 hour. A colour change from orange to deep red occured. The solution was cooled and diluted with water and the precipitate filtered off and redissolved in DCM. An insoluble solid was filtered off and the DCM removed under reduced pressure. A red powder was obtained using the Biotage flash chromatography system with ethyl acetate/hexane (1:1.5) to give a reddish orange powder identified as the title compound (0.14g, 51% yield).

Method 3. Dye acid derivative **6** (0.5 mmol) was dissolved in dichloromethane (20 ml) and the resulting suspension cooled to 0ºC in ice water bath. To this cooled suspension was added in order of 1-hydroxybenzotriazole hydrate (0.07 g, 0.5 mmol) and dicyclohexylcarbodiimide (0.31 g, 1.5 mmol). The reaction mixture turned green 5 minutes after the addition and was left to stir for 20 hours at room temperature. The precipitate which formed was filtered off and DCM removed under reduced pressure

to leave a green powder which was purified twice by column chromatography using EtOAC/hexane (1.5:1) and DCM/MeOH (9:1) as eluents. Title compound was obtained as an orange powder (0.09 g, 53% yield).

1-[5-Amino-4-(4'-methoxy-phenylazo)-benzotriazole-1-yl] ethanone [11]

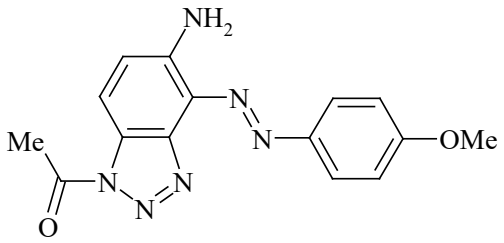

The above compound was isolated as a side product in preparation of **10** using method 1 after column chromatography purification using ethyl acatate/hexane (1:1.5) as an eluent. It is an orange solid with R_f (C) 0.50; ^{1}H NMR δ_H(DMSO-d_6): 1.91 (3H, s, -C*H*$_3$), 3.89 (3H, s, -OC*H*$_3$), 7.07 (1H, d, *J*8.8, Ar-*H*), 7.31 (1H, d, *J*9.0, *H*-4), 7.95 (2H, d, *J*8.8, Ar-*H*), 8.00 (1H, d, *J*9.0, H-5), 8.10 (2H, br s, N*H*$_2$); Anal. Calc. for $C_{15}H_{14}N_6O_2$: C, 58.05; H, 4.52;. Found: C, 58.41; H, 4.78. The compound was recrystallised from MeOH/H_2O and orange crystals were obtained. The melting point was not determined as the compound decomposes prior to melting.

1-[4-(3'-Methoxy-phenylazo)-3*H*-benzotriazole-5-yl]-pyrrole-2,5-dione [12]

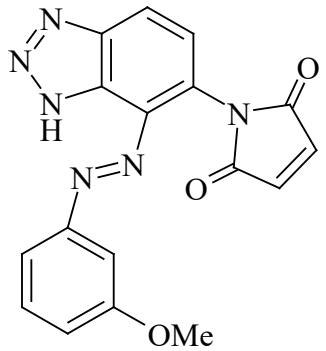

Following the same procedure as for the synthesis of **10** by Method 2, *N*-(2-azonaphthyl-3H-benzotriazole-6-yl) maleamic acid **7** (0.12 g, 3.0 mmol), cobalt naphthenate solution (0.01 ml) and acetic acid anhydride (0.06 ml, 6.0 mmol)

afforded the title compound (0.11 g, 55% yield) as a dark red powder after the purification by column chromatography using (DCM/MeOH (9:1): R_f (B) 0.68; ^{1}H NMR δ_H (DMSO-d_6): 3.89 (3H, s, -OC*H*$_3$), 7.13 (1H, m, Ar-*H*), 7.23 (2H, s, C*H*=C*H*), 7.49 (1H, t, *J*8.0, Ar-*H*), 7.62 (2H, m, Ar-*H and H*-4), 7.72 (1H, m, Ar-*H*), 8.39 (1H, d, *J*8.6, H-5), 15.26 (1H, br s, BT-N*H*); λ_{max} (MeOH-H_2O)/nm: 354.0 (ε/dm^3 mol^{-1} cm^{-1} 11583); *m/z* (FAB) 349.10454 [$C_{17}H_{13}N_6O_3$(M+H)$^+$ < 1.1 ppm]; Anal. Calc. for $C_{17}H_{12}N_6O_3$: C, 58.64; H, 3.47; N, 24.14. Found: C, 58.24; H, 3.86; N, 23.24.

1-[5-Amino-4-(3'-methoxy-phenylazo)-benzotriazole-1-yl] ethanone [13]

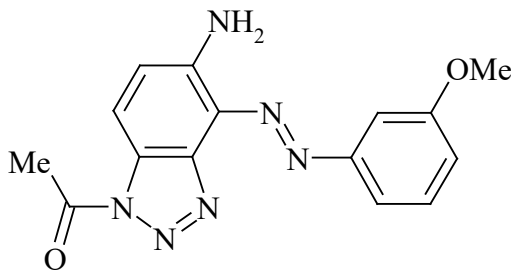

The above compound was isolated as a side product in the preparation of **12** using method 1 after column chromatography purification using DCM/methanol (9:1) as an eluent. It is an dark orange solid with R_f (C) 0.62; ^{1}H NMR δ_H (DMSO-d_6): 1.29 (3H, s, -C*H*$_3$), 3.90 (3H, s, -OC*H*$_3$), 7.14 (1H, d, *J*6.8, Ar-*H*), 7.30 (1H, s, Ar-*H*), 7.49 (1H, t, *J*8.0, Ar-*H*), 7.62 (1H, d, *J*8.6, *H*-4), 7.73 (1H, d, *J*6.8, Ar-*H*), 8.40 (1H, d, *J*8.6, *H*-5); λ_{max} (MeOH-H_2O)/nm: 342.0 (ε/dm^3 mol^{-1} cm^{-1} 1015); Anal. Calc. for $C_{15}H_{14}N_6O_2$: C, 58.05; H, 4.52;. Found: C, 58.70; H, 4.31. The compound was recrystallised from MeOH/H_2O and orange crystals were obtained.

1-[4-(3,5'-Dimethoxy-phenylazo)-3*H*-benzotriazole-5-ylcarbamoyl]-pyrrole-2,5-dione [14]

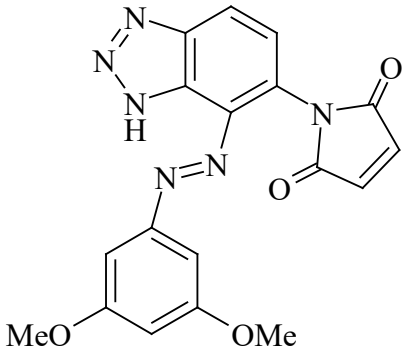

Following the same procedure as for the synthesis of **10** by Method 2, maleamic acid **8** (1.50 g, 3.8 mmol), cobalt naphthenate solution (10 µl) and acetic acid anhydride (0.72 ml, 7.6 mmol) afforded the title compound (0.80 g, 56% yield) as an orange red powder after purification by column chromatography using (DCM/MeOH (9:1): R_f (B) 0.60; ^{1}H NMR δ_H (DMSO-d_6): 3.83 (6H, s, 2xOC*H*$_3$), 6.74 (1H, s, Ar-*H*), 7.34 (2H, s, Ar-*H*), 7.40 (2H, s, *H*C=C*H*), 7.63 (1H, d, *J*8.4, *H*-4), 8.43 (1H, d, *J*8.5, *H*-5), 16.10 (1H, br s, BT-*H*); λ_{max} (MeOH-H_2O)/nm: 362.0 (ε/dm^3 mol^{-1} cm^{-1} 13317); *m/z* (FAB) 379.11548 [$C_{18}H_{15}N_6O_4(M+H)^+$ < 4.5 ppm]; Anal. Calc. for $C_{18}H_{14}N_6O_4$: C, 57.14; H, 3.73; N, 22.22. Found: C, 57.32; H, 4.00; N, 21.98.

1-[4- (Naphthalen-1-ylazo)-3*H*-benzotriazole-5-ylcarbamoyl]-pyrrole-2,5-dione [15]

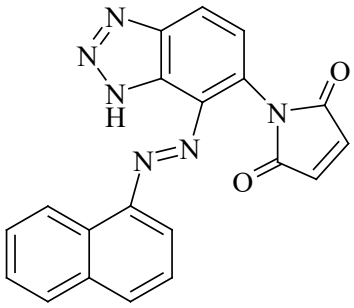

Following the same procedure as for the synthesis of **10** by Method 2, *N*-(2-azonaphthyl-3H-benzotriazole-6-yl) maleamic acid **9** (0.12 g, 0.3 mmol), cobalt naphthenate solution (0.01 ml) and acetic acid anhydride (0.06 ml, 0.6 mmol) afforded the title compound (0.11 g, 55% yield) as a dark red powder after the purification by column chromatography using (DCM/MeOH (9:1): R_f (B) 0.68; ^{1}H NMR(δ_H(DMSO-d_6): 7.37 (2H, s, C*H*=C*H*), 7.68 (3H, m, Ar-H), 7.81 (1H, m, Ar-H), 7.98 (1H, d, *J*8.2, Ar-H), 8.11 (1H, d, *J*8.2, Ar-H), 8.27 (1H, d, *J*8.0, Ar-H), 8.53 (1H, d, *J*8.7, H-4), 9.07 (1H, d, *J*8.7, H-5); λ_{max} (MeOH-H_2O)/nm: 400.2 (ε/dm^3 mol^{-1} cm^{-1} 9389); *m/z* (FAB) 369.10217 [$C_{20}H_{13}N_6O_2$ $(M+H)^+$ < 1.3 ppm]; Anal. Calc. for $C_{20}H_{12}N_6O_2$: C, 65.02; H, 3.30;. Found: C, 63.90; H, 3.42.

8.1.5. Synthesis of N-phenyl maleimides

3-(4-Amino-phenylcarbamoyl) acrylic acid [16]

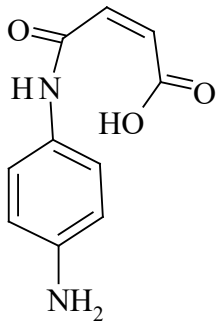

1,4–Phenylenediamine (2.16 g, 20.0 mmol) was dissolved in DCM (20 mL) and maleic acid anhydride (1.96 g, 20.0 mmol) in DCM (5 mL) added dropwise over 30 min. After 12 h of stirring at rt, the resulting precipitate was collected, washed well with DCM and dried, giving the title product (3.93 g, 95%) as an orange powder, mp 179-181 °C (decomp). R_f (A) 0.05. ^{1}H NMR δ_H(DMSO-d_6): 6.27 (1H, d, *J* 12.0, C*H*CHCO$_2$H), 6.46 (1H, d, *J* 12.0, CHC*H*CO$_2$H), 6.53 (2H, d, *J* 8.7, Ar-H), 7.31 (2H, d, *J* 8.7, Ar-H), 10.49 (1H, br s, -CO$_2$*H*). *m/z*(FAB*)* 207.07697 [$C_{10}H_{11}N_2O_3$ $(M+H)^+$ < 1.5 ppm]. Anal. Calcd for $C_{10}H_{10}N_2O_3$: C, 58.25; H, 4.49; N, 13.60. Found: C, 58.28; H, 5.07; N, 13.13.

N-[4-(2,5-Dioxo-2,5-dihydro-pyrrol-1-yl] acetamide [17]

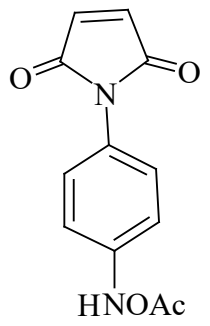

Compound **16** (0.28 g, 1.4 mmol) was added to a solution of sodium acetate (0.11 g, 1.4 mmol) in acetic anhydride (5 mL). The reaction mixture was refluxed and after 5 min the acid dissolved and colour of the solution changed to pale yellow. Stirring was continued for 1 h until TLC showed the reaction to be complete. Water was added to the cooled solution and the pale yellow precipitate collected, washed with water and dried. The pure product was obtained after recrystallization from methanol as pale yellow powder (0.24 g, 85 %), mp 190-192 °C (decomp). R_f (A) 0.48. ^{1}H NMR δ_H(DMSO-d_6): 2.80 (3H, s, C*H*$_3$), 7.00 (2H, s, C*H*=C*H*), 7.27 (2H, d, *J* 8.8, Ar-H), 7.73 (2H, d, *J* 8.8, Ar-H), 9.25 (1H, s, N*H*). *m/z* (FAB) 231.0769. [$C_{12}H_{11}N_2O_3$ $(M+H)^+$ < 6.3 ppm]. Anal. Calcd for $C_{12}H_{10}N_2O_3$: C, 58.54; H, 4.10; N, 11.38. Found: C, 59.46; H, 4.51; N, 11.05.

5-[4-Amino-phenylimino]-5*H*-furan-2-one [18]

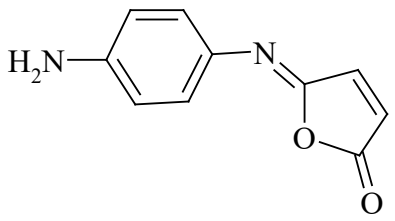

Method 1. 3-(4-Amino-phenylcarbamoyl) acrylic acid **16** (1.03 g, 5.0 mmol) was dissolved in DCM (20 mL) and cooled to 0°C. 1-Hydroxy benzotriazole (0.70 g, 5.0 mmol) and dicyclohexylcarbodiimide (1.24 g, 6.0 mmol) were added respectively. The colour of the solution changed to red after 2 h of stirring. After 12 hours at rt, the precipitate was removed by filtration and the solvent removed under reduced pressure

before the crude product was purified by column chromatrography eluting with MeOH in DCM(1:9) to give the title compound as an orange powder (0.60 g, 63%) .

Method 2. To a solution of acid derivative **16** (0.26 g, 1.26 mmol) in DMA (2 mL), cobalt naphthanate solution (0.01 ml, 0.06g in 10 mL DMA) was added under nitrogen and heated to 40º C. Acetic acid anhydride (0.12 mL, 2.52 mmol) was then added and the reaction mixture warmed to 70-80ºC and stirred for 2 h. The solution was cooled, diluted with water and the precipitate removed by filtration before dissolution in DCM. The orange powder obtained after purification by flash chromatography with ethyl acetate/hexane (1:1.5) and recystallisation from ethyl acetate was identified as the title compound (0.17 g, 72 %), mp 185 °C. R_f (B) 0.30. ^{1}H NMR δ_H(acetone-d_6): 5.10 (2H, br s, N*H*$_2$), 6.65 (2H, d, *J* 8.8, Ar-H), 6.69 (1H, d, *J* 5.5, C*H*=CH), 7.35 (2H, d, *J* 8.8, Ar-H), 7.47 (1H, d, *J* 5.5, CH=C*H*). *m/z* (FAB) 189.1262 [$C_{10}H_9N_2O_2$ $(M+H)^+$ < 1.8 ppm]. Anal. Calcd for $C_{10}H_8N_2O_2$: C, 62.78; H, 4.68; N, 14.07. Found: C, 62.48; H, 5.89; N, 13.55.

3-(4-Nitro-phenylcarbamoyl) acrylic acid [19]

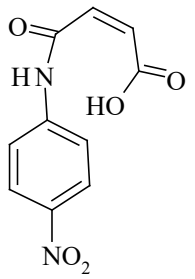

Maleic acid anhydride (2.17 g, 22 mmol) was dissolved in THF (2 mL) and slowly added to a solution of 4-nitroaniline (1.53 g, 11 mmol) in THF (10 ml) and left to stir overnight at rt. The yellow precipitate was collected, washed well with THF and dried giving the title compound as pale yellow powder (2.16 g, 83%), mp 193 °C. R_f (A) 0.08; ^{1}H NMR δ_H(DMSO-d_6): 6.34 (1H, d, *J* 12.0, C*H*CHCO$_2$H), 6.52 (1H, d, *J* 12.0, CHC*H*CO$_2$H), 7.86 (2H, d, *J* 9.2, Ar-H), 8.24 (2H, d, *J* 9.0, Ar-H), 10.87 (1H, s, N*H*CO), 12.85 (1H, br s, CO$_2$*H*). *FAB-MS m/z* 237.05123 [$C_{10}H_9N_2O_5$ $(M)^+$ < 0.7 ppm]. Anal. Calcd for $C_{10}H_8N_2O_5$: C, 50.85; H, 3.41; N, 11.86. Found: C, 50.90; H, 3.40; N, 11.56.

1-(4-Nitro-phenyl)-pyrrole-2,5-dione [20]

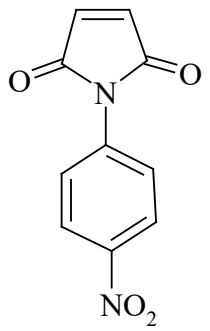

Following the same procedure as for the synthesis of maleimide **17**, *N*-(4-nitrophenyl) maleamic acid **19** (2.16 g, 9.1 mmol) and sodium acetate (0.89 g, 10.9 mmol) were stirred in acetic acid anhydride (25 mL) at rt to give the title compound as a pale yellow powder (1.47 g, 74%) which was recrystallised from MeOH giving colorless plates, mp 162-164°C; R_f (A) 0.38. ^{1}H NMR δ_H(DMSO-d_6): 7.26 (2H, s, C*H*=C*H*), 7.70 (2H, d, *J* 5.0, Ar-H), 8.36 (2H, d, *J* 5.1, Ar-H); *CI-MS m/z* 219.04058 [$C_{10}H_7N_2O_4(M+H)^+$ < 2.5 ppm]. Anal. Calcd for $C_{10}H_6N_2O_4$: C, 55.10; H, 2.80; N, 12.84. Found: C, 54.80; H, 2.67; N, 12.63. Crystal structure deposited in Cambridge Crystal Database, accession number = 212029.

3-(3-Methoxy-phenylcarbamoyl) acrylic acid [21]

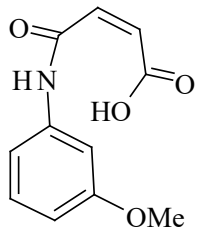

Maleic acid anhydride (1.60 g, 16 mmol) was dissolved in THF (2 mL) and slowly added to the solution of 3-methoxy aniline (0.91 mL, 0.8 mmol) in THF (10 mL) and left to stir overnight at rt. The precipitate was collected, washed well with THF and dried giving the title compound as pale yellow powder (0.91g, 81%), mp 160 °C. R_f (A) 0.1. ^{1}H NMR δ_H(DMSO-d_6): 3.73 (3H, OCH_3), 6.31 (1H, d, *J* 12, C*H*CHCO$_2$H), 6.45 (1H, d, *J* 12, CHC*H*CO$_2$H), 6.66 (1H, d, *J* 8.2, Ar-H), 7.14 (1H, d, *J* 8.0, Ar-H), 7.22 (1H, t, *J* 8.0, Ar-H), 7.31 (1H, s, Ar-H), 10.35 (1H, s, N*H*CO),

13.05 (1H, br s, CO_2H). *m/z* (FAB) 222.07663 [$C_{11}H_{12}NO_4(M+H)^+$ < -4.2 ppm]. Anal. Calcd for $C_{11}H_{11}NO_4$: C, 59.72; H, 5.01; N, 6.33. Found: C, 59.75; H, 5.11; N, 6.14.

5-[3-Methoxy-phenylimino]-5*H*-furan-2-one [22]

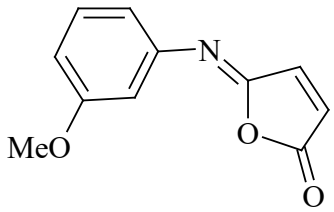

Following the same procedure as for the synthesis of maleimide **18**, *N*-(3-methoxyphenyl)maleamic acid (0.55 g, 2.5 mmol) and sodium acetate (0.25 g, 3.0 mmol) were stirred for 30 min in acetic acid anhydride (10 mL) at rt and then extracted with DCM. The organic layer was dried over $MgSO_4$ and evaporated to give the crude residue. Column chromatrography with DCM-methanol (9:1) afforded the title compound as a yellow oil (0.42 g, 82 %). R_f(A) 0.45. ^{1}H NMR δ_H(DMSO-d_6): 3.73 (3H, s, OCH_3), 6.83 (2H, d, *J* 8.3, Ar-H), 6.90 (1H, s, Ar-H), 7.11 (1H, d, *J* 5.6, C*H*=CH), 7.28 (1H, m, Ar-H),), 7.80 (1H, d, *J* 5.6, CH=C*H*). FAB-MS *m/z* 204.06605 [$C_{11}H_9NO_3(M)^+$ < 0.1 ppm]. Anal. Calcd for $C_{11}H_9NO_3$: C, 64.90 ; H, 4.43; N, 6.90. Found: C, 64.71 ; H, 4.82; N, 6.26.

3-(4-Methoxy-phenylcarbamoyl) acrylic acid [23]

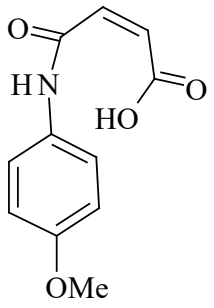

Maleic acid anhydride (2.17 g, 22 mmol) was dissolved in THF (2 mL) and slowly added to a solution of 4-nitroaniline (1.53 g, 11 mmol) in THF (10 ml) and left to stir overnight at rt. The yellow precipitate was collected, washed well with THF and dried giving the title compound as pale yellow powder (2.16 g, 83%), mp 193 °C.

R_f (A) 0.08; ^{1}H NMR δ_H(DMSO-d_6): 6.34 (1H, d, *J* 12.0, C*H*CHCO$_2$H), 6.52 (1H, d, *J* 12.0, CHC*H*CO$_2$H), 7.86 (2H, d, *J* 9.2, Ar-H), 8.24 (2H, d, *J* 9.0, Ar-H), 10.87 (1H, s, N*H*CO), 12.85 (1H, br s, CO$_2$*H*). *m/z* (FAB) 222.05815 [$C_{11}H_{12}NO_4$ $(M+H)^+$ < -4.0 ppm]. Anal. Calcd for $C_{11}H_{11}NO_4$: C, 59.72; H, 5.01; N, 6.33. Found: C, 59.47; H, 5.06; N, 6.09.

5-[3-Methoxy-phenylimino]-5*H*-furan-2-one [24]

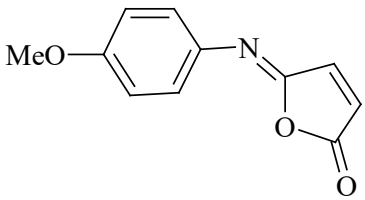

Following the same procedure as for the synthesis of maleimide **18**, *N*–(3-methoxyphenyl) maleamic acid (0.40 g, 1.8mmol) and sodium acetate (0.17 g, 2.0 mmol) were stirred 50 min in acetic acid anhydride (10 mL) at rt. The precipitate was collected, washed well with water and dried. Recrystallisation from acetone afforded the title compound as yellow needles (0.28g, 71 %). Method 2 using Co naphthenate afforded the same product in 75% yield after purification with column chromatography using DCM-methanol (9:1) and recrystallization from acetone, mp 115 °C (decomp). R_f (A) 0.50. ^{1}H NMR δ_H(DMSO-d_6): 3.77 (3H, s, OC*H*$_3$), 6.98 (2H, d, *J* 7.0, Ar-H), 7.05 (1H, d, *J* 5.6, C*H*=CH), 7.40 (2H, d, *J* 7.0, Ar-H), 7.75 (1H, d, *J* 5.6, CH=C*H*); EI-MS *m/z* (203.057 [$C_{11}H_9NO_3$ $(M)^+$ < 0.7 ppm]. Anal. Calcd for $C_{11}H_9NO_3$: C, 64.90 ; H, 4.43; N, 6.90. Found: C, 64.44 ; H, 4.50 ; N, 6.53 .

3-(4-tert-Butoxycarbonylamino-phenylcarbamoyl) acrylic acid [25]

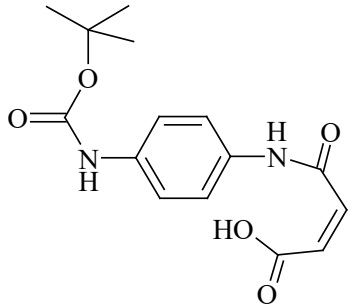

N-(4-Aminophenyl)maleamic acid **16** (0.43 g, 2.04 mmol) was dissolved in a mixture of dioxane, water and a 1M solution of sodium hydroxide (10 mL:5 mL:5 mL) at 0 °C. Di–*ter-t* butyl pyrocarbonate (0.48 g, 2.20 mmol) was added to the cooled solution and stirred for 45 min at rt. The reaction mixture was concentrated under reduced pressure to 10 mL, cooled in an ice bath, covered with a layer of ethyl acetate (10 mL) and acidified with dilute aqueous potassium hydrogen sulphate (1M) to pH 2-3. The aqueous phase was then extracted with ethyl acetate (3 x 15 ml) and the combined organic phase washed with water (2 x 30 mL), dried over anhydrous sodium sulphate and evaporated *in vacuo*. The residue was dissolved in EtOAc, filtered and the filtrate triturated with hexane to give the title compound as a bright yellow powder (0.48 g, 85 %), mp 165 °C. R_f (C) 0.05. ^{1}H NMR δ_H (DMSO-d_6): 1.40 (9H, s, 3 x C*H*$_3$), 6.29 (1H, d, *J* 12.0, C*H*CHCO$_2$H), 6.45 (1H, d, *J* 12.0, CHC*H*CO$_2$H), 7.39 (2H, d, *J* 8.9, Ar-H), 7.50 (2H, d, *J* 8.9, Ar-H), 9.32 (1H, br s, N*H*CO), 10.40 (1H, br s, N*H*CO), 13.36 (1H, br s, CO$_2$*H*), *m/z* (CI) (307.12950 [$C_{18}H_{17}N_2O_5$ $(M+H)^+$ <2.8 ppm]. Anal. Calcd for $C_{18}H_{16}N_2O_5$: C, 58.80; H, 5.90; N, 9.15. Found: C, 58.65; H, 5.71; N, 8.96.

[4-(2,5-Dioxo-2,5-dihydro-pyrrol-1-yl)-phenyl] carbamic acid *tert*-butyl ester [26]

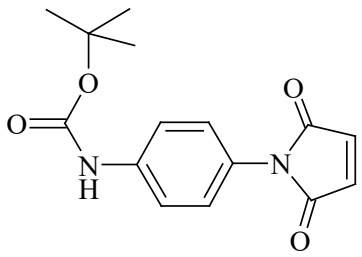

Compound **25** (0.25 g, 0.8 mmol) was added to DCM (50 mL) and the suspension cooled to 0ºC. To the cooled stirred solution was added in order 1-hydroxybenzotriazole hydrate (0.13 g, 0.8 mmol) and morpho CDI (1.40 g, 3.3 mmol). After 5 h of stirring, the reaction mixture was diluted with DCM (30 mL) and extracted successively with water (3 x 50 mL), 1M hydrochloric acid (1 x 40 mL) and sodium bicarbonate (1M, 1 x 40 mL). The organic phase was dried (sodium sulphate) and the solvent removed. The title compound was obtained by recrystallization from methanol as pale yellow powder (0.19g, 83%), mp 179 °C. R_f (C) 0.67. ^{1}H NMR

δ_H(DMSO-d_6): 1.45 (9H, s, 3 x CH_3), 7.14 (2H, s, C*H*=C*H*), 7.18 (2H, d, *J* 8.7, Ar-H), 7.52 (2H, d, *J* 8.7, Ar-H), 9.48 (1H, br s, N*H*CO). CI-MS *m/z* 289.11883 [$C_{15}H_{17}N_2O_4$ $(M+H)^+$ <0.6 ppm]. Anal. Calcd for $C_{15}H_{16}N_2O_4$: C, 62.49; H, 5.59; N, 9.17. Found: C, 61.97; H, 5.42; N, 9.76.

8.1.6. Diels Alder cycloaddition

4-(Dimethyl-hydrazonomethyl)-2-phenyl – isoindole-1,3-dione [27]

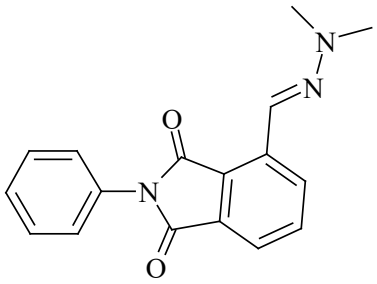

Phenyl maleimide (0.10 g, 0.67 mmol) was dissolved in acetonitrile (2.5 ml) and added to the solution of 2-furaldehyde dimethylhydrazone (0.15 ml, 1.2 mmol) in an acetonitrile-water mixture (2.5 ml:5 ml). The reaction mixture was stirred at 40ºC for 15 minutes by which time TLC showed the reaction to be complete. After 2 days bright yellow needles were obtained from the solution and identified as the title compound (93% yield), mp 178.3 °C; R_f (A) 0.47; ^{1}H NMR (δ_H(acetone-d_6): 3.80 (6H, s, 2xCH_3), 7.44 (1H, s, *H*C=N), 7.50 (4H, m, Ar-H), 7.64 (1H, m, Ar-H), 8.29(1H, m, Ar-H), 8.15 (2H, m, Ar-H).

4-(Dimethyl-hydrazonomethyl)-2-[4-(4'-methoxy-phenylazo)-3*H*-benzotriazole-5-yl)-isoindole-1,3-dione [28]

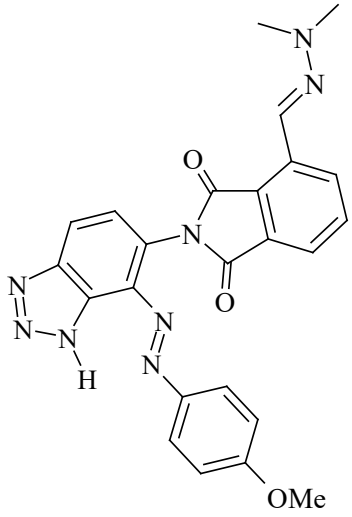

Dye maleimide **10** (7 mg, 0.02 mmol) was dissolved in acetonitrile (2 ml) and water (6 ml). To this solution 2-furaldehyde dimethylhydrazone (0.005 ml, 0.04 mmol) was added and the reaction mixture stirred at 45°C for 30 minutes by which time TLC showed the reaction to be complete. An orange precipitate was obtained from the solution on cooling and identified as the title compound (6 mg, 70% yield): R_f(C) 0.60; mp 185.0 °C, ^{1}H NMR δ_H(DMSO-d_6): 3.12 (6H, s, 2xCH_3), 3.83 (3H, s, CH_3), 7.10 (2H, d, *J*8.9, Ar-H), 7.70 (2H, d, *J*8.9, Ar-H), 7.85 (1H, m, Ar-H), 8.00 (1H, s, C*H*=N), 8.05 (2H, m, Ar-H), 8.16 (1H, d, *J*8.9, Ar-H), 8.38 (1H, d, *J*8.9,Ar-H), 15,62 (1H, br s, N*H*).

8.2. SERRS substrates

8.2.1. General

All chemicals were purchased from Aldrich Ltd. except for polyvinyl alcohol and aminomethylated polystyrene resin 100-200 mesh, which were obtained from Nova Biochem. Cover glass discs of 13 mm diameter and 21.5 mm thickness (BDH) were used in the preparation of PVA-Ag and cold deposited silver discs. Spin coater Electronic Micro Systems Model 4000-1 was used to prepare PVA-Ag substrates. Raman and SERRS spectra were recorded using a Renishaw 2000 Raman spectrometer with 514.5 and 785 nm excitation sources. Solid samples were used for obtaining Raman spectra and solutions of dye in methanol-water mixture were used for SERRS. Static spectra were obtained using 3 accumulations of 3 s and extended (200-2000 cm^{-1}) using 2 accumulations in 10 s. Surface mapping of PVA –Ag discs coated with BT dye maleimide was performed using Renishaw Ramascope 2000 at 514.5 nm with xyz stage control using 5μm steps for mapping 400x400μm^2 disc area. Electron probe microanalysis (EPMA) was done using Cameca SX100 instrument within the Department of Physics at the University of Strathclyde.

8.2.2 Silver colloid

The colloidal silver suspension was prepared by the method based on a report by Lee and Meisel.[117] All glassware was soaked in *aqua regia* for at least 30 minutes prior to use and then rinsed well with water. 500 ml of distilled water was stirred vigorously and heated using a Bunsen burner. When the temperature reached 60ºC, silver nitrate (90 mg, 0.53 mmol) was added and the solution heated rapidly to about 95 –98ºC and trisodium citrate added (1.1 eq, 150 mg, 0.58 mmol). The temperature was maintained at 98ºC for a further 90 minutes, the heating stopped and the mixture stirred until the resulting greenish solution had cooled to room temperature. The quality of silver colloid was checked by UV/Vis spectroscopy. The colloid had a single narrow band at 402 nm and a full width at half maximum (FWHM) of approximately 51 nm (typical values are in the range of λ_{max} = 400-404 nm and FWHW ≈ 60 nm).

8.2.3. Cold deposited Ag films

Silver vapor was deposited onto a glass surface. A small piece of thin silver wire was placed into the molybdenum substrate boat in an Edwards E306A vacuum evaporator. A high vacuum pump was used to evacuate the chamber to a final pressure of $1x10^{-5}$ mbar. The deposition rate and thickness were monitored using an Intellimetrics IL100 crystal thickness monitor. The glass pieces were held approximately 20 cm directly above and parallel to the substrate boat during the evaporation of the silver. Typical deposition rates of 0.01 –0.02nms^{-1} were used.

8.2.4. Polyvinyl alcohol (PVA) substrates

A slight modification of a procedure used by Vo Dinh was used to prepare polyvinyl alcohol - silver substrate deposited on glass discs. PVA (1.6 ml, 5% or 10 % solution in water) was stirred with silver nitrate (0.40 g) for 24 hours. A few drops of PVA - $AgNO_3$ solution were distributed on the surface of the glass discs and the discs were then spun at 2350 rpm for 20 s to ensure uniform coverage of the glass. The coated discs were dried overnight at 60°C under vacuum and then heated at 100°C for two hours. Finally, the substrate was dipped in aqueous $FeSO_4 \cdot 7H_2O$ (wt/vol) for 30 s and then placed in an oven at 100°C for 15 minutes.

8.2.5. TiO_2 – silver discs

TiO_2–silver discs were obtained from Professor A. Mills, Pure and Applied Chemistry, University of Strathclyde.

8.3. SERRS of dyes and dye maleimides

8.3.1. General

A Renishaw 2000 Raman spectrometer with 514.5 nm laser excitation was used for SERRS measurements. The static spectra were recorded using 3 accumulations of 3 s and extended (200-2000 cm^{-1}) using 1 accumulation in 10 s. The methanol-water solutions of dyes were use in SERRS measurements. Normal Raman scattering was obtained from a solid sample presented as fine powders on glass slides. UV/Vis absorption spectra were measured with a Cary Eclipse Varian UV/Vis spectrometer using quartz glass cuvettes with a path length of 10 mm. IR spectra of solid dyes were recorded with a Nicolet Avatar 360 FT-IR using the KBr method for sample preparation. Surface mapping of PVA –Ag discs coated with BT dye maleimides was performed using a Renishaw Ramascope 2000 at 514.5 nm with xyz stage control and applying 5μm steps for mapping 400x400μm^2 disc area

8.3.2. Molecular modelling and frequency calculations

Density functional geometry optimizations and vibrational frequency predictions were calculated using the Gaussian98W program running on a Windows NT workstation. The BLYP method with the 6-31/G (d, p) basis set was used for all density functional calculations. The Raman frequencies predicted from calculations were used as an aid in assigning bands in both Raman and SERRS spectra.

8.4. Synthesis and labeling of modified oligonucleotides

8.4.1. General

The synthesis of the oligonucleotides was carried out using a Peseptive Biosystems Expedite 8909 system. All reagents were supplied by Applied Biosystems, except for the amino link which was purchased from Link Technologies. The estimated loadings of the columns were 1.0 µmol. The following sequences were used: probe 1: 5'- TCT CAA CTC GTA and probe 2: 5'- CGC ATT CAG GAT. Effective coupling of the amino link was ensured by double delivery to the column with an extended coupling time of 15 minutes. Butadiene phosphoramidite was made in our lab and supplied by Dave Robson.

***N* – (2-Methoxy-penta-2,4-dienyl) succinamic acid [29]**

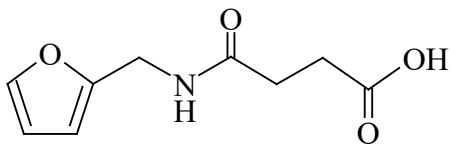

Succinic anhydride (1.68 g, 17mmol) was dissolved in DCM (10 ml) and added dropwise to furfurylamine (1.00ml, 10 mmol). Reaction mixture was stirred for 3 h at rt. and the precipitate isolated by filtration, washed well with DCM and dried. The title compound was obtained as a white powder (2.10g, 95% yield): R_f (DCM-MEOH 9:1) 0.12; mp 122.9 °C; ^{1}H NMR δ_H(DMSO-d_6): 2.34 (2H, t, *J*6.0, *J*7.6, COCH_2), 2.44 (2H, t, *J*6.7, *J*6.6, CH_2CO$_2$H), 2.23 (2H, d, *J*5.6, CH_2NH), 6.21 (1H, s, Fur-H), 6.98 (1H, s, Fur - H), 7.55 (1H, s, Fur - H), 8.31 (1H, s, N*H*CO), 12.05 (1H, br s, CO$_2$*H*); *m/z* (EI) 197.06842 [$C_9H_{12}NO_4$ $(M+H)^+$ < 2.0 ppm]; Anal. Calcd. for $C_9H_{11}NO_4$: C, 54.82; H, 5.62; N, 7.10. Found: C, 54.25; H, 5.87; N, 7.09.

N-(4-[4-(4-Methoxy-phenylazo)-2,3-dihydro-1H-benzotriazole-5-yl)-3,5-dioxo-10-oxa-4-aza-tricyclo[5.2.1.0.^{2,6}] dec-8-en-1-ylmethy) succinamic acid [30]

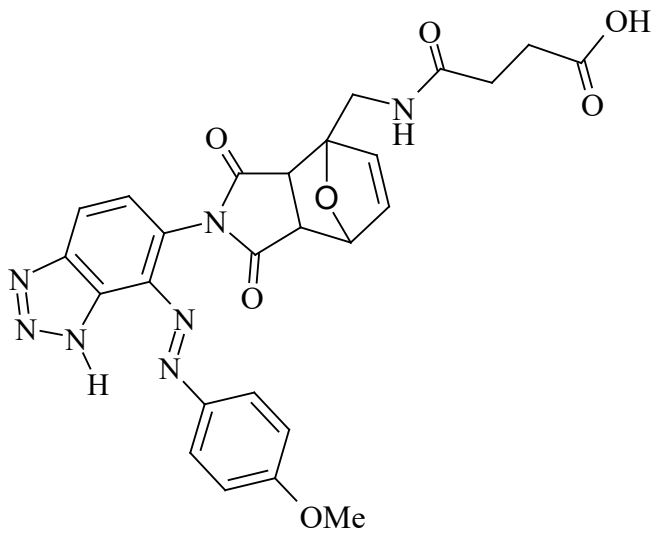

Dye maleimide **10** (0.20g, 0.57 mmol) was dissolved in acetonitrile (4 ml) and water (12 ml). To this, the solution of **29** (0.23g, 1.20mmol) was added and the reaction mixture stirred at 45°C for 1.5 h by which time TLC showed the reaction to be completed. Product was extracted with 3x200mL of EtOAc and solvent removed *in vaccuo*. The solid was redisolved in EtOAc and triturated with hexane to give above compound as yellow solid (0.22g, 71%). R_f(C) 0.30; mp 111.2°C; ^{1}H NMR (δ_H(DMSO-d_6): 2.33 (4H, m, COCH_2,CH_2CO$_2$H), 2.50 (2H, m, CH_2NH), 3.88 (3H, s, 0CH_3), 6.21 (1H, d, *J*5.0, C*H*=CH), 6.37 (1H,d, *J*5.0, CH=C*H*), 6.43 (1H, s, OC*H*), 7.21 (2H, d, *J*9.0, Ar-*H*), 7.51 (1H, d, *J*8.9, Ar-*H*), 7.55 (1H, s, COC*H*), 8.22 (1H, s, COC*H*), 8.27 (3H, m, 2xAr*H*, CON*H*), 8.35 (1H, d, *J*8.9,Ar-*H*), 12.01 (1H, br s, COO*H*); 16.01 (1H, br s, BT N*H*). FAB-MS *m/z* 547.17372 [$C_{26}H_{24}N_7O_7$ $(M+H)^+$ <0.4 ppm].

8.4.2. Synthesis of furan modified oligonucleotides [32a, b]

Compound **29** (0.024g, 0.12 mmol) was dissolved in anhydrous DMF (1 ml) and then activated by reaction with 1,1- carbonyldiimidazole (0.036g, 0.22 mmol). The mixture was warmed to 40˚C for 5 minutes and then allowed to come to room

temperature. The resulting activated acid was loaded into a 1 ml syringe and attached to the column containing oligonucleotide probe 1. An empty 1 ml syringe was attached to the other end of the column, pushed through several times and then allowed to stand for 3 hours. After the time had elapsed, the solution was taken up into one syringe and removed from the column. The column was then washed well with DMF and acetonitrile and dried with nitrogen. The same procedure was repeated using the probe 2 sequence to obtain **33b**.

8.4.3. Synthesis of butadiene modified oligonucleotide [33]

Butadiene phosphoramidate was allowed to couple onto the 5'end of probe 2 during automated synthesis. A 30 min coupling time was used.

8.4.4. Oligonucleotide deprotection and cleavage from solid support

The oligonucleotide was deprotected and removed form the solid support using concentrated ammonia solution. Solid support with synthesised oligonucleotide was placed in an Eppendorf tube, 1 ml of concentrated ammonia added and heated at 55˚C overnight. Finally, the solution containing the deprotected oligonucleotide was placed in a round bottom flask and the ammonia removed *in vacuo*. The solid oligonucleotide was redissolved in distilled water and purified by HPLC.

8.4.5. Synthesis of oligonucleotide cycloadducts

The furan-modified oligonucleotide **33a** (500 µl of 8 x 10^{-6} mol dm^{-3}) in phosphate buffer (25 mM, pH 5.5) was added to the benzotriazole dye maleimide ($MeCN/H_2O$ 3:7, 3eqs, 80 µl). The volume was made up to 1 ml with phosphate buffer and MeCN to keep the amount of MeCN at 30%. The solution was then heated at 40 ^{0}C for 150 mins to complete the cycloaddition. 50 µl aliquots were used for HPLC. The same procedure was followed in all cycloadditions performed.

8.4.6. HPLC purification of modified oligonucleotides

Purification of the oligonucleotides was carried out using a PE Biosystems Biocad Sprint HPLC system running Biocad software. For each sequence, an analytical run was carried out before a full preparative run was attempted. UV detection at 260 nm was used in each case. C-18 Chromolith column (flow rate 4 ml/s) and C-18 column (flow rate 1 ml/min) were used for purifications. The following reverse phase methods were developed (Buffer A = ammonium acetate pH 7, Buffer B = MeCN)

Method 1 for purification of furan modified oligos: 0-5 CV 5% B, 5-30 CV 5-30% B, 30-40 CV 30-100 % B, 40-43 CV 100% B. Total time for method to be completed 19.94 min.

Method 2 for purification of oligo cycloadduct: 0-5 CV 5% B, 5-15 CV 5-10% B, 15-35 CV 10-15% B, 35-45 CV 25-100% B, 45-48 CV 100% B. Total time for method to be completed 22.02 min.

Method 3 for purification of modified oligos using C-18 Supelco column: 0-5 CV 8% B, 5-10 CV 8-20% B, 10-21 CV 20-60% B, 21-23 CV 60-0% B. Total time for method to be completed 38.02 min.

8.4.7. Desalting procedure after purification

The pure oligonucleotide sample was dissolved in 1.0 ml of distilled water and passed through asize exclusion HiTrap™ Desalting column packed with G25 Sephadex Superfine matrix using PE Biosystems Biocad Sprint HPLC system running Biocad software. 15 minutes method was created and both conductivity and absorbance at 260 nm followed. The eluted product was collected in a round bottomed flask, the water removed *in vacuo* and the oligonucleotide redissolved in 1 ml water prior to storage.

8.4.8. Measurement of the concentration of the oligonucleotide stock solutions

Using Beer Lambert Law the absorbance value at 260 nm of the stock solutions is converted into the concentration of oligonucleotide sample:

Beer Lambert Law: A = abc where A = absorbance
a = absorption coefficient
b = path length (1 cm)
c = concentration

The absorption coefficient must be determined for each oligonucleotide is cumulative sum of the absorption coefficients of the individual DNA bases.:

$$A = \{(dG \times n) + (dA \times n) + (dC \times n) + (dT \times n)\} \times 0.9$$

where 0.9 represents a hypochromicity factor.

8.4.9. SERRS of the cycloaddition

When following the cycloaddition by SERRS a 1:1 ratio of furan-modified oligonucleotide to benzotriazole dye maleimide was used. Copper (II) nitrate (100 µl, 0.01 M) solution was added to the reaction mixture to enhance the rate.

The reaction was followed by spotting 10 µl of the reaction mixture onto the PVA-silver coated surface. Spectra were taken using 514.5 nm excitation and 3 accumulations in 3 s.

8.4.10. Fluorescence measurements of labelled oligonucleotides

Cary Eclipse fluorimeter was used to measure the fluorescence of the labelled oligonucleotides. Disposable fluorescence cuvettes were used and all solutions of oligonucleotides were prepared in distilled water.

8.5. SERRS beacons

8.5.1. General

All fluorescence measurements were performed using a Cary Eclipse fluorimeter and disposable fluorescence cuvettes. All solutions were prepared by dissolving used dyes and fluorophores in 70% water: 15% acetonitrile: 15% DMF. Cary Bio 300 UV/Vis spectrometer was used to obtain UV/Vis data. Refractive indices of solvents to estimate the quantum yields were taken from the literature.

8.5.2. Design and purification of SERRS beacon

SERRS Beacon :	5' BTDye – CGC ACC TCT GGT CTG AAA GTT TAT TGG TGC G - FAM
Exact Complement :	5' TTT TTT AAT AAA CTT TCA GAC CAG ATT TTT T
Mismatch :	5' TTT TTT AAT AAA CTT TTA GAC CAG ATT TTT T
Controls:	5' TTT GCG TAA GTC CTA AGA GTT GAG CAT TTT
(both provided by Dr. Enright)	5' GCT GGA ACA GAG ACC ATA GCC GAC GT

The SERRS Beacons were produced by synthesising the desired sequence on a FAM CPG solid support (Transgenomic, Glasgow, UK) using an Expedite 8909 DNA synthesiser and adding the butadiene monomer as the final 5'-residue. Cleavage and deprotection in concentrated ammonia at 50ºC for overnight gave the 5'-butadiene 3'-FAM modified sequence, which was purified by reverse phase HPLC. The benzotriazole azo dye maleimide (10 eq, phosphate buffer pH 5.5 with 30% MeCN) was added to the diene oligonucleotide and left for 12 hours at 40 ºC in the dark. The SERRS Beacon was purified by reverse phase HPLC on a C18 Supelco column with buffer A = 0.1 M triethylammonium acetate pH 6.5, buffer B = 0.1 M triethylammonium acetate with 75 % acetonitrile running from 20 to 70 % B over 25 minutes at 1 $mlmin^{-1}$. SERRS Beacon was then desalted using Sephadex column and dissolved in 1 ml of hybridisation buffer (1 mM $MgCl_2$, 20 mM Tris.HCl, pH 8.0).

8.5.3. Hybridisation Conditions

To the SERRS Beacon (50 µl, 8.4×10^{-7} mol dm^{-3}) in the hybridisation buffer wad added the desired sequence (5 equivalents) and solution made up to 100µl with the buffer. The temperature was then increased to 80°C and then slowly decreased to room temperature to enable hybridisation.

8.5.4. SERRS measurements using silver colloid

Citrate reduced silver nanoparticles were produced as described in previous section. For the analysis the SERRS Beacon mixture from above (25 µl) was added to silver nanoparticles (260 µl). When aggregating agent was used, 10 µl of spermine tetrahydrochloride (1×10^{-5} mol dm^{-3}) was added to 250 µl of the colloid and 25 µl of the SERRS Beacon solution. A final concentration of the SERRS Beacon was 3.7×10^{-8} mol dm^{-3}. Extended SERRS spectra (200-2000 cm^{-1}) were obtained with a Renishaw Ramascope 200 with 514.5 nm excitation suing 5 accumulations in 10 sec. Different concentrations of silver colloid were used. To make up 50% silver colloid, 5 ml of stock colloid solution was diluted with 5 ml of distilled H_2O. 25% colloid was made by diluting 2.5 ml of stock solution with 7.5 ml of distilled H_2O.

8.5.5. SERRS measurements using PVA-silver disc

The silver/PVA films were prepared as described previously. The SERRS Beacon mixture (10 µl) was added to the disc and left to sit for 20 minutes. The film was washed well with water and then wet examined using the Renishaw Ramascope as before but using 10 % of the laser power.

References

1. J. D. Watson, F.H. Crick, *Nature*, 1953, **171**, 737-738.
2. a) E. Pennisi, *Science*, 2003, **300**, 409-412.
   b) A.D.Roses, *Nat.Genet*., 2003, **33**, S217.
3. M. Chee, R. Yang, E. Hubbel *et al*., *Science*, 1996, **274**, 610-614.
4. I. M. Mackay, K. E. Arden, A. Nitsche, *Nucleic Acids Res*., 2002, **30**(6), 1292-1305 and references thereafter.
5. S. Verma, F. Eckstein, *Annu. Rev. Biochem*., 1998, **67**, 99-107.
6. N. E. Broude, *Trends Biotechnol.,* 2002, **20**(5), 249-256.
7. S. L. Beaucage, M. H. Caruthers, *Tetrahedron Lett.,* 1981, **22**, 1859-1862.
8. R. L. Letsinger, W. B. Lunsford, *J. Am. Chem. Soc*., 1976, **98**, 3655-3661.
9. H. Koester, N.D. Sinha, J. Biernat, *Tetrahedron Lett*., 1983, **24**, 245-248.
10. K.L. Agrawal, A. Yamazaki, P. J. Cashion, H.G. Khorana, *Angew. Chem. Int. Ed*., 1972, **11**, 451-550.
11. J. Skeidsvoll, P.M. Ueland, *Anal. Biochem.,* 1995, **231**, 359-365.
12. R.S. Tuma, M. P. Beaudet, X. Jin, L. J. Jones *et al.*, *Anal. Biochem.,* 1999, **268**, 278-288.
13. M. J. Lim, W.F. Patton, M. F. Lopez *et al., Anal. Biochem*., 1997, **245**, 184-1895.
14. A. Waggoner, *Methods Enzymol.,* 1995, **246**, 362-373.
15. A. P. Feinberg, B. Vogelstein, *Anal. Biochem.*, 1984, **137**(1), 266-267.
16. Z. R .Zhu, J. Chao, H. Yu, A. S. Waggoner, *Nucleic Acids Res.,* 1994, **22**(16), 3418-3422.
17. M. Bruchez, M. Moranne, P. Gin, S. Weiss, A. P. Alivisatos, *Science*, 1998, **281**, 2013-2016.
18. a) W. C. Chan, S. M. Nie, *Science*, 1998, **281**, 2016-2018.
    b) G. P. Mitchell, C. A. Mirkin, R. L. letsinger, *J. Am. Chem. Soc.,* 1999, **121**, 8122-8123.
19. H. Cai, Y. Xu, N. Zhau, P. He, Y. Fang, *Analyst*, 2002, *127*, 803-808.
20. K. T. Kitchin, J. L. Brown, *Anal. Biochem.,* 1995, *229*, 180-187.
21. E. M. M. Menders, H. Kimura, P. R. Cook, *J. Cell. Biol*., 1999, **144**, 813-821.

22. A.C. van der Laan, R. Brill, R. G. Kuimelis, R. Vinayak *et al*,. *Tetrahedron Lett.,* 1997, 2249-2252.
23. P. Hagmar, M. Bailey, G. Tang, J. Haralambidis *et al.*, *Biochim. Biophys. Acta*, 1995, **1244**, 259-268.
24. M. Lyttle, H. Adams, D. Hudson, R. M. Cook, *Bioconjugate Chem.,* 1997, **8**, 193-198.
25. G. De Bellis, M. Maroni, R. Pergolizzi, M. Luzzana, *Nucleic Acids Res*., 1990, **18**, 4951-4952.
26. P. R. Banks, D. M. Paquette, *Bioconjugate Chem.,* 1995, **6**, 447-458.
27. F. F. Chehab, Y. W. Kan, *Proc. Natl. Acad. Sci. USA*, 1989, **86**, 9178-9183.
28. R. Vinayak, *Tetrahedron Lett.,* 1999, **40**, 7611-7613.
29. a) C. E. O'Ferral, G. U. Lee, L. A. Chrisey, *Nucleic Acids Res*., 1996, **24**(15), 30130-3039.
    b) B. T. Houseman, E. S. Gewalt, M. Mrksich, *Langmuir*, 2003, **19**, 1522-1531.
30. a) R. Eghanain, J. J. Storhoff, R. C. Mucic, R. L. Letsinger, C.A. Mirkin, *Science*, 1997, **227**, 1078-1081.
    b) R.A. Reynolds, C. A. Mirkin, R. L. Letsinger, *J. Am. Chem. Soc.,* 2000, **122**, 3795-3796.
31. R. Bermejo, E. Fernandez, J. M. Alverez-Pez, E. M. Talavera, *J. Luminescence*, 2002, **99**, 113-124.
32. P. S. Nelson, M. Kent, S. Mithini, *Nucleic Acids Res.,* 1992, **20**, 6253-6260.
33. P. Theisen, C. McCollum *et al., Tetrahedron Lett.,* 1992, **33**(35), 5033-5036.
34. M. Adamczyk, C. M. Chan, J. R. Fino, P. G. Mattingly, *J. Org. Chem*., 2000, **65**, 596-601.
35. M. H. Lyttle, t. G. Carter, D. J. Dick, R. M. Cook, *J. Org. Chem.,* 2000, **65**, 9033-9038.
36. www.glenreserach.com
37. B. Mullah, A. Andrus, *Tetrahedron Lett.,* 1997, **38**(33), 5751-5754.
38. S. Dey, L. Sheppard, *Org. Lett.,* 2001, **3**(25), 3983-3986.
39. T. S. Seo, Z. Li, H. Ruparel, J. Ju, *J. Org. Chem.,* 2003, **68**, 609-612.
40. L. J. Brown, J. P. May, T. Brown, *Tetrahedron Lett.,* 2001, **42**, 2587-2591.
41. L. Shi, www. gene-chips.com
42. M. Street, *Australasian Biotechnol.,* 2002, **12**(1), 38-39.

43. B. Lemieux, A. Aharani, M. Schene, *Mol. Breeding*, 1998, **4**, 277-289.
44. S. Jin-Oh, S. J. Cho, C.O. Kim, J. Won Pak, *Langmuir*, 2002, **18**, 1764-1769.
45. T. R. Hughes, M. Mao, A. R. Jones *et al.*, *Nat. Biotechnol.,* 2001, **19**, 342-347.
46. S. M. Dhanasekaran, T. R. Barrette, D. Ghosh *et al., Nature*, 2001, **412**, 822-826.
47. M. Chee, R. Yang, E. Hubbell *at al., Science*, 1996, **274**, 610-613.
48. D. D. Shoemaker, E. E. Schadt, C. D. Armour *et al*., *Nature*, 2001, **409**, 922-927.
49. M. L. Bulyk, X. Huang, Y. Choo, G. M. Church, *Proc. Natl. Acad. Sci. USA*, 2001, **98**(13), 7158-7163.
50. a) P. S. Bernard, C. T. Wittwer, *Clin. Chem.,* 2002, **48**(8), 1178-1185.
    b) I. M. Mackay, K. E. Arden, A. Nitsche, *Nucleic Acids Res.,* 2002, **30**(6), 1292-1305.
51. L. J. Kricka, *Ann. Clin. Biochem.,* 2002, **39**, 114-129.
52. P. H. Holland, R. D. Abramson, R. Watson, D. H. Gelfand, *Proc. Natl. Acad. Sci.USA*, 1991, **88**, 7276-7280.
53. L. G. Lee, C. R. Connell. W. Bloch, *Nucleic Acids Res.,* 1993, **21**(16), 3761-3766.
54. www.stratagene.com and references thereafter.
55. I. A. Nazarenko, S. K. Bhatnager, R. J. Hohman, *Nucleic Acids Res.,* 1997, **25**, 2516-2521.
56. a) D. Whitcombe, J. Theaker, S. P. Guy, T. Brown, S. Little, *Nat. Biotechnol*., 1999, **17**, 804-807.
    b) N. Thelwell, S. Millington, A. Solinas, H Booth, T. Brown, *Nucleic Acids Res*., 2000, **28**(19), 3752-3761.
57. S. Tyagi, F. R. Kramer, *Nat. Biotechnol.,* 1996, **14**, 303-308.
58. V.V. Didenko*, BioTechniques*, 2001, **31**, 1106-1121.
59. P. Wu, L. Brand, *Anal. Biochem.,* 1994, **218**, 1-13.
60. a) L. G. Kostrikis, S. Tyagi, M. M. Mhlaga, D. D. Ho, F. R. Kramer, *Science*, 1998, **279**, 1228-1229.
    b) J. A. M. Vet, A. R. Mjithia, S. A. E. Marras, S. Tyagi, *Proc. Natl. Acad. Sci. USA*, 1999, **96**, 6394-6399.
61. www.metabion.com for BHQ
62. www.molprobes.com for QSY7

63. J. P. May, L. J. Brown, I. Rudloff, T. Brown, *Chem. Commun.,* 2003, 970-971.
64. S. A. E. Marras, F. R. Kramer, S. Tyagi, *Nucleic Acids Res.,* 2002, **30**(21), e122.
65. S. De, A. Pal. N. R. Jana, T. Pal., *J. Photochem. Photobiol. A*, 2000, **131**, 111-114.
66. B. Dubertet, M. Calame, A. J. Libhaber, *Nat. Biotechnol.,* 2001, **19**, 365-370.
67. P. Zhang, T. Beck, W. Tan, *Angew. Chem. Int. Ed.,* 2001, **40**(2), 402-405.
68. S. Tyagi, S. A. E. Marras, F. R. Kramer, *Nat. Biotechnol.,* 2000, **16**, 245-248.
69. N. E. Broude, *Trends Biotechnol.,* 2002, **20**(6), 249-256.
70. Q. G. Li, J. X. Liang, G. Y. Luan, Y. Zhang, K. Wang, *Anal. Sci.,* 2000, **16**, 245-248.
71. W. Chen, G. Martinez, A. Mulchandani, *Anal. Biochem.,* 2000, **280**, 166-172.
72. J. J. Li, X. Fang, S. M. Schuster, W. Tan, *Angew. Chem. Int. Ed*., 2000, **39** (60), 1049-1052.
73. J. J. Li, R. Geyer, W. Tan, *Nucleic Acids Res*., 2000, **28**(11), e52.
74. D. L. Sokol, X. Zhang, P. Lu, A. M. Gewirtz, *Proc. Natl. Acad. Sci. USA*, 1998, **95**(20), 1158-11543.
75. V. Raman, K. S. Krishnan, *Nature*, 1928, **121**(3048), 501-506.
76. D.A. Skoog, F. J. Holler, T. A. Nieman, *Principles of Instrumental Analysis,* 5th Ed., Saunders College Publishing, 1998.
77. M. Fleischmann, P. J. Hedra, A.J. McQuillan, *Chem. Phys. Lett*., 1974, **26**(2), 163-166.
78. R. P. van Duyne, D. L. Jeanmarie, *J. Electroanal. Chem.,* 1977, **84**, 1-20.
79. K. Kneipp, Y. Wang, H. Kneipp, L. T. Perelman *et al*., *Phys. Rev. Lett*, 1997, **78**(9), 1667-1670.
80. M. Moskovits, *Rev. Mod. Phys.,* 1985, **57**, 783-792.
81. J. A. Craighton, *The Selection Rules for SERS*, ed. R. Clark and R. E. Hester, Chickester, 1988.
82. H. Xu, J. Aizapurua, M. Kaell, P. Apell, *Phys. Rev. E*, 2000, **62**(3), 4318-4324.
83. A. Otto, I. Mrozek, H. Grabhorn, W. J. Akemon, *J. Phys. Condens. Mat*., 1992, **4**, 1143-1212.
84. J. T. Krug II, G. D. Wang, S. R. Emroy, S. Nie, *J. Am. Chem. Soc*., 1999, **121**, 9208-9214.

85. P. Hildebrandt, M. Stockburger, *J. Phys. Chem.,* 1984, **88**, 5935 –5944.
86. K. Kneipp, H. Kneipp, V. Bhaskarankartha *et al*., *Phys. Rev. E,* 1998, **57**(6), 6281-6284.
87. Y. Sun, Y. Xia, *Science*, 2002, **298**, 2176-2179.
88. G. McAnally, C. McLaughlin, R. Brown, D.C. Robson *et al*., *Analyst*, 2002, **127**, 838-841.
89. C. J. L. Constantino, T. Lemma, P. A. Antunes, R. Aeoca, *Anal. Chem.,* 2001, **73**, 3574-3678.
90. N. Weissenbacher, B. Lendl, J. Frank *et al., J. Mol. Struct.,* 1997, 410-415.
91. C. J. McHugh, R. Keir, D. Graham, W. E. Smith, *Chem. Commun*., 2002, **6**, 580-581.
92. N. Taranenko, J. P. Alarie, D. L. Stokes, T. J. Vo Dinh, *J. Raman Spectrosc*., 1996, **27**, 379-384.
93. K. E. Schafer-Peltier, C. L. Haynes, M. R. Glucksberg, R. P. van Duyne, *J. Am. Chem. Soc*., 2003, **125**, 588-593.
94. Q. Yan, W. Priebe, J. B. Chaires, R. S. Czernhszewicz, *Biospectrosc.,* 1997, **3**, 307-316.
95. M. Ermishov, A. Sukhanova, E. Kryukov *et al., Biospectrosc.,* 2000, **57**, 272-281.
96. L. R. Allain, T. J. Vo Dinh, *Anal. Chim. Acta*, 2002, **469**, 149-154.
97. L. A. Gearheart, H. J. Poehn, C. J. Murphy, *J. Phys. Chem. B*, 2001, **105**, 12609-12615.
98. D. Graham, B. J. Mallinder, W. E. Smith, *Angew. Chem. Int. Ed*, 2000, **39**, 1061-1063.
99. R. Brown, W. E. Smith, D. Graham, *Tetrahedron Lett.,* 2001, 2197-2199.
100. A. Grondin, D. Robson, W. E. Smith, D. Graham, *J. Chem. Soc., Perkin Trans.2*, 2001, 2136-2141.
101. C. Rubin, I. G. R. Gutz, O. Sala, *J. Mol. Struct.,* 1983, **101**, 1-5.
102. D. Graham, A. R. Kennedy, S. J. teat*, J. Heterocyclic Chem.*, 2000, **37**,1555-1558.
103. J. F. T. Corrie, *J. Chem. Soc., Perkin Trans. 1*, 1994, 2975-2981.
104. F. Keanna, M. D. Ogan, Y. Lu, M. Beer, J. Varkey, *J. Am. Chem. Soc.,* 1986, **108**, 7957-7963.
105. S. Nozaki, *J. Pep. Res.,* 1999, **54**(2), 162-168.

106. C. J. McHugh, *PhD Thesis*, University of Strathclyde, 2003.
107. M. P. Cava, A. A. Deana, K. Muth, M. J. Mitchell, *J. Organic Synth.,* 1973, **5**, 944-946.
108. J. E. T. Corrie, M. H. Moore, G. D. Wilson, *J. Chem. Soc., Perkin Trans.1*, 1996, 777-781.
109. a) G.B. Gill, G.D. James, K. V. Oates, G. Pattenden, *J. Chem. Soc., Perkin Trans 1*, 1993, 2567-2579.
    b) C. S. Chaurasia, J. M. Kauffman, *J. Heterocyclic Chem.,* 1990, **27**, 727-732.
110. K. Brady, A. F. Hegarty, *J. Chem. Soc., Perkin Trans. 2*, 1980, 121-126.
111. a) U. Pindur, G. Lutz, C. Otto, *Chem. Rev.,* 1993, **93** (2), 741-761.
    b) D. Rideout, R. Breslow, *J. Am. Chem. Soc*., 1980, **102**, 7816-7817.
112. I. Khan, *PhD Thesis*, University of Strathclyde, 2003.
113. R. Keir, D. Sadler, W. E. Smith, *Appl. Spectrosc*., 2002, **56**(5), 551-559.
114. P. A. Masier-Boss, S. H. Liebermann, *Appl. Spectrosc.,* 1999, **53**(7), 862-873.
115. G. McAnally, *PhD Thesis*, University of Strathclyde, 2000.
116. M. Volkan, D. L. Stokes, T. Vo Dinh, *Appl. Spectrosc.,* 2000, **54**(12), 1842-1848.
117. P.C. Lee, D. Meisel, *J. Phys. Chem.,* 1982, **86**, 3391-3395.
118. O. Siimian, L. A. Bumm, R. Callaghan *et al*., *Phys. Chem*., 1983, **87**, 1014-1017.
119. D. Graham, B. J. Mallinder, W. E. Smith, *Biopolymers (Biospectrosc*.), 2000, **57**, 85-88.
120. D. Graham, C. McLaughlin, G. McAnally, J. C. Jones *et al*., *Chem. Commun*., 1998, 1187-1188.
121. H. Y. H. Chan, M. J. Weaver, *Langmuir*, 1999, **15**, 3348-3355.
122. J. C. Jones, C. McLaughlin, D. Littlejohn *et al., Anal. Chem*., 1999, **71**, 596-601.
123. C. H. Munro, W. E. Smith, M. Garner *et al*., *Langmuir*, 1995, **11**, 3712-3720.
124. D. Graham, B. J. Mallinder, D. Withcombe, W. E. Smith, *Chem. Phys. Chem*., 2001, **2**, 746-749.
125. P. A. Limbach, *Mass Spectrom. Rev.,* 1996, **15**, 1297-1314.

126. A. Castro, J. G. K. Williams, *Anal. Chem.,* 1997, **69**, 3915-3919.
127. D. Graham, B. J. Mallinder, W. E. Smith, *Angew. Chem. Int. Ed*., 2000, **36**(6), 1061-1063.
128. a) R. Breslow, *Acc. Chem. Res*., 1991, **24** (6), 159-164.
   b) R. Breslow, U. Maitra, D. Rideout, *Tetrahedron Lett.,* 1983, **24**, 1901-1903.
129. K.W. Hill, J. Taunton_Rigby, J. D. Carter *et al*., *J. Org. Chem.,* 2001, **66**, 5352-5362.
130. R. Breslow, C. J. Rizzo, *J. Am. Chem. Soc.,* 1991, **113**, 4340-4341.
131. D. Graham, W. E. Smith, A. M. T. Linacre, C. H. Munro *et al., Anal. Chem*., 1997, **69**, 4703-4707.
132. www.amershambiosciences.com for Sephadex information.
133. J. V. Goodpaster, V. L. McGuffin, *Appl. Spectrosc.,* 1999, **53**(8), 1000-1008.
134. S. Tyagi, S. E. Marras, F. R. Kramer, *Nat. Biotechnol.,* 2000, **18**, 1191-1196.

Contents of the Appendix CD

1. Fluorescence Quenching and FRET
2. Common Fluorophores and Their Properties
3. Crystallographic Data
4. DFT Calculation and Raman Spectra of Dye Maleimide 10
5. Publications
6. Presentation 1: Euroanalysis Conference, Dortmund 2002
7. Presentation 2: Final Year Presentation, Glasgow 2003
8. Poster 1: IR and Raman Discussion Meeting, Glasgow 2002
9. Poster 2: Symposium on Nucleic Acid Chemistry and Biology, Cambridge 2003
10. Curriculum Vitae